NTNU – Trondheim
Norwegian University of
Science and Technology

Parameters Contributing to the Formation of NOx in the Silicon Furnace

The effect of the charging frequency and raw material composition on the formation of NO

Ingeborg Brede

Materials Science and Engineering
Submission date: June 2013
Supervisor: Gabriella Tranell, IMTE
Co-supervisor: Bente Faaness, ELKEM

Norwegian University of Science and Technology
Department of Materials Science and Engineering

Preface

This research project started during my summer internship at the smelting plant Elkem Thamshavn during the summer of 2012. They have provided practical and theoretical education for this work. All of the experimental work included in this report has been done at the smelting plant in cooperation with operators and engineers working at the plant. The data that has been analyzed have been based on industrial measurements. The operators and engineers have also helped in understanding the results, and their observations have been important when it comes to investigating the furnace operational conditions.

Regarding the theoretical aspects of the report, there have been several key people contributing both from the Elkem organization and academic environment. Bente Faaness, Jan Erlend Andersen and Roar Livik are all engineers working at the plant and they have helped plan the experimental work. Edin Myrhaug has given a lecture about the silicon process and the formation mechanisms, and Nils Eivind Kamfjord has contributed with his PhD thesis. During the writing process my supervisor Gabriella has given advice about the discussion part and the structure of the report.

Dmitry Slizovskiy has contributed greatly with the data processing and with analyzing the data from the pilot-scale experiment and the charging experiment done at Elkem Thamshavn. He also helped during the charge experiment seeing that the data was measured correctly. Ole Kjos from SINTEF, a Norwegian research organization, helped set up the FTIR-measurement device.

At last, I would like to thank my class-mate Trygve Schanche. Throughout this project we have discussed subjects such as matlab, thermodynamics and the silicon process in general.

Abstract

NO_x is a harmful gas emitted primarily by the transport industry, agriculture and petroleum industry. The emissions contribute to acid rain and global warming. The gas also has certain health risks; when exposed to NO-based pollution there can be higher risk of lung-cancer and the pollution gives an asthmatic reaction for asthmatics. As a consequence of the Gothenburg protocol, there has been established a ceiling for the emissions of NO_x; Europe is to cut emissions by 41 %. As a result of this protocol the industry in Norway has joined forces creating the "NO_x-fund", which is an association providing support for research regarding reducing emissions. In Norway the silicon industry has the highest emissions yearly of the onshore industry, which means they have to contribute. In this project the mechanisms for formation of NO is investigated in an industrial silicon furnace and also in a pilot scale furnace.

In the silicon furnace, NO is primarily formed by the combustion of SiO gas, which is a by-product of the reaction in the crater of the furnace. Following, the combustion of SiO produces oxygen radicals and energy. In a combination of a high local temperature, oxygen radicals and air, NO will be formed. A lot of parameters can reduce the production of SiO gas and also control the temperature. Examples of these parameters can be the routines of tapping, charging and stoking, raw materials and access to oxygen.

One parameter contributing to the formation of NO is the raw materials. To study the effect of raw materials, a pilot-scale experiment has been done by the Norwegian research organization SINTEF together with the silicon industry in Norway. In this experiment the effect of the carbon materials is studied by varying the carbon source between coal and coke. The purpose was to create cases with a wet charge and a dry charge. In the dry charge the humidity and volatile content is low and in the dry charge the carbon is coal consisting of a high volatile and humidity content. The results of this experiment show that the amount of NO_x is reduced during charging due to an evaporation of water and combustion of volatiles on the charge surface. This effect was larger for the periods with the wet charge because of a larger amount of volatiles and water.

From the pilot-scale experiment there was a relationship between the reduction in NO_x and charging due to the fresh raw materials. At the silicon producing plant Elkem Thamshavn, the furnace is continuously charged automatically. The effect of the charging frequency was studied in an industrial scale experiment by changing the charging frequency from 400 seconds to 2000 seconds. The results of this experiment show that there is an indication that less frequent charging increases the amount of NO_x. In addition to the charging frequency the effect of water was also studied. The result of this study is the same as for the pilot scale experiment, and the conclusion remains that water is an important parameter regarding the reduction of NO during charging.

Sammendrag

I hovedsak er arbeidet som har blitt gjennomført i denne oppgaven relatert til NO_x-utslipp i silisiumsindustrien. Relatert til dette emnet har det blitt gjennomført to experimenter og i begge forsøkene har det vært fokus på effekten av råmaterialer og charging av ovnen. Mekanismen for NO_x-dannelse er tilknyttet forbrenning av SiO som danner oksygen-radikaler. Disse oksygen-radikalene kommer i kontakt med nitrogen fra luft og ved en høy lokal temperatur vil det dannes termisk NO_x

Pilot-skala forsøket ble gjort i samarbeid med norsk silisiumsindustri og forskningsorganisasjonen SINTEF. I forsøket er driftstilstanden på ovnen en konstant, mens parameterne som varieres er karbon og posisjonen for innslipp av luft. Karbon kilden varierer mellom koks og kull. Formålet med å variere karbonkilden er å undersøke hvilken effekt de ulike egenskapene til karbon har på utslipp av NO_x. Resultatene viser at vannmengden og innholdet av flyktige materialer øker under charging samtidig som at utslippet reduseres. Når koks blir brukt som karbon kilde er utslippet større i forhold til om kull er brukt. Denne forskjellen er mest sannsynlig grunnet en mindre mengde med flyktige materialer og vann. En konklusjon som kan dras fra disse resultatene er at vann og flyktige materialer bidrar til å redusere temperaturen på charge-overflaten og dette vil bidra til et mindre utslipp. I tillegg vil flyktige materialer reagere med oksygen under forbrenning, noe som betyr at forbrenningen av SiO gass må konkurrere med forbrenningen av flyktige. Vann kan også inngå i en reaksjon med SiO gass og redusere mengden oksygen radikaler som blir brukt til å danne NO.

I det industrielle forsøket er råmaterialsammensetningen konstant, og variabelen i dette tilfellet var hyppigheten av charging. Bakgrunnen for dette forsøket er å undersøke om en hyppigere charge-frekvens bidrar positivt i forhold til utslipp av NO_x. Når ovnen blir charget sjeldnere vil ovnen få tid til å varmes opp og brenne ned charge-nivået. Ved en generelt høyere temperatur er det forventet at det gjennomsnittlige utslippet vil bli større. Basert på resultatene har det blitt et høyere gjennomsnitt i når ovnen ble charget ved en lavere frekvens, det ble også produsert mer NO_x per støvmengde noe som tilsier at kontinuerlig charging medvirker positivt til utslipp. Et annet resultat fra dette forsøket er at det er observert høye utslipptall ved et lavt vann-nivå, noe som tilsier at vann er relevant med tanke på å redusere utslipp. Dette samsvarer med resultatene fra pilot-skala forsøket.

List of Content

1 Introduction

In 2010 the Gothenburg Protocol set an emission ceiling for NO_x; Europe is going to cut its emissions by 41 % (UNECE). As a consequence of the protocol made in 1999, the Norwegian Climate and Pollution Agency (KLIF) have been cooperating with Norwegian industry with the goal of reducing NO_x. Emissions based on data from the industry have been estimated, and it has been reported that Silicon producers have the highest NO_x-emissions amongst the onshore industry in Norway (Klif).

The term NO_x is a common notion for the two gases NO and NO_2.These gases are formed by the transport industry because of the combustion of fuel. The transport industry has the highest reported emissions of the gas per year (Norske Utslipp, 2012). Other large contributors to the emissions of NO_x are the offshore industry and also agriculture.

When NO_x is emitted to the atmosphere along with SO_x, formation of acid rain might occur. Acid rain is formed when these oxides react with other compounds in the atmosphere like water or oxygen. This reaction in combination with sunlight can form HNO_3, which means that a strong acid can be found in fog or rain (WHO).The acid rain could again lead to a change of pH in water, and disrupt the natural buffer capacity of water. Water could get contaminated with dissolved metals.

With an increase of nitrates in water, eutrophication may occur. A consequence of this is depletion of oxygen in water, which will lead to a reduction of the animals living in water.

Oxidation of NO will form the greenhouse gas N_2O. Along with the other greenhouse gases, N_2O will contribute to global warming (Bireswar & Amitava, 2008).

Another effect of NO_x-emissions is the decomposition of NO_2 producing an oxygen radical in contact with sunlight. This radical will react with oxygen and produce ozone. Also, the decomposition of NO_2 can react and become air particulate matter $PM_{2.5}$, which are particles found in the air (WHO). These particles can be both organic and inorganic. Ozone on ground level is harmful for the health because it can cause asthma attacks

Known health issues because of exposure of the gas can be divided into long-term exposure or short-term exposure (WHO) (Bireswar & Amitava, 2008):

Long-term exposure: People induced to long-term exposure of NO_2 can decrease lung-function. Studies have shown that NO_x also increases the risk for lung cancer in areas where the air pollution is high (Raaschou-Nielsen & Andersen, 2000).

Short-term exposure: As previously mentioned short-term exposure can cause asthma attacks.

Research focusing on the mechanisms of formation of NO_x has been carried out in the PhD work of Nils Eivind Kamfjord, where he looked into the correlation between silica-dust and emission of the gas. He also investigated the effect of furnace design. Although, he has done a lot of work indicating the effect of other parameters such as the effect of raw materials, experiments with raw materials have not been done.

The aim of this study is to investigate how the raw material mixture and charging contributes to NOx-formation in a silicon furnace. The effect of volatiles and water has been studied in a pilot scale furnace. The charging and the charging frequency are the relevant parameters for the industrial scale experiment.

2 Terminology related to the silicon process

The report includes terminology from the silicon process. A list of important keywords used about the silicon process is given in bullet points below (Schei, Tuset, & H.Tveit, 1998):

- ***Arc furnace*** is the name of the furnace used to produce metallurgical grade silicon. In an industrial furnace there are normally three electrodes providing heat, and the power load of the electrodes are normally from 20-40MW.
- ***Charging*** is commonly used for when the furnace is filled with raw materials. In a modern furnace this happens through an automatic feeding system that fills up raw materials in the center of the feeder and around the electrodes. The charging can be done frequently in small batches or one time per hour in bigger batches.
- ***Stoking*** is an operation done by the process operators. In this task the raw materials are distributed throughout the furnace. The purpose of stoking is to fill the gas channels created from consumption of raw materials around the electrode and the the formation of SiO in the crater. This is done by that the operators use a lance to move the raw materials to the wanted location in the furnace.
- ***Crater*** is used to describe where the silicon producing reactions happen. This area consists of molten metal and is found at the tip of the electrodes.
- ***Charge*** is the area of the furnace that consists of raw materials. This area stretches from the top of the furnace to the crater.
- ***Raw materials*** are the materials feed to the furnace. The materials used are quartz that provides the silicon and different carbon materials like woodchips, coke and coal that is used as a reductant.
- ***"Process parameters"*** is often used to describe the different factors that can contribute to that the furnace is operated preferably. By changing raw materials, temperature, stoking pattern, charging or the current of the electrodes the condition of the furnace can change drastically.
- ***"Blows" on the charge surface*** is when the $SiO_{(g)}$ reaches the top of the charge by going through gas channels from the crater. The reacts with oxygen creating silica fume, and the combustion is exothermic creating high temperatures. This is observed as a white light by operators.
- ***SiO/SiO_2*** is used to describe the silica fume that is produced from the process. The structure of this fume is close to the structure of SiO_2, however in reports and calculations both terms are used.

3 Theory

3.1 The Silicon process

Since this project is focused on the silicon industry and more specifically the conditions of the furnaces at Elkem Thamshavn it is natural to go into the silicon process. Fig. 1 describes the different unit processes of the silicon process.

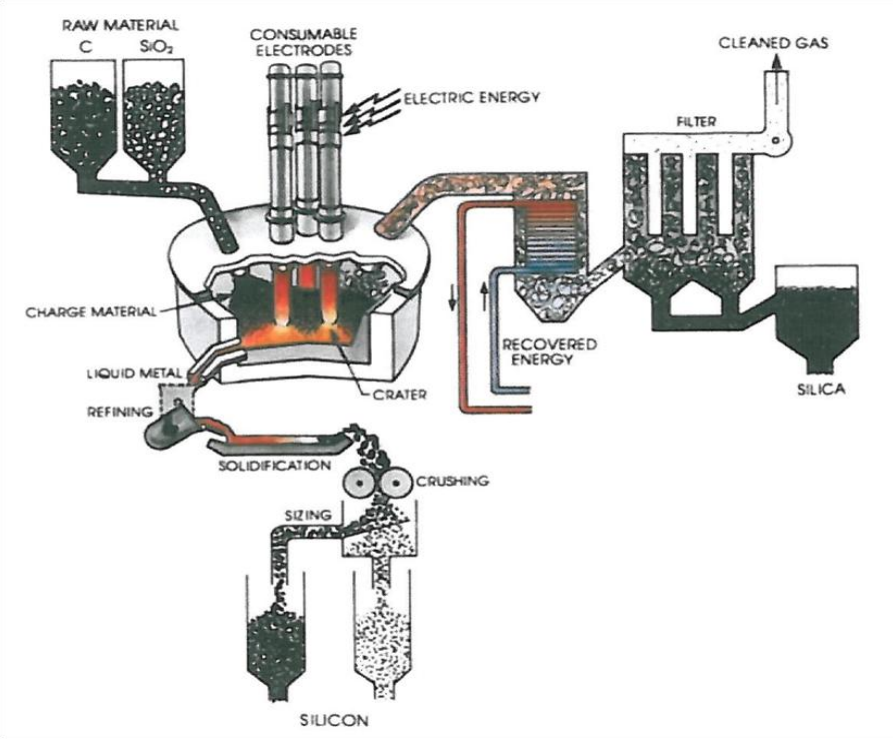

Fig. 3.1: The parameters of the silicon process (Schei, Tuset, & H.Tveit, 1998).

Primarily silicon is produced in a submerged arc furnace as it is shown in Fig. 3.1. Normally in an arc furnace, raw materials (quartz and carbon materials) are charged from the top and the furnace is heated with the help of three graphite electrodes. In a normal medium-sized furnace it is common with a power load of 20-40 MW. Current passes through the electrodes and heats up the crater due to an electrical resistance. The position of the electrode in the furnace is important because it will influence the distribution of the heat. The electrodes heat up the crater to a temperature of about 2000°C. At that temperature the silicon dioxide is reduced to silicon. Carbon materials are used to reduce the silicon dioxide. This overall carbothermic reaction is described by reaction (3.1) below.

$$SiO_2 + 2C = Si\ (l) + 2CO \qquad (3.1)$$

Further the pure silicon will be tapped from a tap hole, which is at the bottom on the furnace. After the molten metal is tapped it will be refined, solidified and then crushed into the final product. Silicon is used in several different products. It is used as an alloying element for the aluminum industry, and the Al-Si alloys are commonly used in the automobile industry. Ferrosilicon is used as an alloying element in the steel industry. In computers and other electrical devices, silicon is often used in semiconductors or circuits that can be found in computer-chips.

As seen from Fig. 3.1 the silicon process produces silica as a by-product. Silica fume is condensed silicon dioxide and it is commonly used as a binder for fiber cement. In the fiber cement the silica will work as a binder that will increase the packing density and make the cement stronger (Elkem).

The modified chemical reaction, which includes the losses of Si units as SiO gas, is given as equation (3.2). As the overall reaction (3.2) shows, the products are molten silicon, silicon oxide gas and carbon oxide gas. A further oxidation of the silicon oxide gas produces silica fume, and this reaction is described later on in the chapter.

$$SiO_2(s) + (1+x)C(s) = xSi(l) + (1-x)SiO(g) + (1+x)CO(g) \quad (3.2)$$

For the overall reaction, *x* is the silicon recovery. The silicon recovery is how much silicon that can be recovered from the process based on how much silicon goes into the furnace and how much silicon goes out of the furnace.

The process can be described by dividing the furnace into two parts: the inner zone and the outer zone. The equilibrium assumptions for these zones the pressure is set as 1 bar. The pressure ratio in the inner zone is $p_{SiO}/p_{co} \approx 2$. The reactions and equilibrium temperatures for the inner and outer zone is given in reaction (3.3) and (3.4) below.

$$3SiO_2 + 2SiC = Si + 4SiO + 2CO, \; T_{eq} = 1811°C \quad (3.3)$$

$$2SiO_2 + 6C = 2SiC + 6CO, \; T_{eq} = 1512°C \quad (3.4)$$

Based on these equilibrium assumptions it is needed 5 SiO_2 to produce 1 Si, this gives a silicon recovery of only 20 %.

In an industrial furnace it is common with a silicon recovery of 80-90 percent. This means in practice that there is a difference between the silicon recovery that is obtained in the industry and that is found by equilibrium conditions. A conclusion of this is that the silicon process is a non-equilibrium process and the result of this is it is not likely to get a silicon yield of 100 % purely based on assuming equilibrium conditions. Primarily, the silicon recovery is so low because SiO(g) produced from the crater evaporates and goes off in the off-gas system. To increase the silicon recovery

the SiO(g) has to react with carbon in the charge, this property of the carbon is called the reactivity of carbon. Including the capture of SiO(g), non-equilibrium assumptions have to be made regarding pressure and temperature to achieve a high silicon recovery.

In fig. 3 a model used to analyze the furnace reactions is shown. The model divides the furnace into two zones: The outer reaction zone and the inner reaction zone. In the outer reaction zone the pre-reactions involving silicon oxide gas is shown. In the inner reaction zone the reaction producing silicon, silicon oxide gas and carbon monoxide is given. The purpose of this model is to get an understanding of the mass- and gas flows that are important in understanding the process. In Fig. 3.2 a silicon recovery of 100 percent is assumed and a mass balance is made so that no SiO(g) goes out of the furnace. This means that all of the SiO(g) is recovered by reacting with carbon and condensation of SiO(g).

By increasing the temperature in the inner zone of the furnace, a lower SiO(g) content of the gas is required to produce silicon. At equilibrium conditions the reaction rate of the SiO(g) producing reactions is low although they are endothermic reactions, which means that the temperature will rise. At 1980°C silicon can be produced at a lower content of SiO(g) in the gas.

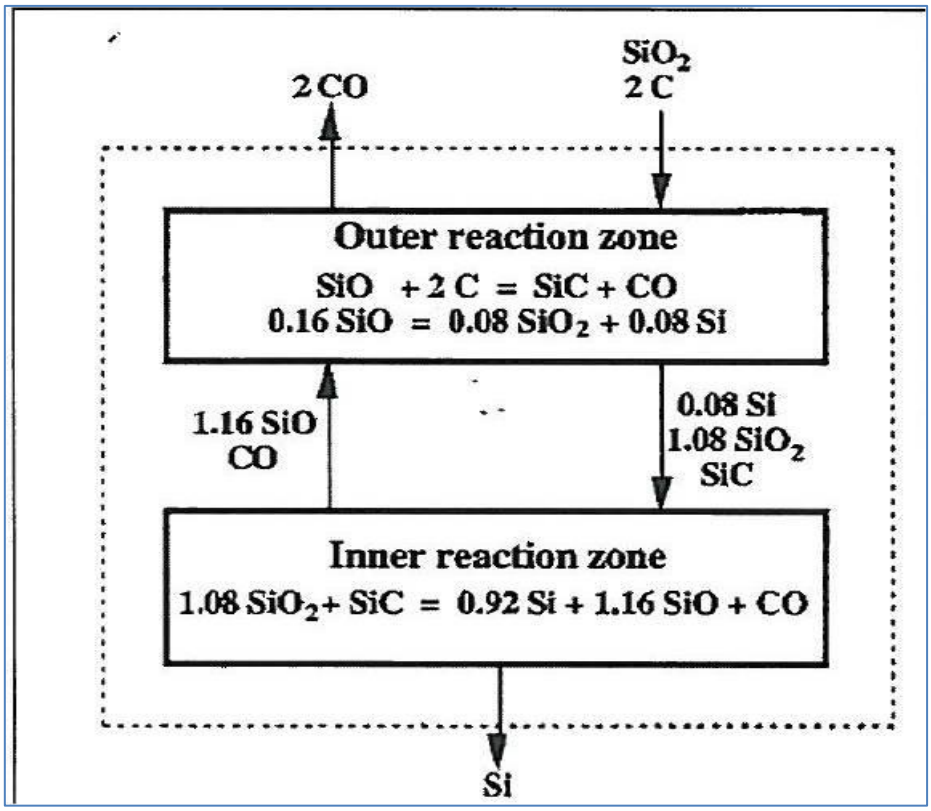

Fig. 3.2: (Schei, Tuset, & H.Tveit, 1998) The process model assuming 100 % silicon yield.

A sketch of the material- and gas flows in a furnace is given by Fig. 3.2. The red arrows in Fig. 3.2 are assumed to be the gas flow of SiO(g), and they go up from the high pressure carbon zone. These gas flows creates channels that can be found along the electrodes and in the between the electrodes. When the SiO(g) comes to the crater it can be seen on the surface as “blows”, which is basically a brighter light.

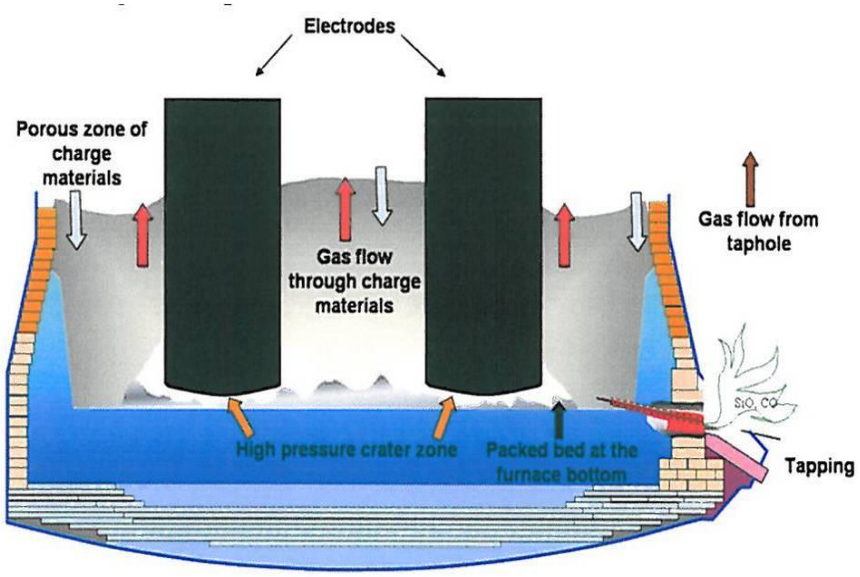

Fig. 3.3: Cross section of the silicon furnace showing the material and gas flow (Tveit & Kadkhodabeigi).

The white arrows in Fig. 3.3 show how the furnace is charged with raw materials. The raw materials in the furnace are commonly called the "charge" of the furnace.

3.1.1 Changing process parameters

Later in the experimental part there will be a description of two experiments. The first experiment is a pilot-scale experiment and the second experiment is an industrial experiment. In both of these experiments there has been a change in process parameters. In later parts of the theory it is described how NO_x can relate to a change in raw materials, charging and stoking. However, it is relevant to see what kind of effect these parameters generally have on the process.

Raw Materials

As previously mentioned, the two raw materials that are essential for the silicon production is quartz and different carbon materials.

Quartz is the raw material that brings silicon to the process. By changing the siliconoxide source, the final product of the process will be influenced. This is because of the quartz contains elements that are more noble than silicon, there will be a reduction of these elements and it will end up in the final product. The thermal properties of quartz could influence the SiO(g) formation, hence influence formation of NO_x. However, the quartz has not been studied in this thesis. The particle size of the quartz might change the gas flow in the charge if the quartz-particles are fines. This is because SiO(g) will go up to the charge from the crater, and by having small particles

the density of the charge will increase and make it difficult for the SiO(g) to get up to the charge. The consequence of this could be that the silicon yield can be affected.

Carbon materials like coke, coal and woodchips will be thoroughly described under the chapter about how the raw materials influence the NO formation. Changing the carbon materials is a more critical change in the silicon process regarding NO formation because it does influence the silicon yield. Both the carbon reactivity and the particle size of the carbon are important parameters in this case. The reactivity of carbon is given as how well the carbon reacts with SiO(g) from the crater. The particle size is important because if the particles are too small they will be taken by the gases with high velocity above the crater and go off in the off-gas system. In this case there will be low control of how much carbon is in the system. The carbon amount in the furnace is might also change the position of the electrodes, which could change the heat distribution. As a conclusion the carbon can change the whole process.

Charging

Charging mainly has the purpose of feeding the furnace with raw materials. This parameter does not change the process directly, but rather influences the top of the charge surface. When the new raw materials are fed to the furnace, the temperature of the materials is around 25°C. This will decrease the temperature of the top of the charge. Heating up the fresh raw materials will also demand some energy, although this depends on the frequency of the charging. If the carbon contains water or other elements that easily evaporates, the first reactions that happens on the charge is that these elements will evaporate.

In the industry there are two ways to charge the furnace: “Continuous” or “Batch”. When the furnace is charged continuous it is normally done by feeding the furnace around every minute. However, the amount of raw materials per feeding is small. This provides a charge surface with an even temperature. This way of charging also prevents the charge from burning down, which creates a high temperature in the charge and also the combustion of SiO(g) to silica fume.

In batch charging the raw materials are fed to the furnace normally one time per hour. In this case the mass of every charging is large, because the furnace needs to be filled with raw materials for another hour of furnace operation. In this case the temperature on top of the charge will be high because the charge is fully heated up and burned down by the time of the next charge-period.

Stoking

During the stoking of the furnace the purpose is to even out the raw materials on top of the charge. Another reason for stoking the furnace is to cover the gas channels that lead to losses of SiO(g). By stoking the furnace often, it is likely that blows to a certain extent will be prevented. The most important effect of stoking is in this case that the gas channels get covered with raw materials because it hinders the combustion of SiO(g).

3.2 NOx formation mechanisms

In processes where combustion takes place, NO_x can be formed by these three mechanisms: Thermal, Fuel and Prompt (De Nevers, 2000).

When there is fuel NO_x, the gas has been formed by combustion of the nitrogen in fuel. Prompt NO_x is formed by an interaction between oxygen and nitrogen in an environment with active hydrocarbons. In a silicon furnace the NO_x will mainly be formed with a combination of high temperature and the presence of nitrogen and oxygen in the air.

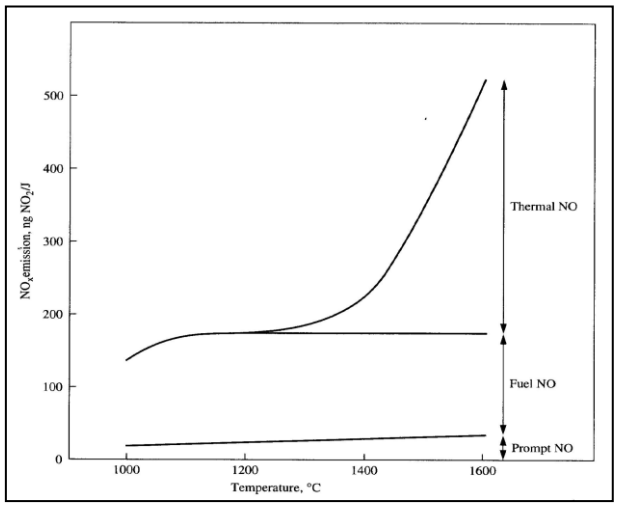

Fig. 3.4: The formation mechanisms and their dependency of temperature (Zeldovich).

Zeldovich mechanism

The principle of thermal NO_x was described by Zeldovich (Zeldovich). This principle states that at high temperatures NO will be formed by radicals of nitrogen and oxygen. As seen from Fig. 3.4, this mechanism is highly dependent on the temperatures reached in the mixture of oxygen and nitrogen in the air.

The Zeldovich mechanism is essentially given by two reactions:

$$O + N_2 = N + NO \qquad (3.5)$$

$N + O_2 = O + NO$ (3.6)

In addition to these two reactions there is an extra reaction called the extended Zeldovich mechanism:

$N + OH = NO + H$ (3.7)

This correlation is stated further by Turns (Turns), which has given the reaction rate coefficients in the Table 3.1 below (Kamfjord).These coefficients show that the reactions are strongly dependent on temperature.

Table 3.1: Given for reactions 3.5, 3.6, 3.7, hence K3.5, K3.6, K3.7. These are the reaction rate coefficients given in [m^3/kmol*s]

Forward rate	Backward rate
K3.5 = $1,8*10^{11}exp(-38370/T)$	K3.5 = $3,1*10^{10}exp(-425/T)$
K3.6 = $1,8*10^{7}exp(-4680/T)$	K3.6 = $3,8*10^{6}exp(-20820/T)$
K3.7= $7,1*10^{10}exp(-450/T)$	K3.7 = $1,7*10^{11}exp(-24560/T)$

$O_2 = 2O$ (3.8)

Looking at the rate of the reactions producing NO_x, the slowest reaction is given by reaction 3.5. Reaction 3.8 is faster than all of the reactions included in the formation of the gas. Kamfjord (Kamfjord) has chosen to use the assumptions by Turns (Turns) in his thesis and as a result of this it has been created en equation to describe the formation of NO given in equation 3.9.

Equation 3.9 states that NO is dependent on temperature in the gas, nitrogen concentration, oxygen concentration and pressure. If NO is to be calculated by this equation the terms has to be defined. First, the reverse equations can be neglected. If the goal is to look at what produces NO gas it can be assumed that the concentration of nitrogen oxide is small, hence the reaction will go forward. The concentrations of nitrogen and oxygen have to be found as well to be included in the equation. [N] is found by assuming steady state, following dN/dt=0. The oxygen reaction (3.8) is defined to be in equilibrium, and as a consequence of this definition the oxygen radicals' concentration can be found.

$$\frac{d[NO]}{dt} = 3.6 \times 10^{11} \times e^{(-\frac{38370}{T})} \times \frac{\sqrt{(K_{eq} \times P)}}{RT} \times [N_2] \times \sqrt{[O_2]} \qquad (3.9)$$

K_{eq} is given as the equilibrium constant for expression 3.9. P is given as the pressure of air, at a value of 1 atm. R is the gas constant (8.3145kJ/mol). The temperature is T. The

concentrations of oxygen and nitrogen are $[O_2]$ and $[N_2]$. There is also a reaction rate coefficient, which is in this expression given as 2*K3= $3.6*10^{11}$ [m^3/kmol*s].

Following, expression 3.9 can be transformed into an equation looking into the NO formation as a function of time. As previously mentioned, the concentrations of oxygen and nitrogen can be considered as steady-state, which means that the content does not change as a function of time. By integrating the equation on the terms of [NO] =0 at t=0, the expression will look like equation 3.10:

$$NO(t) = 3.6 \times 10^{11} \times e^{(-\frac{38370}{T})} \times \frac{\sqrt{(K_{eq} \times P)}}{RT} \times [N_2] \times \sqrt{[O_2]} \times t \quad (3.10)$$

3.3 How does the formation of NO take place in a Silicon furnace?

3.3.1 SiO(g) and O

As previously mentioned, the formation of NO is seen to be dependent on the amount of oxygen radicals at a given temperature. This amount is given when equilibrium between O and O_2 is obtained. However, in the temperature range that is relevant (1133-1563K (Kamfjord)), the Gibbs free energy is positive for reaction (3.10). The consequence of this is that there has to be another source providing oxygen radicals.

Common for both the furnace surface and the tapping area is that silica is produced in both of these areas of the furnace. Silica is produced as a consequence of the combustion of SiO gas. The reaction producing SiO gas takes place in the crater zone and flows up to the surface reacting with carbon or making silica. Further in Kamfjord's work it has been shown that there is coupling between silica fume and formation of NO in Fig. 3.5. Fig. 3.5 is taken from an industrial silicon furnace on the surface.

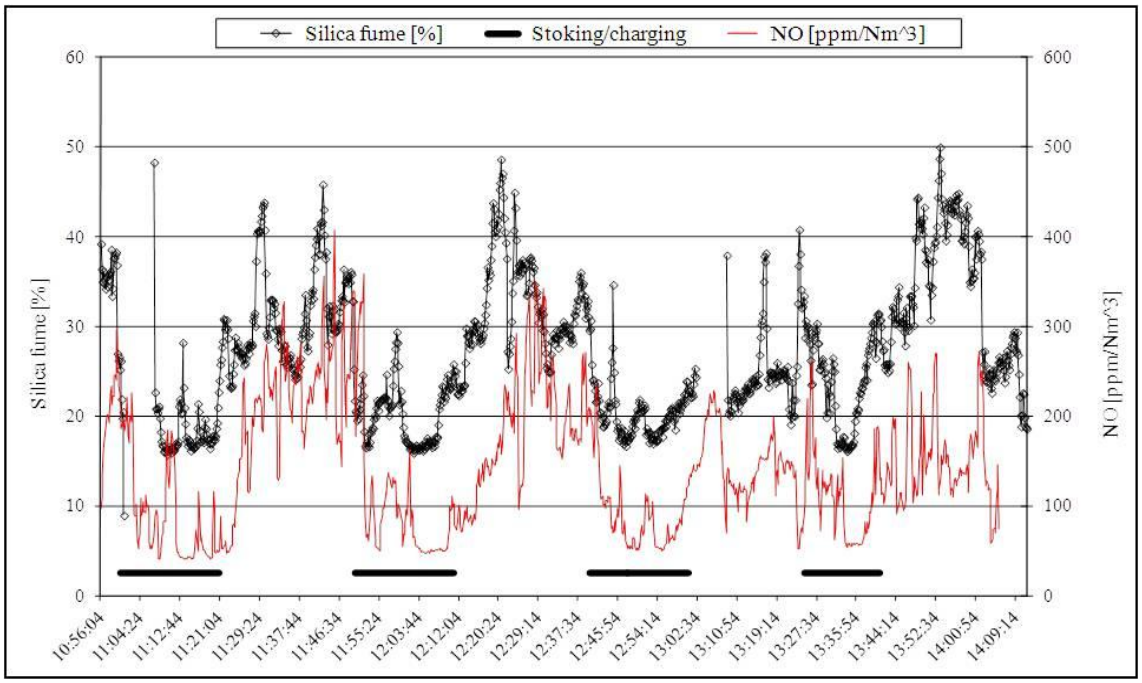

Fig. 3.5: NO and the coherence with silica fume (Kamfjord).

Kamfjord (Kamfjord) used assumptions based on the work of Jachimowski and MacLain (Jachimowski & McLain, 1983) and also Britten and Tong (Britten, Tong, & Westbrook, 1990). In their theories the combustion of silanes is investigated. These studies has shown an estimation of reaction rates primarily for silanes combusted by H_2, but the SiO_2 reactions has been included in the work.

These reactions are given as equation 3.11, 3.12 and 3.13:

$$SiO + O + M = SiO_2 + M \quad (3.11)$$

$$SiO + OH = SiO_2 + H \quad (3.12)$$

$$SiO + O_2 = SiO_2 + O \text{ (radical)} \quad (3.13)$$

In reaction 3.11 the M stands for a third body molecule.

With these three reactions on hand, it is natural to look at reaction (3.13) as a source for oxygen radicals. In industrial furnaces this means that SiO(g) combustion is the primary source generating NO_x. When more SiO(g) is produced, there will be more combustion, which will further lead to more NO. Also the SiO(g) combustion reaction is exothermic, which means it gives off heat. Temperature is also a parameter, which has to be considered in the formation theory.

3.3.2 Formation of NO on the surface of the furnace

As previously mentioned in the chapter about the silicon furnace, silicon monoxide is a product of the reaction that takes place in the crater of the furnace. This gas will flow up to the surface of the furnace and make a gas path either along the crater wall or close to the electrodes (Tranell, Ringdalen, Ostrovski, & Steinmo). When the gas reaches the surface combustion of silicon monoxide and carbon oxide will take place.

The surface of the furnace is defined as the top of the charge, which is the where the furnace is fed with raw materials. The raw materials will include a variation of chemical components in both the quartz and the carbon materials. Volatile materials in the coal/coke will combust, and if there is any water it will evaporate.

Different chemical components with nitrogen content in the raw materials might react to form NO. However, this will not be thermal NO_x, but rather fuel NO_x or prompt NO_x. These reactions will take place when nitrogen reacts with hydrocarbons. Coals that have volatile matters will have amounts of hydrocarbon.

Since there is a correlation between the fume and the NO formation, it is likely that NO is primarily formed thermally. As mentioned the combustion with SiO(g) will give a high temperature needed to form NO, because the reaction is exothermic.

Kamfjord gives a description of what happens after stoking and charging and divides it into two three different stages as given in Fig. 3.6.

At first there is the primary formation mechanism:

- The temperature of the charge will decrease as can be seen in the chapter about charging.
- The decrease in temperature will make the SiO gas condensate and will hinder the SiO(g) from combusting at the furnace surface
- After a while the new materials will heat up and eventually there will be combustion of SiO(g), volatiles and evaporations of water. These reactions will compete for oxygen.
- This phase will primarily have fuel and prompt NO_x formation mechanisms.
- There will be a permeability of raw materials, which will lead to an increase in fume formation.

The second phase is known as the transient time phase:

- Some of the water would have evaporated and some of the volatiles have combusted. This leads to that more of the SiO gas will flow up from the crater and combust. NO formation will in this time will be a mixture between the different formation mechanisms.

The third stage will be the secondary formation:

- When all of the water has evaporated and all of the volatiles have combusted the primary NO formation mechanism will be because of the SiO gas.

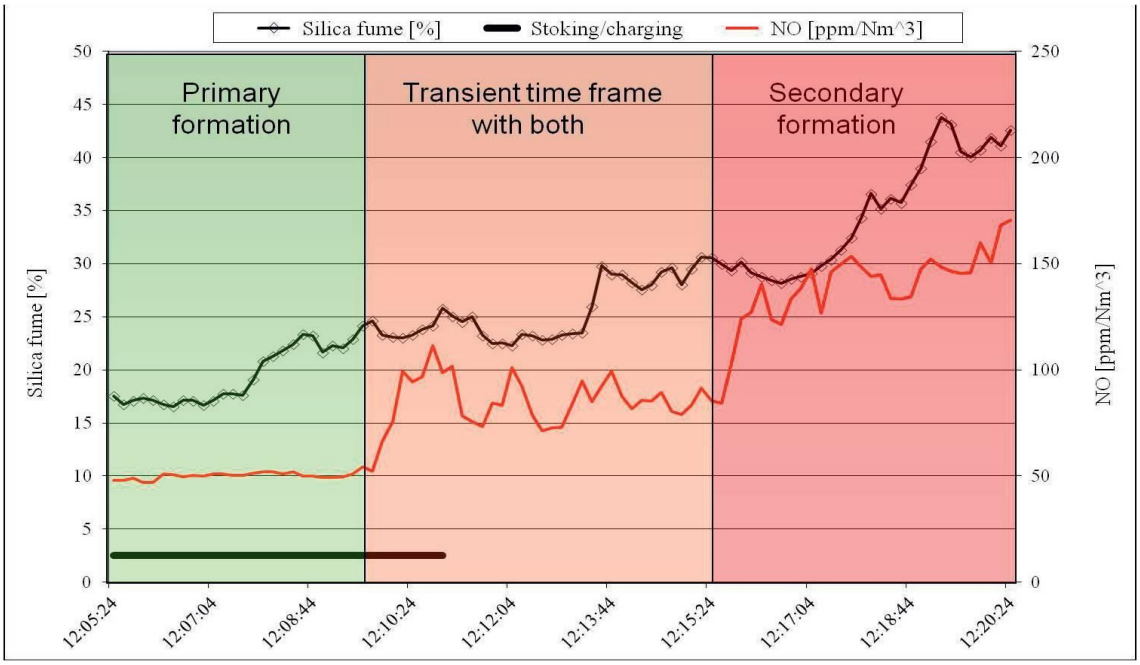

Fig. 3.6: Reactions at the furnace surface by Kamfjord (Kamfjord).

3.3.3 Formation of NO in the tapping area

In comparison to the furnace surface, there are no raw materials potentially contributing to NO formation in the tapping. This means that the only way to form NO is by combustion of SiO(g).

Gases from the crater close to the tapping channel might combust and produce NO_x. During tapping the main purpose is to get the metal to flow easily. Gases, like SiO(g) will escape, combust and create oxygen radical. This radical will react with air and give NO. However, the furnace surface is open, and will have access to unlimited amounts of oxygen. The tapping channel is only open during tapping. If there is produced any NO gas it is not likely to be the main source of emissions in the silicon furnace.

Kamfjord (Kamfjord) has indicated in his work that tapping might be of importance when it comes to the formation of NO because if the metal is not tapped regularly, but

instead creates a pool of metal beneath the electrodes, this molten metal might react and give an increase in SiO(g). The increase in SiO(g) might give an increase in fume, and produce more NO.

3.4 Parameters in the silicon process contributing to NO formation

3.4.1 Charging

Charging is the term for when the furnace surface is fed with new raw materials. The temperature of the raw materials before they are fed to the furnace is around room temperature (25°C). This means that a cold layer of materials will be on top of the charge and will thereby reduce the temperature of the charge. This temperature reduction is described by Kamfjord to drop from 800°C to 400°C. After the reduction the temperature will gradually increase again.

There are two ways to charge; either the furnace can be charged continuously or the furnace can be charged in batches once an hour. When the furnace is charged continuously the charge gets a constant flow of cold raw materials. This is likely to have an effect of the temperature on the charge. When the furnace is charges once an hour, the temperature would have increased and created a higher temperature on the surface. As previously mentioned a local high temperature will have an effect on the formation of NO, and hence there will be a peak in the emissions trends when the furnace has not been charged in a while.

Fig. 3.7 shows what happens when the feeding stopped for about an hour at the plant Elkem Thamshavn. The graph shows a text saying “Peak”, and that peak represents an increase in the emissions of NO_x because the charge level was burned down when there was a lack of new materials on the surface. This plant produces MG-Silicon and micro silica. Normally the feeder in the centre of the furnace has a frequency of around 9 min at Elkem Thamshavn, where as the other feeders around the electrodes has a frequency of 7 minutes. In this case the furnace was not charged, and there was a peak in the emissions measured at the pipe.

.

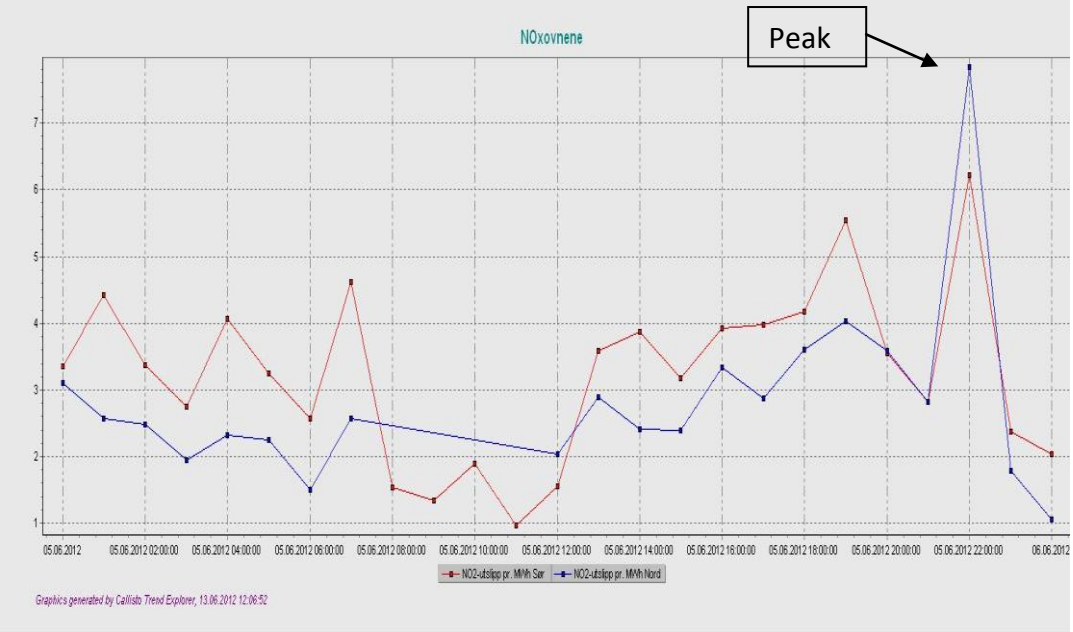

Fig. 3.7: Increase in NO emissions during lack of charging based on data from the system at Elkem Thamshavn.

The same trends has been shown when the charge drops to the crater of the furnace or during batch charging.

3.4.2 Stoking

When the furnace has been fed with new raw materials it is natural to try to even out the raw materials through the furnace, especially if some of the raw materials have aggregated by the furnace walls. The purpose of this is to try reducing SiO(g) losses by filling gas channels of SiO(g) going up from the crater of the furnace, and to get as much of the materials to take place in the reaction to SiC.

The frequency of stoking will have an effect on the formation of NO gas mainly because it will fill the gas channels, such that it hinders the combustion of SiO(g) on the surface of the furnace. Instead of combusting on the surface there will be a condensation of SiO(g) further down in the charge. In addition it can keep the temperature of the surface even. As seen in the chapter about charging the temperature will drop when new raw materials are charged on the surface. Stoking will also contribute to this effect when raw materials are distributed throughout the furnace.

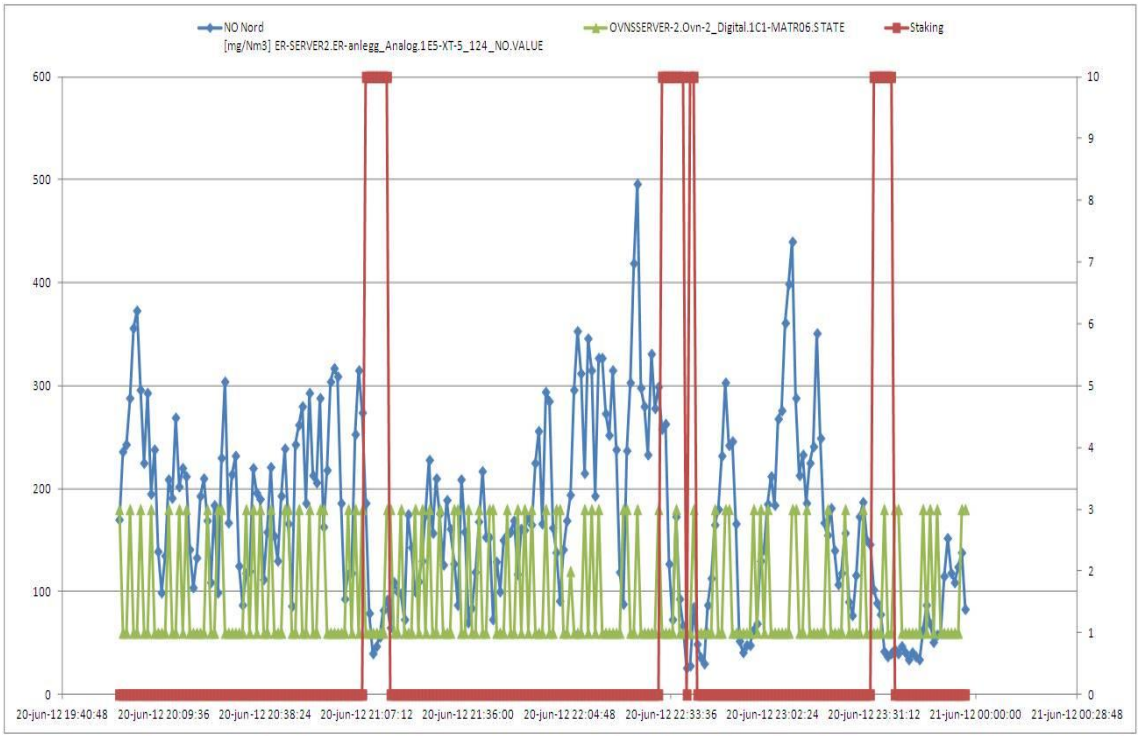

Fig. 3.8: Stoking, charging and the NO emissions from "furnace 2" at Elkem Thamshavn (ELKEM (Åslaug Grøvlen)).

Fig. 3.8 is made from data taken at Elkem Thamshavn made by Åslaug Grøvlen (ELKEM (Åslaug Grøvlen)). This shows the frequency of the feeder in the center of the furnace, and also what happens during stoking. As can be seen from the figure the stoking tends to decrease the emissions of NO, likely because it fills up the gas channels. The graph for the feeders are marked with green and shows that if the frequency is higher, the measured NO tends to be low and there is an increase in emissions when there is a longer period between the feeders.

3.4.3 Raw Materials

Quartz and carbon materials like coke, coal, charcoal and woodchips are used in the production of metallurgical grade silicon. It is natural to investigate the effect the raw material/reductant mix has on the emissions, primarily because it has an effect on the yield of the silicon, which means it is also likely to have an effect on the fume produced.

The carbonaceous raw materials can contain volatiles, which are C_xH_y materials. Also, the raw materials may include water, which means that water will also evaporate on the surface. Kamfjord (Kamfjord) has mentioned that the surface has a different environment than the tapping area primarily because of these additional matters. Combustion of volatiles and water will compete with the combustion reaction of SiO(g) at the surface, and thereby reduce the emissions of NO.

However, this will again depend on the carbon materials. There is a difference in how much water and volatiles the carbon materials will contain. The reactivity of the carbon materials is also highly important for the process seeing that it is the ability the carbon has to react with SiO gas from the crater and hence the amount of SiO(g) that will pass un-reacted through the furnace.

There have been several studies on the effect of humidity on emissions. Stuart Neill and Guo (Guo, Neill, & Smallwood, 2008) investigated the effect of addition of water regarding NO formation in a counter flow CH_4/air premixed flames. This was done by a numerical simulation using a chemical reaction mechanism by GRI-Mech 3.0. The conclusion to this work was that an addition of water reduces the temperature of the flame and following there will be a reduction of NO formation. The study also shows that the NO formation can be reduced by a chemical effect that is due to that the water addition increases the production of OH-radicals instead of O and H.

A study done by Bhargava and Colket (Bhargava, Sowa, Casleton, & Maloney, 2000) has showed the effect of humidity when looking at the combustion of air in premixed flames in a humid air turbine. They found that the steam tends to lower the concentration of oxygen atoms and instead found an increase in the OH-atom concentration. Also, the equilibrium temperature decreased. All of these factors will decrease the formation of NO.

Another parameter that can contribute to a change in silicon yield is the size of the raw materials. The carbon material particle size varies from 1mm to 30mm. It is important to notice that the specific surface decreases when the particle size increases. Also if the particles are too small they may be carried out of the process by high velocity gas flows. This might change the carbon content of the process. Particle size can also change the density of the charge. The process is dependent on the gas flow of SiO to react with carbon in the charge, and the gas must be able to flow through the charge to avoid an increase in pressure below the charge surface.

3.4.3.1 Properties of different carbon materials (Schei, Tuset, & H.Tveit, 1998).

Charcoal is characterized by having a high carbon reactivity and high moisture content because it is made out of wood. Charcoal also has a high fixed carbon content of around 46 %, which is lower than for coal and coke. Another property is the low volatile content. Volatiles give the process extra chemical energy and will increase the energy in the off-gas system because the volatiles will be burned at the surface.

Coke is made out of coal pyrolysed under CO. This is done so that the coal will lose its volatiles and give a high amount of fixed carbon (around 75 %) that is important in the process. *Coal* has a fixed carbon content of around 51 %, and has a high amount of volatiles. The moisture and ash level is low for both these materials.

Woodchips has a low fixed carbon content of around 12 %. However these particles are used to segregate the carbon and quartz in the furnace. Without the woodchips there might be a dense charge, and it is preferred that the charge gives possibilities of gas flow. The woodchips also have a high volatile content and moisture content. Moisture has to be evaporated when fed in the charge.

The particle size of the carbon material is important. Air is used to cool down gases above the furnace surface, and this air is also important in making the gases combust. Because of inlet of air there will be high gas velocities carrying away carbon particles to the gas outlet. The result of this will be a reduction of carbon in the charge.

3.4.4 Design

Another important parameter is the design of the furnace and the off-gas system. As seen before in the chapter about formation mechanisms the inlet of air and the temperature is of importance when NO is formed.

Kamfjord (Kamfjord) did experiments in his work investigating the supply of air and the air flow with a pilot scale furnace. His conclusions of these experiments were that if the inlet of air is close to the charge surface, there will be higher NO emissions than if the inlet of air would be closer to the off-gas channels. Kamfjord also concluded that if the amount of air was decreased there was more NO produced, because there will be less cooling effect from the oxygen. This indicates that also the velocity of the gas in the hood of the furnace will have an impact on the formation of NO. Further it can be stated that a low velocity of the gases in the hood of the furnace will increase the time where the gases can be heated. It will be a general increase in temperature in the furnace, which will give an environment more likely to produce NO.

3.5 Parameters important in this study

Now there has been a general overview of the different parameters in the silicon furnace contributing to the formation of NO gas. In this study the parameters raw materials and design will be investigated. Elkem Thamshavn had a design change in furnace 2 in 2010, and the effect of this design change could have changed the gas flow velocities on the surface. This change in gas flow on the surface could have decreased the temperature in the specific region of the furnace, and could have had an effect. The study regarding the raw materials is due to a change in the carbon materials and could have affected both of the furnaces.

The parameters that could affect the NO_x formation mechanisms are summarized below:

- Temperature change at the surface of the furnace due to a change in gas flow velocities because of the openings in the wall.

- The effect of coal fines in the carbon mixture.
- The effect of change in coal particle size on the emissions.

Elkem Thamshavn

At the plant they have two furnaces: Furnace 1 and Furnace 2. Furnace 2 is the biggest furnace and produces around 80 tons of metal per day. Furnace 1 is somewhat smaller with a production of around 50 tons per day. Another difference is that furnace 1 has a smaller geometry than furnace 2. There is also a design difference, where furnace 2 has two gas outlets and furnace 1 has one gas outlet. Normally furnace 2 is used for combined operations, where it produces both silicon and the fine micro silica. Furnace 1 is primarily used for production of silicon and normally has a higher silicon yield than furnace.

4 Experimental

There are two experiments studied in this report. The first study is done based on the results of a pilot-scale experiment administrated by SINTEF, which is a Norwegian research organization. The other experiment is done at the silicon production plant Elkem Thamshavn. This experiment is done to relate results from the pilot-scale experiment and those from an industrial plant. Both of the experiments will be described in this chapter.

4.1 Measurement equipment and design on a pilot scale furnace (SINTEF).

In order to do controlled experiments, NO was also investigated in a 440 kVA pilot scale furnace as an experiment done by SINTEF cooperating with the industrial silicon producers. This furnace is set up such that inlet of air can be controlled and also controlled variations of raw materials (Olsen, Solheim, Panjwani, & Andersson, 2013).

4.1.1 The pilot-scale furnace.

Fig. 4.1 shows a sketch of the pilot scale furnace from Kamfjords thesis (Kamfjord). The hood of the furnace is made with two rings; upper and lower. The purpose of these rings is to control the inlet of air and also where the air comes from. These rings are adjustable and contain fifty holes on the lower part and fifty holes on the upper part. The meaning of this is that the gas flows on the charge furnace can be controlled. The diameter of these rings is 3.5 cm.

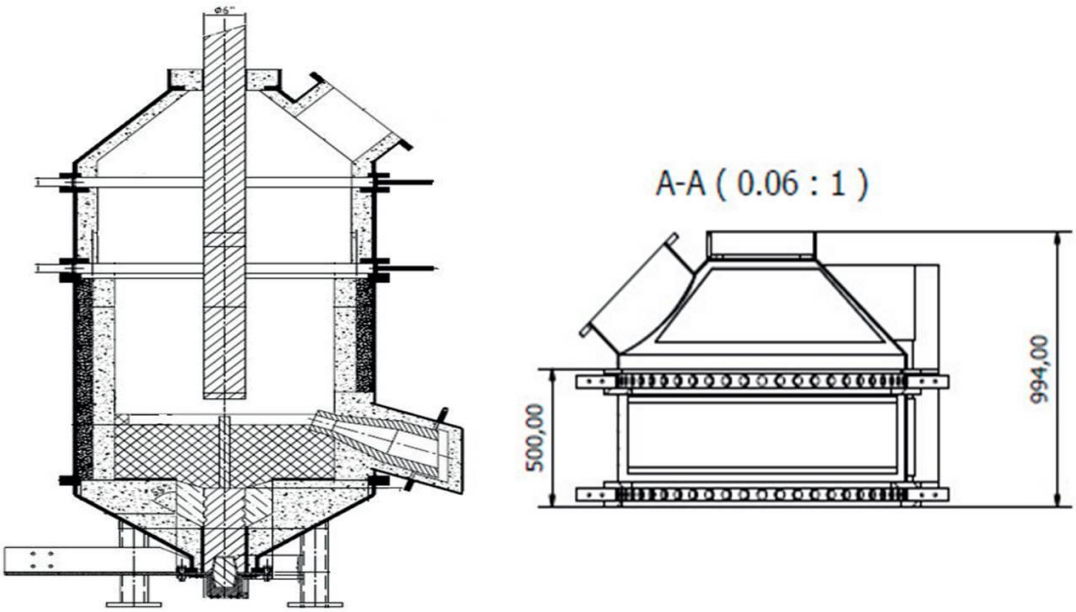

Fig. 4.1: Pilot scale furnace (Kamfjord).

The lower opening is close to the charge and is approximately 15 cm above the charge, where as the upper ring is 65 cm above the charge. There are also hatches placed on each side of the hood so that there is a possibility to stoke and charge the furnace.

4.1.2 Hypothesis

The goal of this experiment is to investigate the effect of charging and stoking. More specific the furnace is charged with carbon materials where the amount of volatiles and water is varying. Listed below are some hypotheses that will be investigated further.

- Carbon materials with volatiles will have an effect on the formation of NO.
- Water will slow down the formation of NO.

4.1.3 Experimental set-up

The furnace started Monday 23.10, and after two days the furnace was ready to tap metal on Wednesday 25.10. The experimental set-up is given below in Table 4.1. It is important to notice that the furnace was stoked and charged between tapping based on operational matters like temperature and gas blows from the crater.

Table 4.1: The experimental matrix. Tap nr is given as how many times the furnace was tapped. Sats is given as the combination of raw materials put into the furnace during charging. The meaning of wet/dry is whether or not the carbon materials contain volatiles/humidity. V is for volatiles and T stands for dry carbon materials. The term upper/lower is based on which of the rings in the hood that is kept open.

Tapp nr	Run	Sats	Wet/dry (Carbonmaterials)	False Air inlet Upper/Lower Open
1	1	7	V	U
2	2	8+9	V	L
3	3	5+6	T	L
4	4	6+10	T	U
5	5	11	V	L
6	6	10	T	L
7	7	13	V	U
8	8	14	T	U
9	9	15	V	U
10	10	16	T	U
11	11	17	V	L
12	12	18	T	L
13	13	19	V	U

As Table 4.1 shows the furnace was tapped thirteen times. After every tapping the furnace was charged with a new type of carbon material. This means that the amount and composition of quartz was kept constant. As can be seen from the table the composition of the carbon materials varied between wet and dry. With wet and dry it is referred to the amount of humidity and volatiles that can be found in the carbon. The terms “wet” and “dry” carbon will be explained further in the experimental chapter.

Because a part of this study was to examine the effect of the inlet of air on the emissions, the rings described earlier in the chapter varied between upper and lower.

As an example in tap 1 the upper rings were kept open. The effect of the rings will not be studied in detail in this thesis, because the raw materials and the charging will have the primary focus.

In Table 4.2 the experimental set-up is given based on the composition of the raw materials compared to table 1 that gave the general set-up. Here it can be seen that the silicon yield, the fix carbon and the quartz composition is expected to be constant during the experiment. The variation in carbon is whether or not coal or coke is fed to the furnace.

Table 4.2: Experimental set-up based on composition of raw materials.

Run	Ring open	Type	Fix C	Quartz	Coke	Woodchips	Coal	Expected Si-yield	Water content
1	Upper	Wet	98 %	25		6,77	16,93	96 %	4,35
2	Lower	Wet	98 %	25		6,77	16,93	96 %	4,35
3	Lower	Dry	98 %	25	9,65	4,9		96 %	1,15
4	Upper	Dry	98 %	25	9,65	4,9		96 %	1,15
5	Lower	Wet	98 %	25		6,77	16,93	96 %	4,35
6	Lower	Dry	98 %	25	9,65	4,9		96 %	1,15
7	Upper	Wet	98 %	25		6,77	16,93	96 %	4,35
8	Upper	Dry	98 %	25	9,65	4,9		96 %	1,15
9	Upper	Wet	98 %	25		6,77	16,93	96 %	4,35
10	Upper	Dry	98 %	25	9,65	4,9		96 %	1,15
11	Lower	Wet	98 %	25		6,77	16,93	96 %	4,35
12	Lower	Dry	98 %	25	9,65	4,9		96 %	1,15
13	Upper	Wet	98 %	25		6,77	16,93	96 %	4,35

Following, in Fig. 4.2 the composition of the carbon material is shown. For the dry carbon, coke and woodchips with a low humidity and volatile content is used. As for the wet carbon, coal and woodchips have a higher content of volatiles and humidity.

Dry Carbon	Wet Carbon
Coke 0.97% Humidity 5.91% Volatiles	Coal 8.9% Humidity 38.9% Volatiles
Woodchips 5.6% Humidity 72.9% Volatiles	Woodchips 42.1% Humidity 72.9% Volatiles

Fig. 4.2: The composition of dry and wet carbon.

4.1.4 Measurement in the off-gas system.

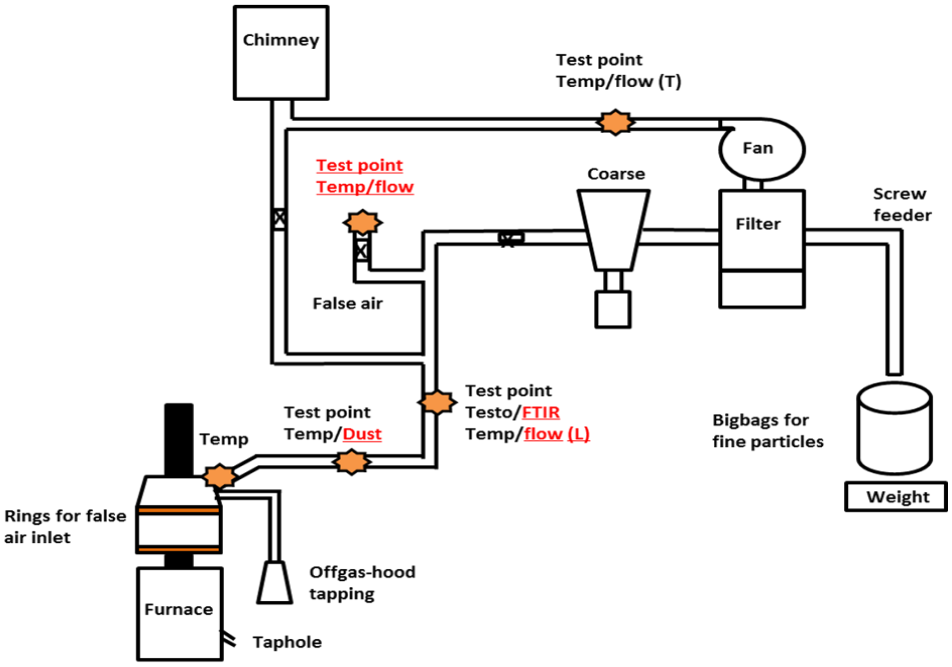

Fig. 4.3 The off-gas system. This figure shows where the measurement devices are places. The most important devices for my thesis are FTIR (FTIR), TESTO (TESTO, 2012) and NEO (NEO MONITORS).

Fig. 4.3 shows the off-gas system of the furnace and where all the measurement devices are placed. The devices that are relevant for this purpose are the devices related to the gas and emissions. However, process parameters and also the

temperature give information about how the furnace is operated, which is needed to understand the results.

Measurements done regarding the operational factors of the furnace were done manually by the operators where they wrote the information down or logged it directly from the furnace. Examples of operational factors could be the time when the furnace was charged, stoked, tapped or general comments about how the furnace is running.

Primarily the NO in the off-gas system was measured by the TESTO 350XL (TESTO, 2012)(see Appendix A.3). This equipment measures NO_x as a sum of NO and NO_2. Also measurements for temperatures and CO can be done with the TESTO 350XL. NO is given as ppm and has a range from 0 ppm to 39.9 ppm. If the value if higher than this given range only 5 % of the measured value is given until the levels of NO reaches 300 ppm. The TESTO 350XL has an electrochemical cell for NO with a chosen ppm range that is put into the equipment. If the range is higher the cell can be changed to a cell with a different range.

The dust was measured by weighing the dust after each tapping, and also with the NEO LASERDUST MP Monitors (NEO MONITORS) (See Appendix A.2). The NEO LASERDUST is a device measuring the fume by sending a light through the channel and the monitor measures the percentage of light that is lost. The device is logging data every second, but this can be adjusted to a different scale. The NEO LASERDUST measured either as percentage of light that is lost or mg/Nm^3.

The FTIR (FTIR) (see Appendix A.4) is used for measuring water, CO, H_2O, SO_2 and other gases. This equipment works in such a way that air is sucked in through a filter, gets analyzed and then the air get blown out after the analysis. During the analysis of the gases a beam of infra-red light is sent toward the gas-sample. Based on how the different gases absorb this light a value for the different gases is given. The device is connected to a computer used for logging the data from the analysis. The data is analyzed every 55 seconds, but might have certain delays that will give a variation in time.

Tapped metal from the furnace was also weighed and a silicon yield is calculated based on silicon that goes into the furnace and silicon that goes out of the furnace.

4.1.5 Silica particles

During each tapping, silica powder was collected and the weight of the powder was measured. In addition a sample of the powder from each tap was taken. There was a change in carbon materials in every other tap, where the furnace was charged with either charcoal or coke. Because of the different characteristics of the carbon materials

it is likely that it would have had an impact on the silica produced. In order to study this powder the particle size and the type of impurities must be studied in detail.

BET-method

Samples from each tap were measured with the BET-method. The BET-method is a short name for the Brunauer-Emmett-Teller-method and is a theory found first by the authors Brunauer, Emmett and Teller (Fagerlund). The method is in this case is used to find the specific surface area of silica particles taken from the pilot-scale furnace.

The theory behind this method is based on the absorption of gases from the surface of the particle. When the particle is in an environment with a gas under equilibrium conditions, a certain temperature and at a relative vapor pressure, the particle will absorb some of the gas. How much the particle absorbs depends on the relative vapor pressure and also the surface of the particle. An absorption isotherm is therefore the correlation between relative vapor pressure and the amount of gas that the particle has absorbed at a constant temperature.

These absorption isotherms are the key for finding the specific surface area of the particle. By using a dynamic BET-device the isotherms will be found and thus the surface area will be given. Before the isotherms can be measured the particles are placed in a measurement bulb. The bulb has to be weighed before and after the sample is filled up in the glass bulb. After the weighing the sample, the sample has to be dried for a day to remove any moisture from the sample. The sample is dried for almost a day at a temperature of 250°C. After the sample is dried it is weighed again so that the accurate sample weight can be found. Following, the sample is placed on the device where it degassed to remove any gas the surface of the particles and the sample is filled with nitrogen. Isotherms are calculated based on the amount of gas that is absorbed by the silica particles. Based on the weight of the sample and also the relative vapor pressure the specific surface area is calculated. An example of the results and the software used to get the surface area is given in Appendix 5.

4.1.6 Data processing

Because of the different equipment that is used for the pilot-scale furnace, most of the work is in analyzing and processing the data. In this process there are certain factors that can be crucial to the results. Dmitry Slizovskiy, a NTNU postdoctoral student has done most of the data processing. He also worked with validating the data. In such a complex process there were some periods in the experiment that was influenced by the open tapping hood or problems with the measurement devices.

As mentioned before devices such as the FTIR and TESTO were used for measuring several parameters such as NO, water, CO and SO_2. The NEO LASERDUST was used for

measuring the silica fume. However, these devices were logging at different times. The consequence of this is that the data has been difficult to compare for further studies. Some bullet points are given below to show what has been the case:

- The TESTO measured data every five seconds measuring in ppm.
- The FTIR measured data every fiftyfive seconds, however sometimes the time difference would be fiftytwo or fiftythree. These data have been interpolated so that it gives data every five seconds based on the linear interpolation. FTIR measures gas in volume percent or in ppm.
- The NEO LASERDUST logged data also every five seconds and measures the dust as mg/Nm^3. Further the data was transformed into volume percent. These measurements give the amount of silica going through the off-gas system. The amount of silica was also weighed between every tap. Comparing these values the amount of dust was different for every tap and to get the correct data the dust concentration was normalized based on the weight of the dust.

When the time scale was corrected the data was put together. Further the data was ready to be analyzed.

A parameter that has to be taken into consideration when looking at the results is the open tapping hood. The hood is supposed to be open during tapping, but then close then the furnace runs normally. The mechanism did not work correctly and at some points during the experiment the tapping hood was actually open. False air coming from this opening could have influenced the results. Fig. 4.4 shows how the tapping hood with 50 mm during the experiment

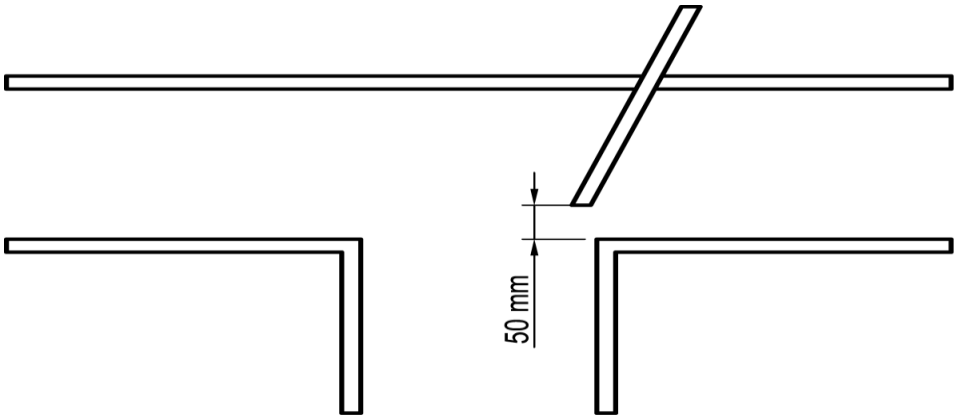

Fig. 4.4: Open tapping hood

As a conclusion of the data processing, Fig. 4.5 shows the data that is valid to use in a further analysis. The dust measurements were only working between 22 hours into the

experiment until 32 hours into the experiment. During the time the dust was being measured there was also a time when the tapping hood was partly open.

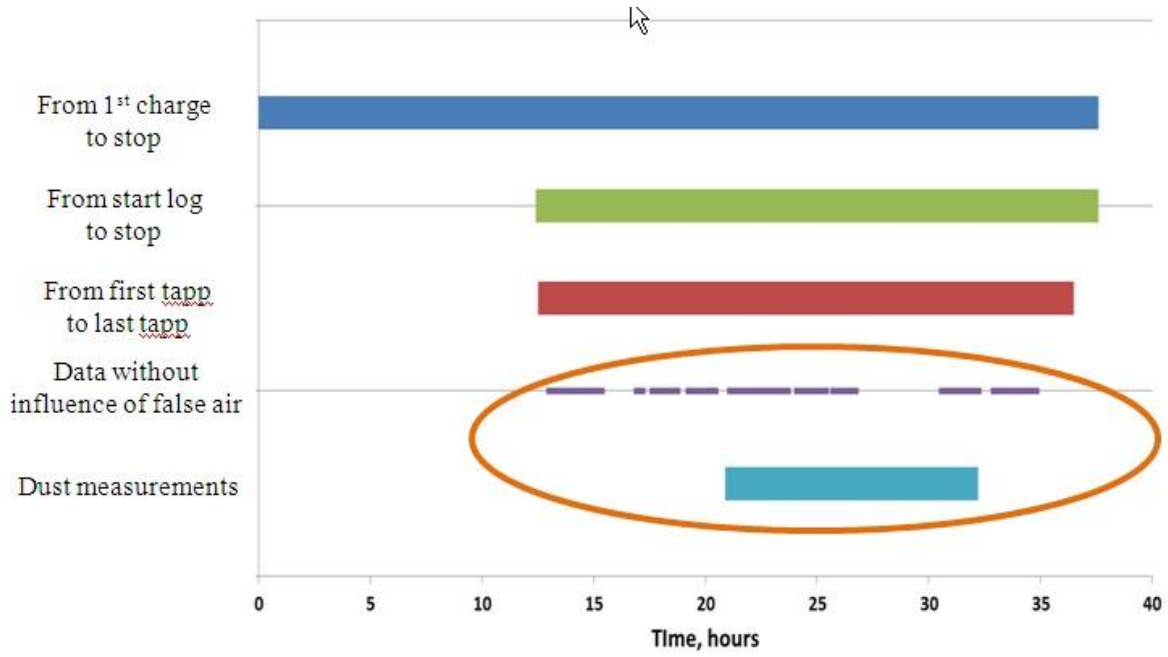

Fig. 4.5: The complete data set and the time that is valid for analysis.

From Fig. 4.5 there are some conclusions to which tapping runs/periods that can be used as results:

- Tap 2, 4, 5, 6, 7, 8, 11 and 12 are good periods to use for further analysis
- Tap 1, 3, 9, 10 and 13 are not good to use for analysis because the results might have been influence by false air from the open tapping hood.

4.2 Industrial Scale Experiment at Elkem Thamshavn.

As a result of the pilot scale experiment, an industrial scale experiment was planned. The pilot scale experiment is going to give information about the effect of raw materials, inlet of oxygen and the effect of water. However, the experiment does not take account for another important parameter which is the charging of the furnace. By doing an experiment where the frequency of the feeders is decreased, the effect of batch-charging versus continuous charging can be studied on behalf of the emissions.

As mentioned in the theoretical part of the thesis, the furnace is charged every 9 minutes. However, the frequency can be changed and set to other values. During these experiments the furnace will be set to around 7 minutes. The meaning of the term cycle time is that the feeder goes through 6 positions in 7 minutes, which means that the center feeder actually will charge every minute. If the cycle time is 15 minutes, the center will be charged every 2.5 minutes.

By provoking the furnace with a change in charging frequency there is a possibility of getting a reaction from the furnace that can change the NO_x emissions. The feeder in the center of the furnace will most likely have the biggest impact on the emissions and is therefore important concerning the experimental set-up; if the furnace does not respond to a less frequent charging pattern, then the other feeders will most certainly not influence the emissions.

As a summary, the goal of this experiment is to answer the questions below:

- Will a small change in the frequency of the feeders have an impact on the emissions?
- If the feeders have an effect, how much will the continuous charging improve the formation of NO in a furnace?

The experimental set-up will therefore consist of changing the charging-rate to 3000 seconds instead of 400 seconds, and to take certain conditions to account the furnace will be charged at this rate for 2-4 hours depending on how the furnace can tolerate the change. Every batch is approximately 150 kg, and it is assumed the furnace can tolerate five times bigger batch than this, which will give a cycle time of 2000 seconds. Table 4.3 below summarizes the cycle times.

Table 4.3: This table gives the cycle time and the charging rate. The cycle time is the time the feeder needs to get from one position to the same position at the new cycle. Charging rate is how often the furnace is charged from one feeder.

Cycle time (s)	Charging rate (s)
400 (normal)	67
1000	167
2000	333
3000	500
4000	667

Following, there will be done experiments with the other feeders if the center feeder has an effect on the results. Also, if a trend can't be found, this experiment has to be done over several days to see if the furnace conditions might have impacted the results. This experiment will be summarized later on in this chapter; however a quick explanation of the feeders is needed to understand the experiment.

Fig. 4.6 shows the feeders have been divided into where they are placed in the furnace. Electrode 1, 2 and 3 each is surrounded by two feeders. Then there is a feeder in the middle, which is the most dominating feeder.

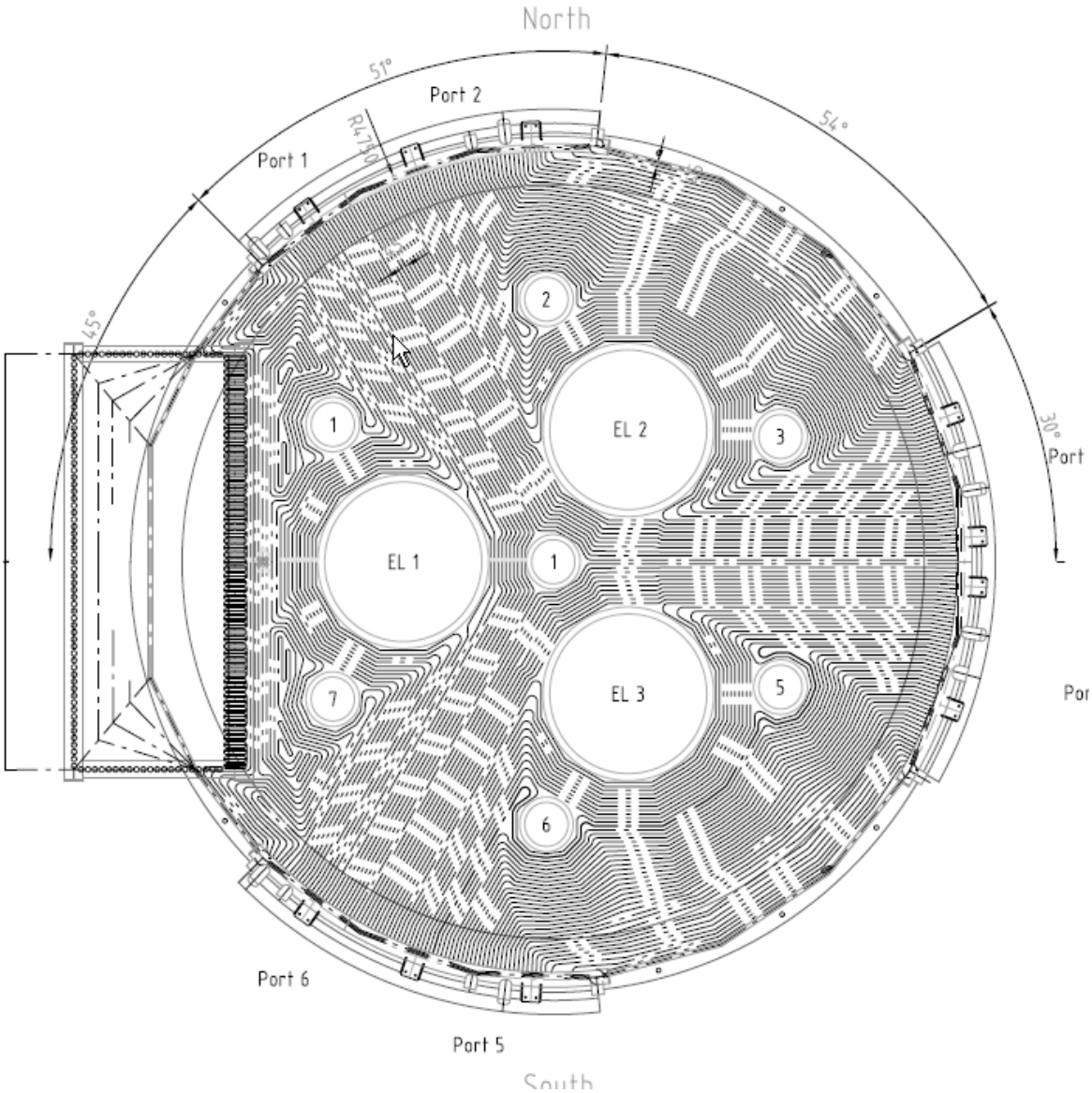

Fig. 4.6: This figure shows the electrodes and the feeders surrounding the electrodes. The feeder in the center is marked as 1, and is the feeder with most impact.

4.2.1 Experimental Set-Up

The consequences of having a low frequency of the feeders can be fatal for the furnace because of a massive temperature increase and the furnace is not charged with large batches of raw materials. The plan for this experiment is put up in Table 4.4. From this table it is shown three experiments. The first experiment is when both the center feeder and the other feeders have a cycle time of 2000 seconds. In the second experiment the center feeder will have a higher cycle time whereas the cycle time of the other feeders are kept normal. As for the third experiment the cycle time of the center feeder will be kept normal and the other feeders will have a higher frequency.

Table 4.4: Experimental set-up summarized in this table. Position gives the area where the feeder is, column two is the description of the values and the value-column gives the values of how the furnace is charges. Cycle time is how long the feeder used to go from one position to the same position of the cycle. Seeing there are six positions it takes the feeder 400 seconds to go from one position to the same position in the cycle.

Position	Description	Value (seconds)
Center	Cycle time center	2000
	Feeding time	10
Feeders around electrodes	Cycle time other feeders	2000
Electrode 1	Feeding time electrode 1	10
Electrode 2	Feeding time electrode 2	10
Electrode 3	Feeding time electrode 3	10

By changing the cycle time, there must also be a change in how long the feeders will charge. Normally the feeding time is around 3 seconds, but since the cycle time is five times bigger the feeding time will also have to be 5 times bigger.

4.2.2 Equipment

Measurements that are relevant for this report are; the temperature of the off-gas, the gas flow, NO gas and the power of the furnace. The fume is registered before the filter. The weight of the fume will be registered at the filter if such data is to be used.

The volume of the gas is done by calculations that are based on the gas velocity and temperature at a certain location in the system. In this case that is also measured in the chimney at the same location as the NEO LASERGAS II SP. To summarize where the equipment is found look at Table 4.5.

Table 4.5: The measurement devices at Elkem Thamshavn.

Measuring	Reason	Placement
NO2/NO [mg/Nm^3]	Main parameter for analyzing the results	Chimney
Flow [Nm^3/s]	The total gas flow out of the chimney. If the gas flow is little but the concentration of NO is high the results might be misunderstood when analyzing them.	Chimney
Silicon yield Si(metal)/Si(quartz) Si(metal)/Si(Silica)	Silicon yield says something about the condition of the furnace. Also it will give an indication of the silica produced from the furnace.	
Dust %	The amount of dust correlates with emission of NO	Off-gas system before filter
Power load [MWh]	Condition of the furnace	

4.2.2.1 NEO LASERDUST/NEO LASERGAS

Elkem Thamshavn already has installed both the NEO LASERDUST (NEO MONITORS) and the NEO LASERGAS (NEO MONITORS) (see appendix). Both of these devices log every second at the plant. The principle of this equipment is that is sends a laser-beam through the pipe, where it gets absorbed and gives the values of the gas. The data from the NEO LASERGAS is gives as mg/Nm^3 and the data given from the NEO LASERDUST is given as the percent of light transmitted. The inverse values from the NEO LASERDUST give the percent of dust. Fig. 4.7 shows where the measurement devices are located.

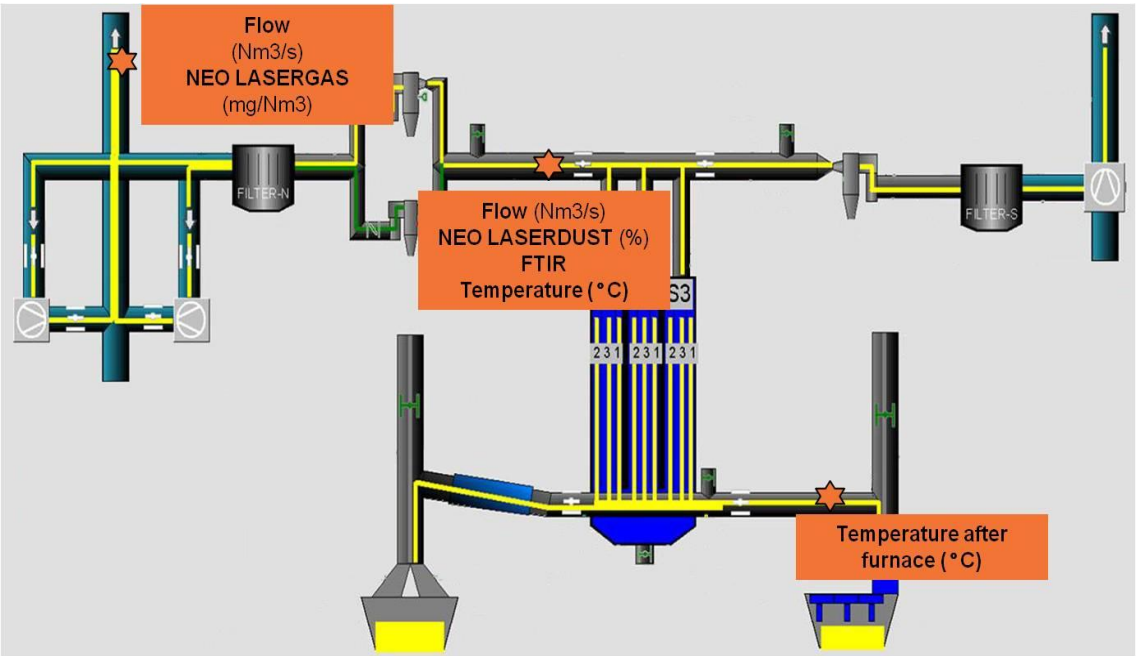

Fig. 4.7: This shows an overview of the furnace and where the measurement devices are located.

4.2.2.2 FTIR (FTIR)

There was placed a FTIR-device before the filter (appendix A.4). This location is close to the flow measurement and also the dust measurement. The FTIR is described earlier in the part about the pilot-scale experiment. In this area of the off-gas system the temperature is around 180°C, which is within the temperature range that the FTIR can tolerate.

The lance placed in the off-gas system has a diameter of around 4 cm, and as Fig..4.8 and Fig..4.9 shows from the pictures the diameter of the opening was around 9 cm.

Fig..4.8: This figure shows the opening in the off-gas system where the FTIR was placed before the filter. The diameter needed for placing the FTIR in the off-gas system is 4cm. This opening is 9cm and is actually too big for the FTIR. Wool was used to cover the FTIR so that false air will not influence the results.

Fig..4.9: The diameter of the opening is around 9 cm.

This diameter difference was solved by putting some isolation to covering the lance and as can be seen from Fig. 4.10 and Fig. 4.11 the isolation was again covered with duck-tape to make sure there were no movements. By covering the opening with isolation there will be no influence of false air.

Fig. 4.10: The NEO LASERDUST and the FTIR is shown in this figure.

Fig. 4.11: This figure shows that the measurements were done close to each other.

4.2.3 Data processing

Also, in this experiment different equipment for measuring gas and dust was used. The FTIR is logging with a time difference between fifty and fifty-five seconds, where as the devices from NEO LASERGAS/LASERDUST was logging every second.

Having data from every second during 26 hours gives a lot of data and a huge amount of data make it difficult to make graphs in excel. The variation in time difference from the FTIR also makes it difficult to compare results from the NEO-devices. Given below is a summary of what has been done to the data regarding the time:

- Data from Elkem Thamshavn logging system logs every second. Flow, dust, NO, power and temperature has been collected from this system.
- The data from Elkem Thamshavn have been extrapolated. This means that we have transformed time difference from one second until five. This was done by taking the average values from the five last values for every five value.
- Because the feeders are charging the furnace every 400 seconds, the data from Elkem Thamshavn was also extrapolated to a time difference of 400 seconds. This was done by the same principle as for the 5 second values.
- The data from the FTIR was linearly interpolated in the same way as for the pilot-scale furnace. The variation in time difference ranged from 50-55 seconds and had to be transformed into 5 second values. To compare with the 400 second values from the Elkem Thamshavn data the FTIR-data was also transformed into values with a time difference of 400 seconds.

5 Results and discussion: Pilot-Scale Experiment

5.1 Results

In the pilot-scale experiment the focus of the experiment is looking into the effect of the raw material mixture. In practice this is done by varying the carbon source between coal and coke. These two carbon materials are different when it comes to moisture content and amount of volatiles creating a wet or dry charge. The results from the pilot scale experiment will be presented in this chapter.

Fig. 5.1 is a scheme showing which parameters can form NO and can be related to this report. Raw materials are added to the furnace by the charging process. Since charging and raw materials are related to each other, the two parameters are studied in this thesis. In the pilot-scale experiment the carbon materials have been studied. From the theory part it is implied that the two properties of carbon that could influence the formation of NO are water and volatiles since the fixed carbon in this case is kept constant to create a constant silicon yield.

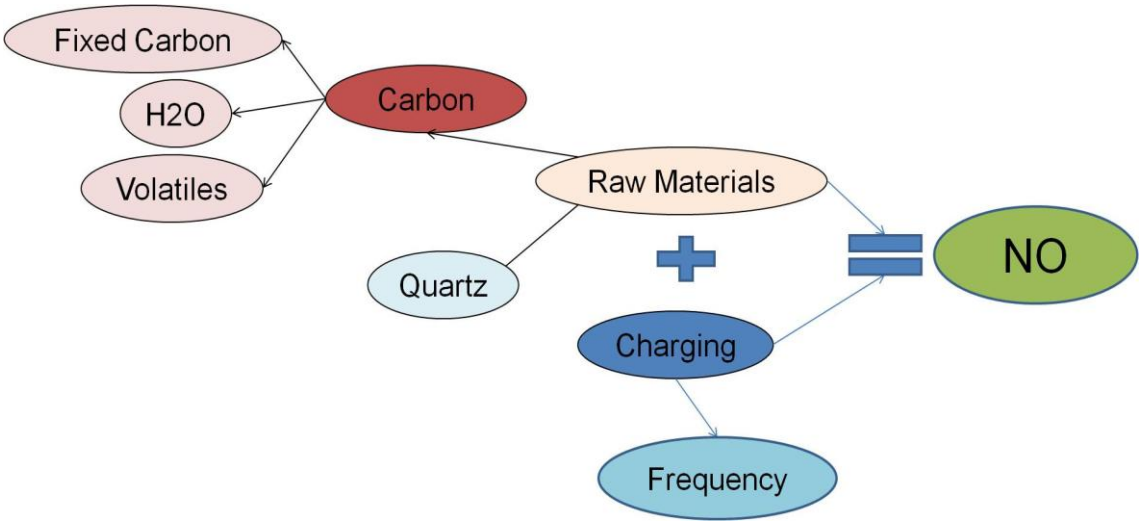

Fig. 5.1: This scheme shows how raw materials are charged to the furnace with primarily a silicon source and carbon source used to reduce the quartz. Following the important parameters of the carbon is the content of volatiles and water. For the charging process the frequency of the charging is assumed to be important for the amount of NO that is formed.

Because the open tapping hood influenced the results with false air, there was found one valid time-period for each of the four periods “Dry Charge + Lower openings”, “Dry Charge + Upper openings”, “Wet Charge + Lower openings” and “Wet Charge + Upper openings”. These four cases will be repeated throughout the results, and the dynamics of the periods can be found in the appendix (A.7).

In this experiment, huge amounts of data is collected and analyzed. Detailed reports and publications will be made from this experiment. Since the focus will be on the industrial experiment there will only be relevant results regarding the raw materials will be included and it is natural to divide the results into a part about the water content and the effect of the volatiles. First, there will be a part about the data measurements and the dynamics of the gases.

5.1.1 General Results: Measurements & Dynamics.

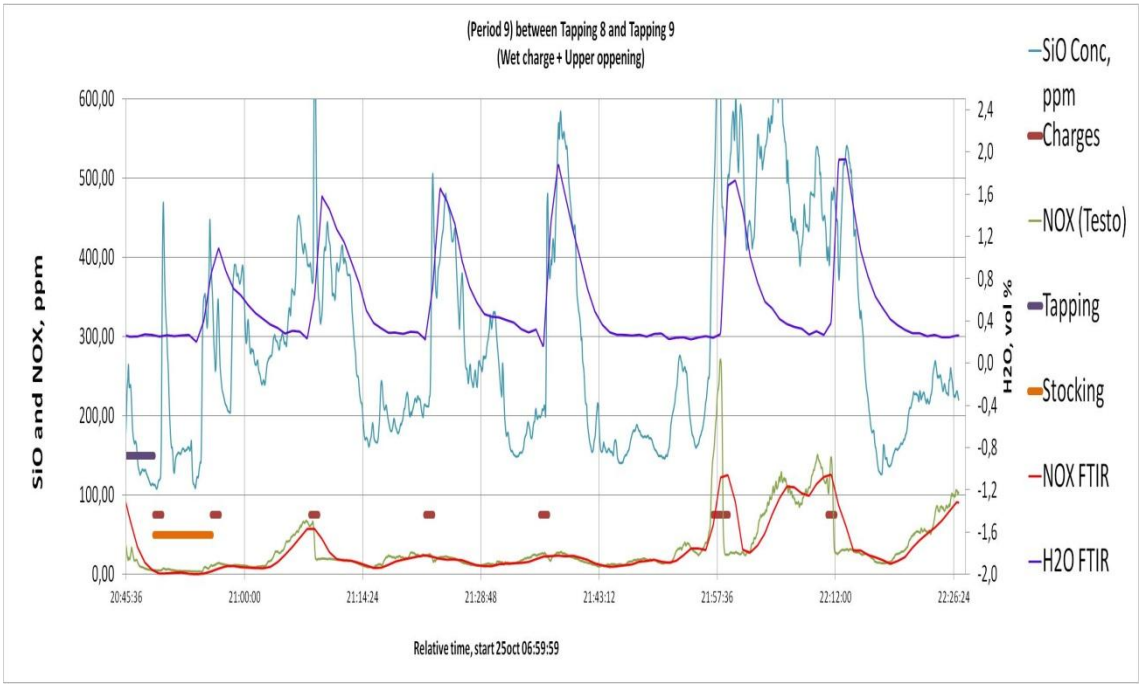

Fig. 5.2: The graph shows an overview of the important parameters that have been measured during the experiment.

Fig. 5.2 is showing an overview of the important parameters that have been measured during the experiment. The FTIR measurement device measures water, NO and other relevant gases like CO and SO_2. TESTO is another measurement device that is used to measure NO_x. The measurements from the TESTO device are more frequent than the measurement from the FTIR. From the figure the NO_x from the FTIR is compared to the NO_x from the TESTO. The NO_x plot made by data from TESTO show a higher resolution compared with the data from the FTIR. The data from TESTO have a higher resolution because the device measures more frequent.

Included in the plot is also the charging and stoking. These data are collected based on observations when running the furnace. One operator is in charge of writing down the times when the furnace is charged or stoked. The tapping process is also registered in the same document by observation. The tapping process can also be observed by looking at the measurements of temperature and power.

Silica (dust) is another parameter that is necessary to measure for the understanding of the formation of NO. The silica fume is measured by NEO LASERDUST and the fume is also collected into bags that are weighed during every tapping.

Most importantly, the graph shows the dynamics of the measurements. The dynamics are used to look at the response of NO and water during charging and stoking. Also, the dynamics are used to validate the data to see that they fit with time and scale.

5.1.2 H_2O-content of carbon

These graphs in Fig. 5.3 and Fig. 5.4 show an overview of the different cases while keeping the position of the inlet of air constant. For both figures the NO_x is marked as red and green. The variation in water can be seen as the blue line.

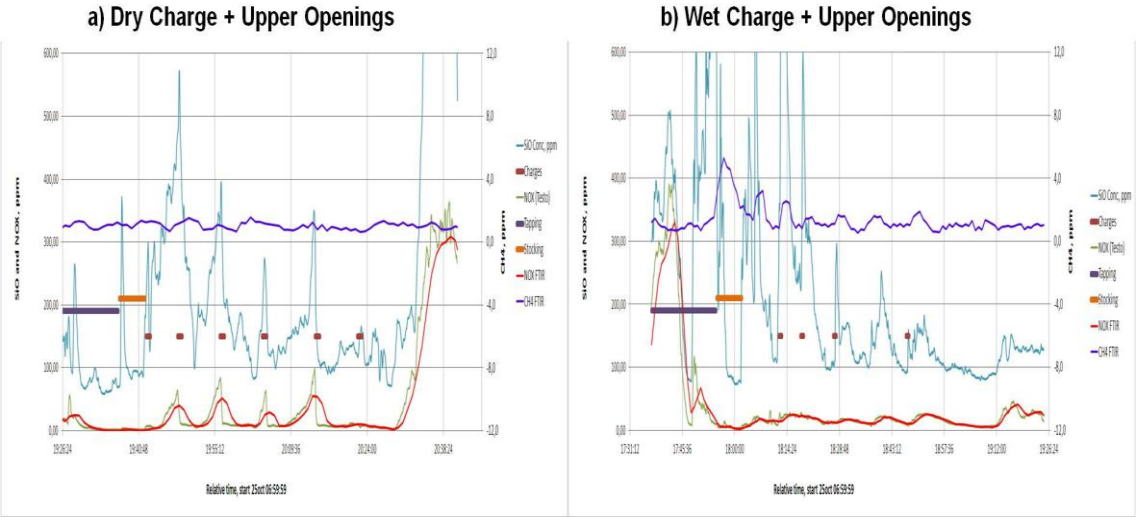

Fig. 5.3: a) In this case the carbon materials are dry, which means that the carbon is low on humidity and volatiles. b) With a wet charge there is a high content of humidity and volatiles.

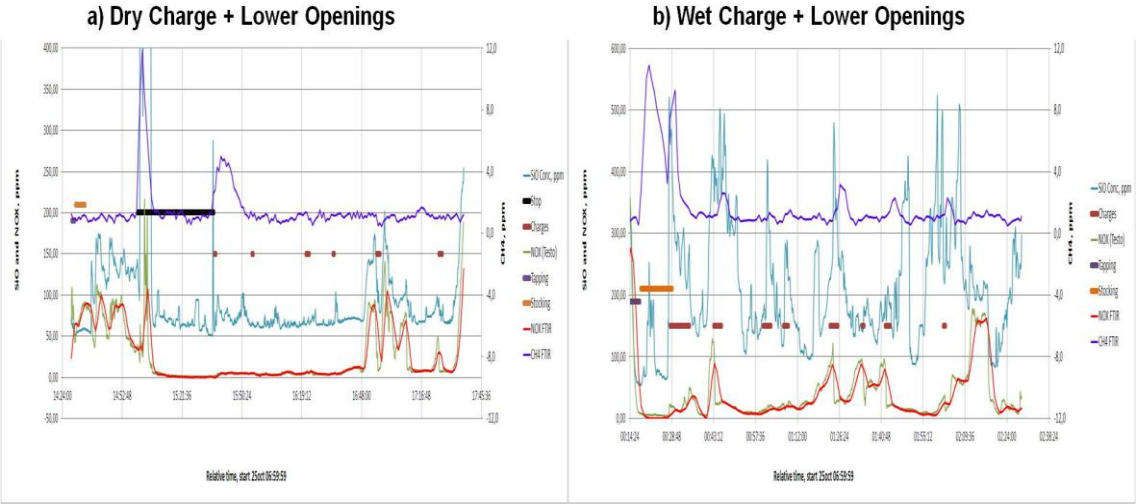

Fig. 5.4: a) In this case the carbon materials are dry, which means that the carbon is low on humidity and volatiles. b) With a wet charge there is a high content of humidity and volatiles.

In Fig. 5.5 the overview figures has been zoomed in to look at the effect of water. From the figures the axes show negative values. This is related to the program used to normalize the data. The data is normalized to be on the same scale. The software is called “Eureqa” and can be downloaded for free to normalize data.

The figure (Fig. 5.5) shows that the NO_x varies more for the process with a dry charge in contrary to the wet charge. For the wet charge there are almost no larger peaks in NO. In the graph to the left there is a peak of NO and this is because of the tapping.

In Fig. 5.5 and Fig. 5.6 the stoking (marked as red) is included to show how the stoking relates to water. The stoking for the pilot furnace is a combination between adding raw materials and create an even charge and for such a small furnace this can be compared to charging for an industrial furnace. Observed from these figures is that there is a reduction in NO_x when the furnace is stoked/charged. This can be related to theory and could be due to a reduction of the overall temperature at the charge surface.

For the lower openings in Fig. 5.6 the wet charge seems to have a larger effect on the formation of NO. This will be further explained in the discussion part.

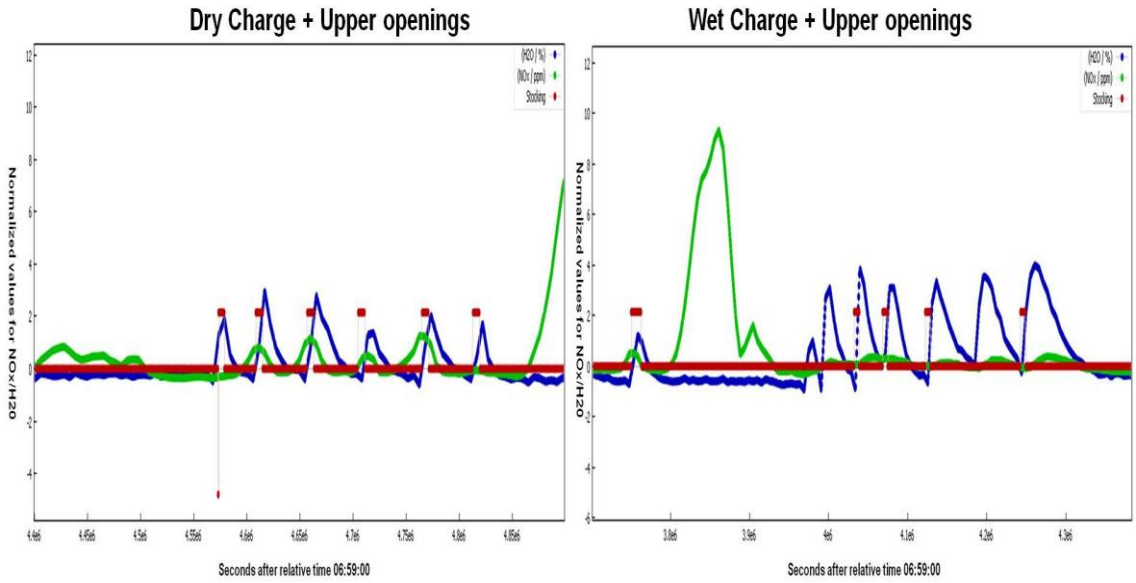

Fig. 5.5: Left - Dry charge. Right - Wet charge. The position of the inlet of air is kept constant.

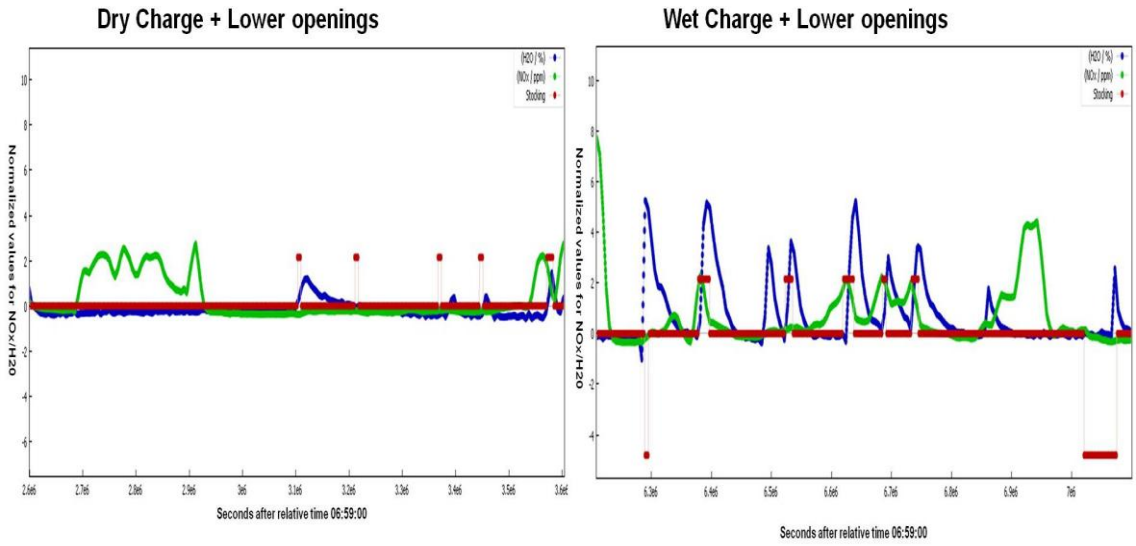

Fig. 5.6: Left - Dry charge. Right - Wet charge. The position of the inlet of air is kept constant.

To see the clear effect of the water content, NO_x versus silica fume was plotted based on all the data. Basically the graph in Fig. 5.7 illustrates a trend of that at most of the low emissions can be found when the silica-fume concentration is low.

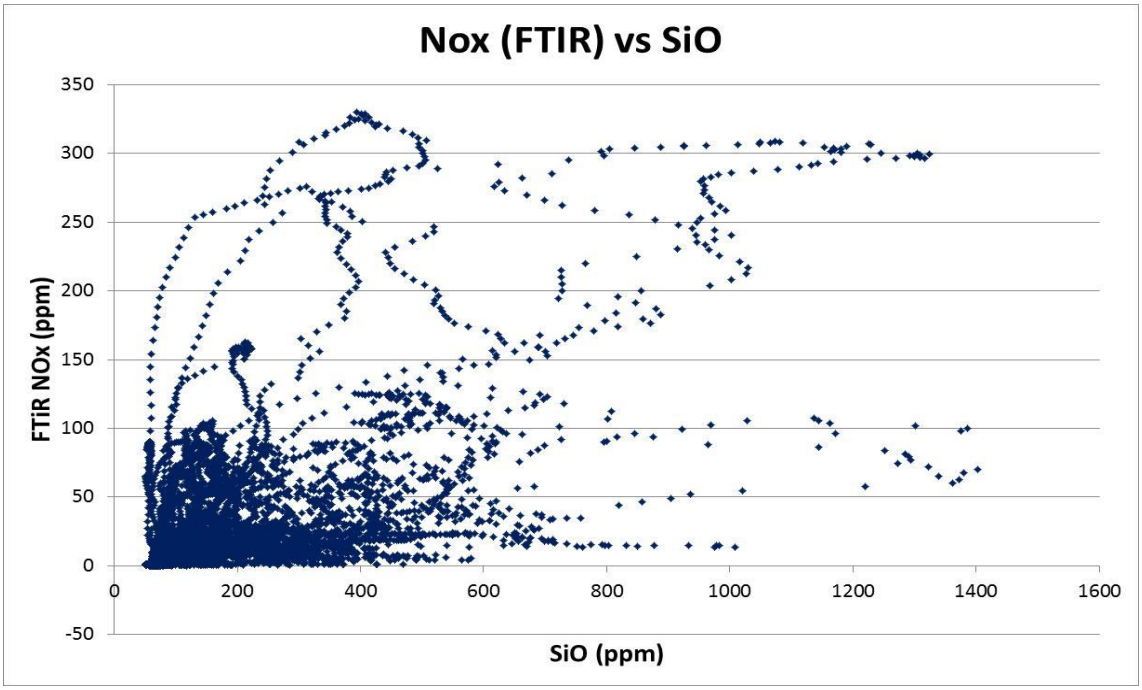

Fig. 5.7: This figure shows the NOx versus the silica fume.

The same plot as above is given for different concentrations of water and these plots are given in Fig. 5.8 to Fig. 5.10. The following graphs indicates that the variation of NO is higher and more spread if the concentration of water is low. As the water content increased the NO is gradually decreasing and hence more concentrated around a low dust concentration and low values for NO. The emissions are more spread when the water content is above 0.3 vol% in comparison to if the water content is above 0.4 vol%. The same trend can be found when the H_2O concentration is above 0.8 vol%. Plots for H_2O over 0.5 vol% and 0.6 vol% can be found in the appendix.

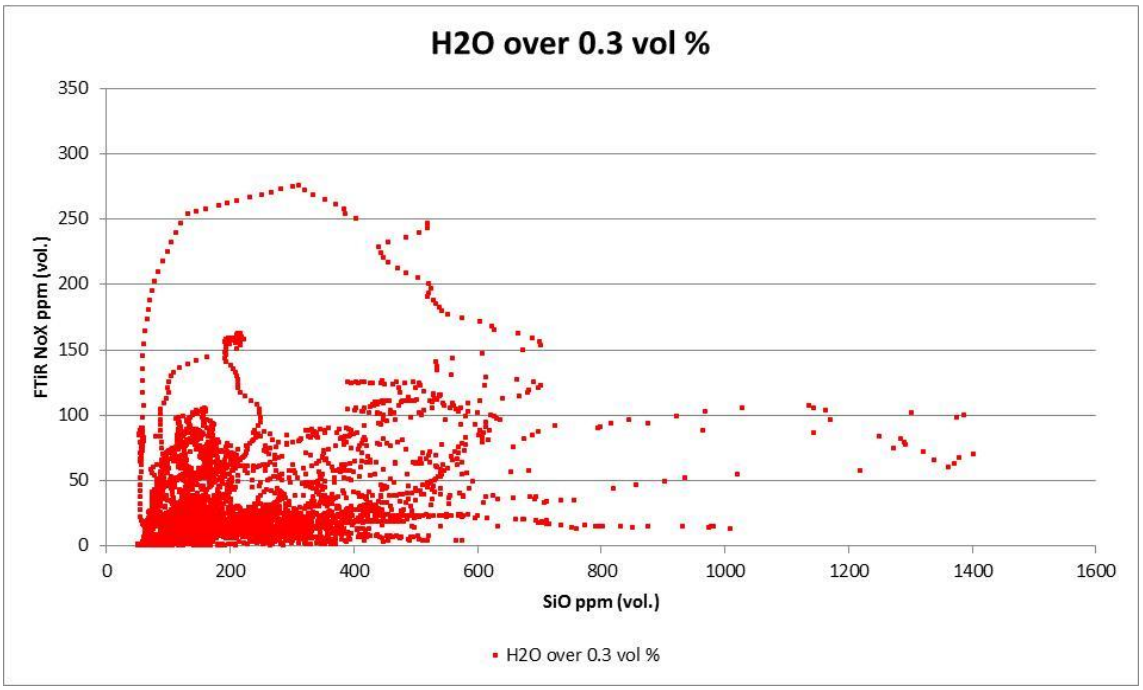

Fig. 5.8: NO_x vs. SiO: H_20 concentration from 0.3 vol% and over.

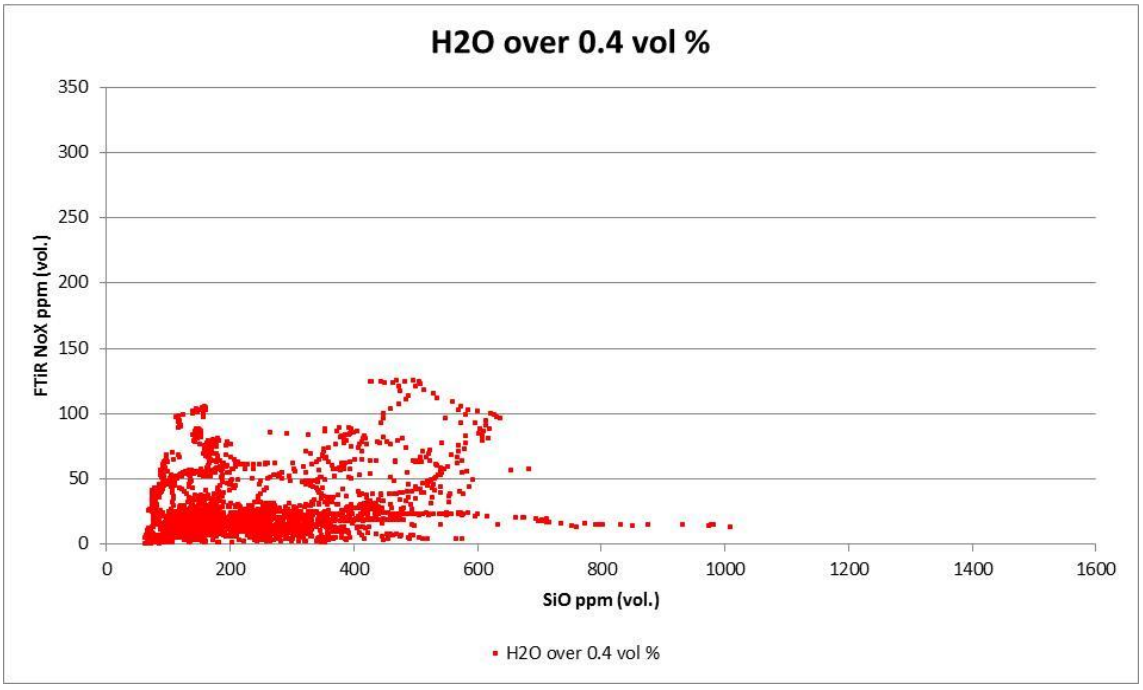

Fig. 5.9: NO_x vs. SiO: H_20 concentration from 0.4 vol% and over.

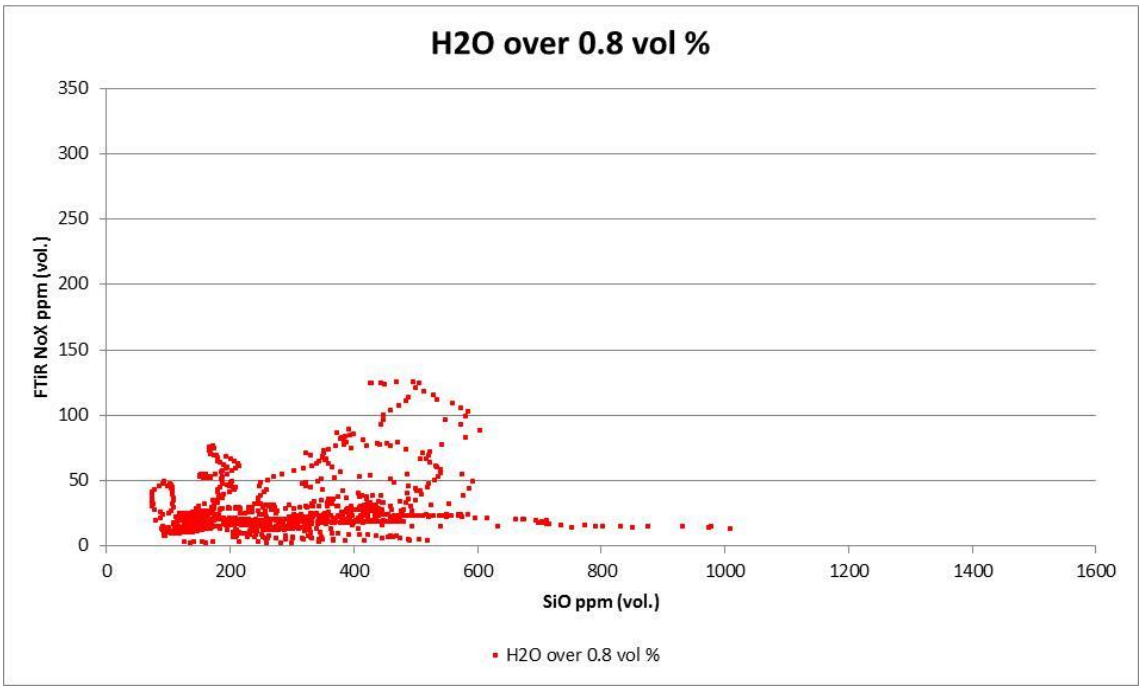

Fig. 5.10: NO_x vs. SiO: H_20 concentration from 0.8 vol% and over.

Fig. 5.11 below shows the phenomenon of that higher water content give lower values of NO_x. In this case the water is plotted against the silica fume. The graph also shows that for a low water content and a high fume concentration give a high NO_x. From this figure the trend is that for a low fume concentration and high water content most of the emissions are less than 150 ppm. When the water content is low and the silica concentration is high there can be observed emissions over 150 ppm.

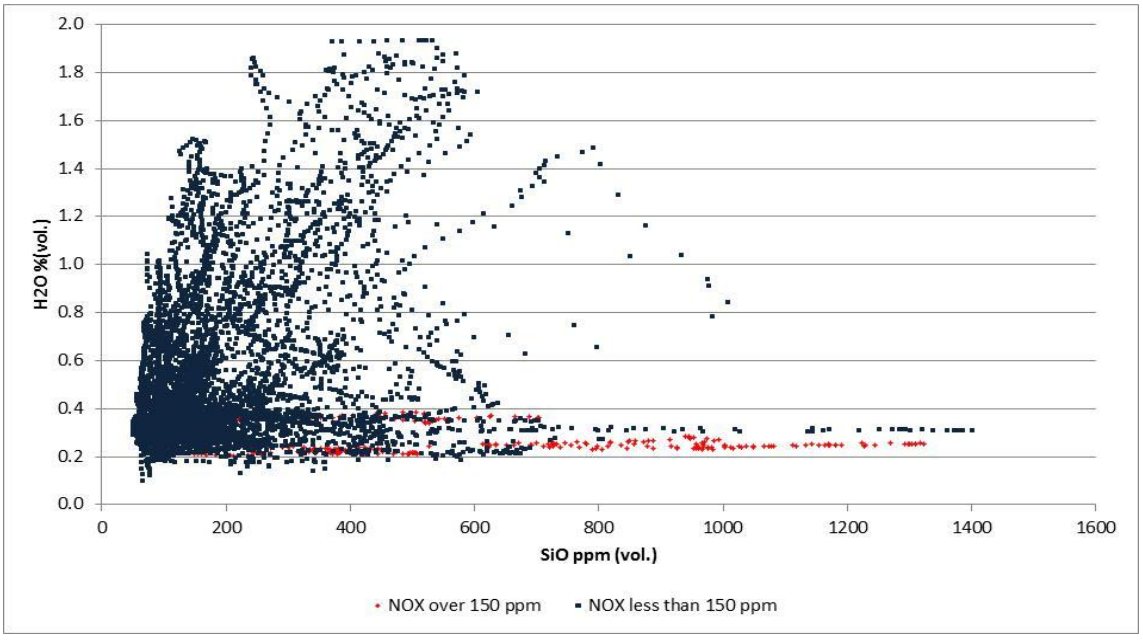

Fig. 5.11: Water versus Silica fume with NOx plotted for values below and over 50 ppm.

5.1.4 Volatile content of carbon

From Fig. 5.12 to Fig. 5.15 the four cases are shown with CH_4. These four graphs show the dynamics and variation of the volatiles. The volatile content of the dry charge is low compared to the wet charge, and is can be seen from the graphs where the peaks are higher for CH_4 in the graphs showing the wet charge.

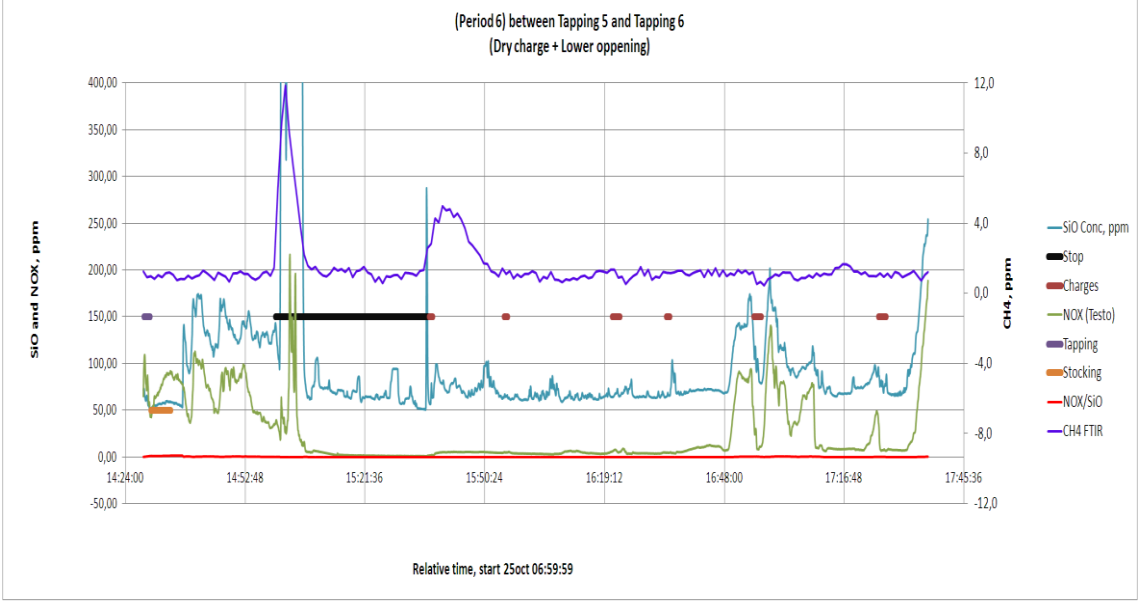

Fig. 5.12: This figure is for the dry charge with lower openings. The CH_4 concentration is marked as the blue line.

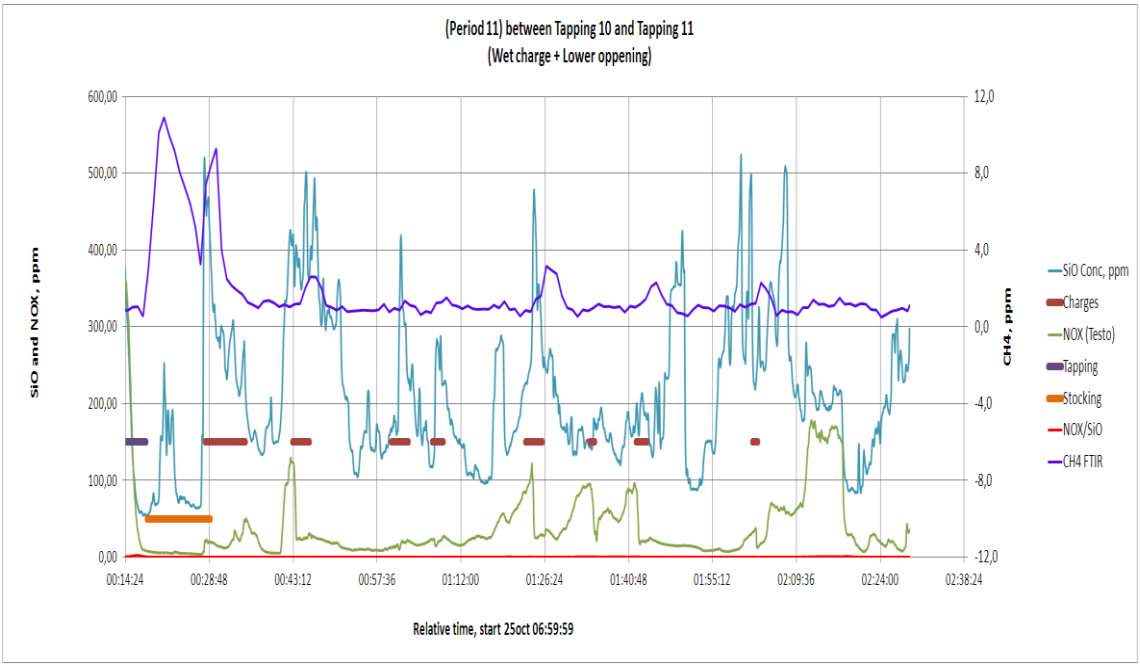

Fig. 5.13: This graphs shows the wet charge when the inlet of air was close to the charge.

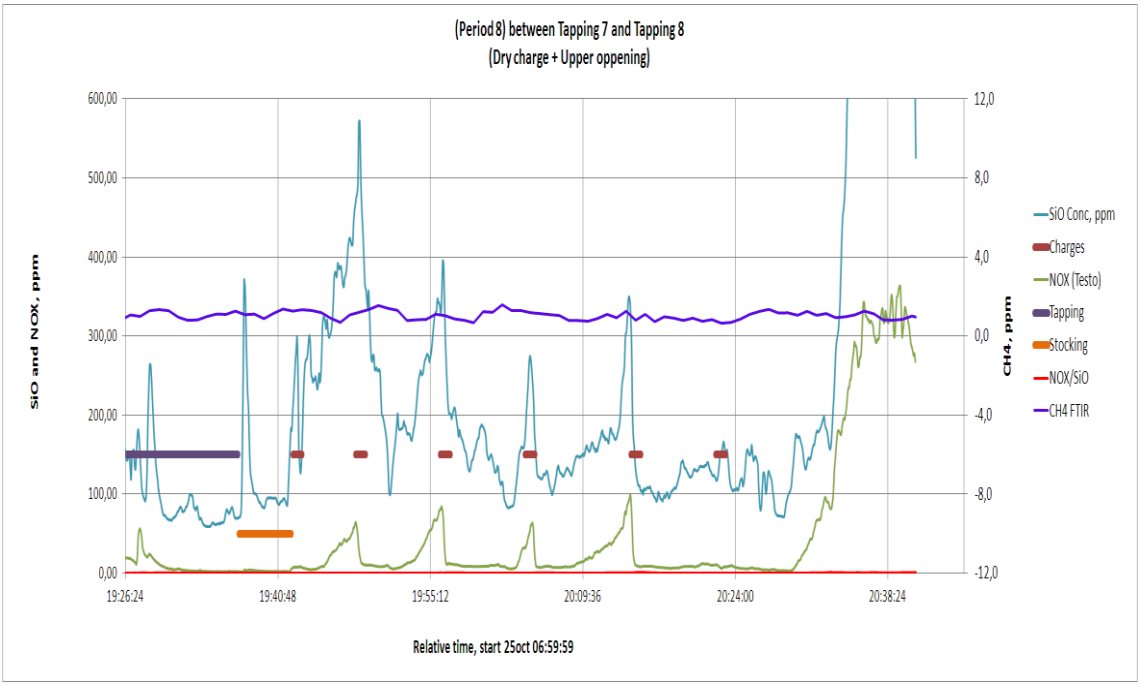

Fig. 5.14: This graph shows the data from the wet charge then the openings are in the upper position.

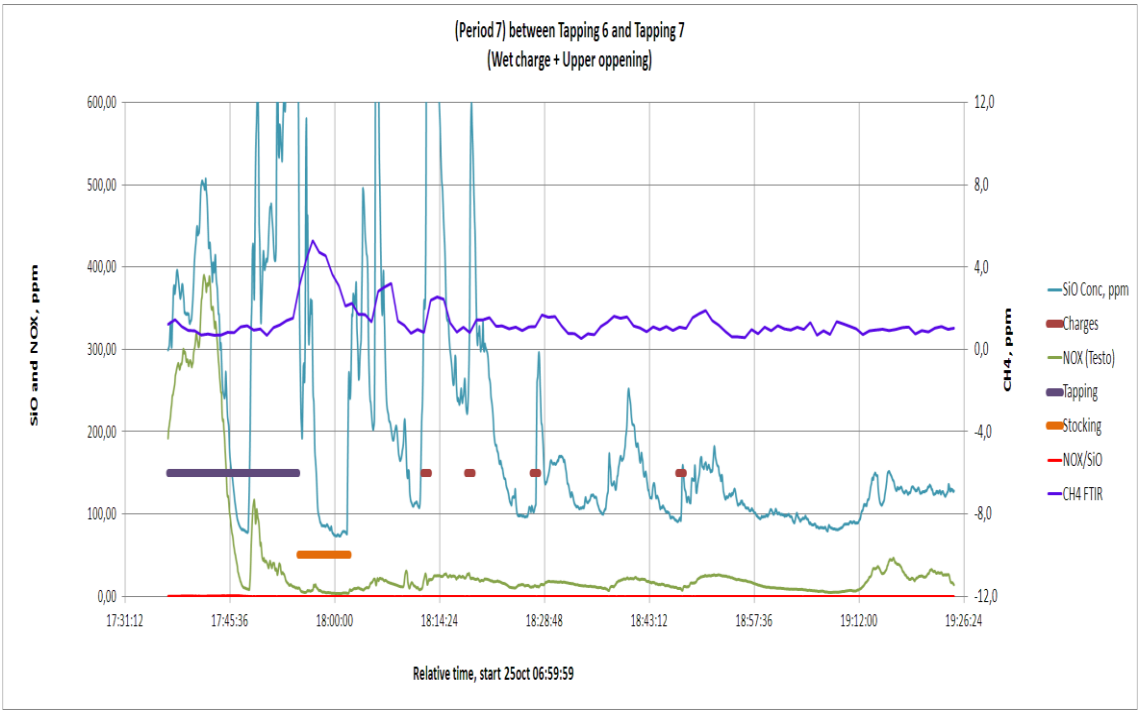

Fig. 5.15: This graph shows the wet charge with the upper openings. Peaks of CH4 can be seen from this figure.

The volatile content of the dry carbon is generally lower than for the wet charge. Because of this the effect on the NO formation will be found for the wet charge. From Fig. 5.16 it can be seen that for CH_4 less than 2 ppm a high concentration of NO_x can be

found. For CH_4 over 2 ppm the concentration of NO_x is low even though the concentration of silica fume is high.

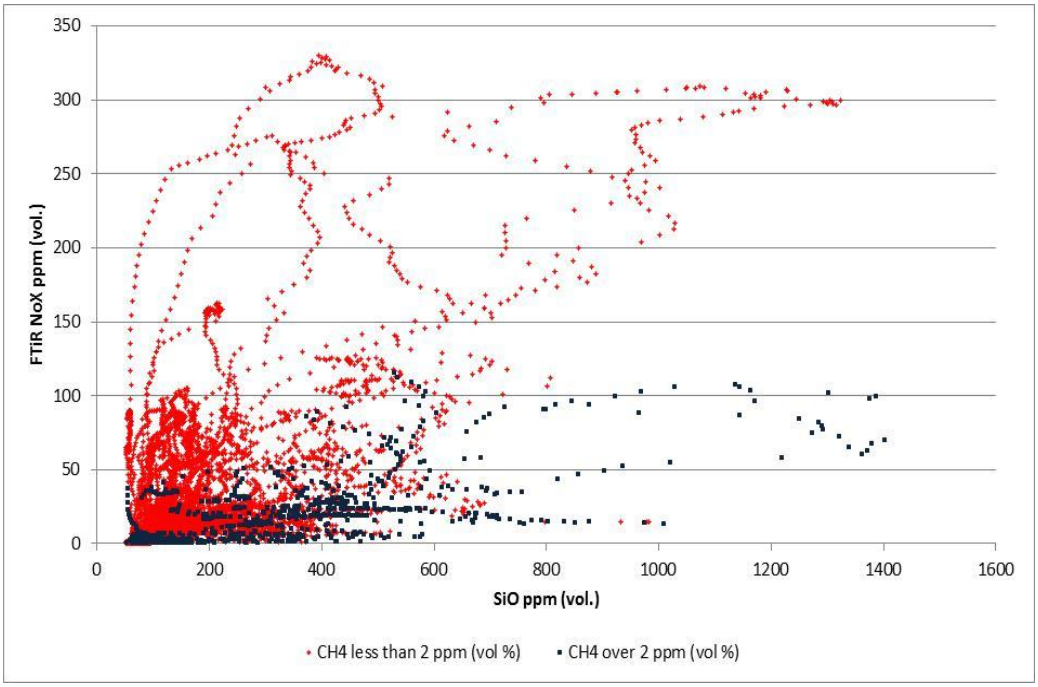

Fig. 5.16: Effect of CH4.

5.2 Discussion

In this experiment the yield is set to be constant. The formation of NO correlates with the silica fume, and it can be assumed that the variation in NO_x will be affected by other parameters rather than the silicon yield. The combustion of SiO(g) happens on the top of the charge surface, and the following discussion will include how the raw materials influence this combustion.

It is important to notice that these experiments have been done in conditions where there are many parameters that can contribute to the formation of NO. It is difficult to assume what is the most important parameter. The type of NO_x that is produced in such a system is classified as "thermal" NO_x and is dependent on temperature, oxygen radicals and nitrogen present in the system.

The oxygen radicals are created by the combustion of SiO(g) given by reaction (5.1). This reaction is exothermic and creates heat, which is found in the furnace as blows.

$$SiO(g) + O_2 = SiO_2 + O \text{ (radical)} \qquad (5.1)$$

In this case, the charge can influence the reactions in two ways. The fresh charge materials can reduce the temperature that is created by the combustion of SiO(g) on the charge surface. Also, water and volatiles, from the raw materials, could react with oxygen and slow down both the fume production and the NO formation.

5.1.1 Comparison of the wet charge and dry charge.

It is natural to start this discussion with the difference between the wet and dry charge.

Charging the furnace will have an impact on the NO formation even though the characteristics of the charge materials are different. In the pilot-scale experiment, the charging process is a combination between feeding the furnace with fresh materials and making sure the charge surface is even (stoking). In the industrial scale furnace, the raw materials are fed to the furnace continuously and during stoking, which is less frequent, the raw materials get distributed.

The consequence of charging is that the furnace could "rinse" itself, which means that the charge materials, from the surface, fall down to the crater and take place in the silicon producing reaction. The "rinsing" could give blows of SiO(g) and following create peaks of fume and NO_x.

Throughout the results there have also been peaks in NO_x, which cannot be explained by charging, stoking or stops. These peaks can be related to blows, which can be seen by looking at the temperature measurements or by observing the furnace. However, in this discussion the focus will be on the charging.

Primarily the difference between the wet and dry charge can be found by looking at the water content and the volatile content. It is observed high peaks of water and volatiles during charging while the raw materials are classified as wet.

5.2.2 Wet Charge

The wet charge consists of coal and woodchips. The coal has a humidity of 8.9 % and a volatile content of 38.9 %. The woodchips have 42.1 % humidity and 72.9 % volatiles. In this case the quartz is kept constant, hence the properties of the quartz that can be related to the formation of NO is not a parameter that is studied in this case.

5.2.2.1 Effect of Water and volatiles

A conclusion from the scatter plots in the results is that the concentration of NO_x decreases with an increasing content of water and volatiles. This can be related to the theory seeing that the charging of raw materials itself reduces the overall surface temperature. The system has to heat up the new layer of charge materials and uses some energy to heat up the system. Also, the water needs to be evaporated, a process that also takes energy. The volatiles can contribute to a reduction of volatiles by reacting with oxygen and stealing some of the oxygen used in the combustion of SiO gas. However, these mechanisms will be described in chapter seven when the industrial experiment and the pilot scale experiment are compared to each other. In this chapter the focus will be the difference between the wet charge and the dry charge, because the trend is easier to see in a controlled furnace operation.

Fig. 5.17 is a plot showing the effect of water and volatiles. The trend of the dynamics is the most important part of the figure. The axes and lines are not clear to see, so they are added to the appendix for a clearer view (appendix A.7). This figure show the typical behavior of water and volatiles (CH_4) during charging, which is the process of feeding fresh raw materials to the furnace. During the charging process there is an increase in the content of water and volatiles. This increase is due to evaporation of moisture and combustion of volatiles. At the same time of the evaporation of water and combustion of volatiles, the emissions decrease.

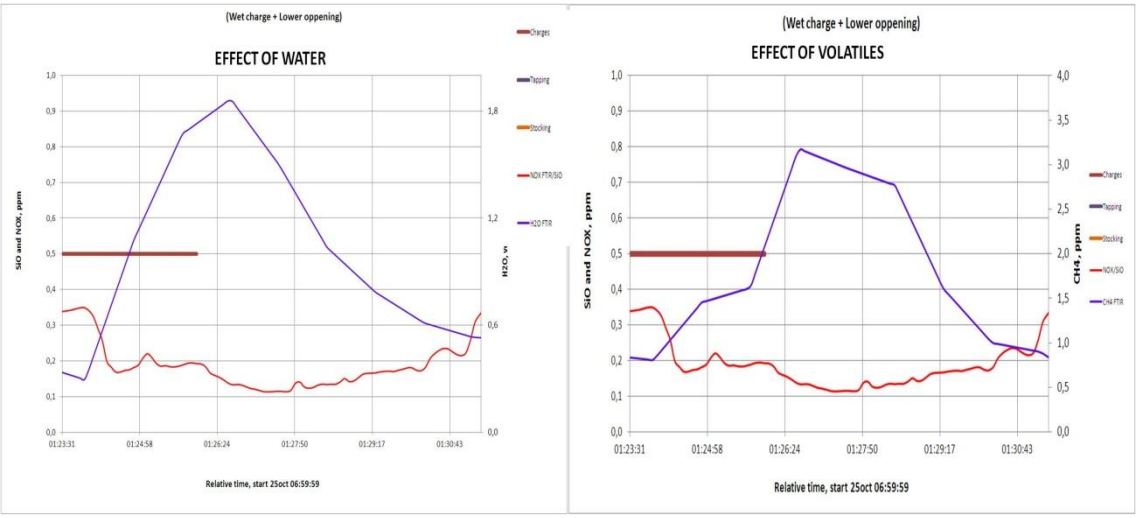

Fig. 5.17: This figure shows the effect of the water and volatiles (marked in blue).

Fig. 5.18 is a plot where volatiles and water are plotted in the same figure. Basically the figure states that both the silica fume and emissions decrease during charging. Another interesting observation from this figure is that the evaporation of water happens at a quicker rate than the combustion of volatiles. The evaporation of water will happen fast because water evaporates at 100 °C. The raw material will reach this temperature quickly and the condensation will begin.

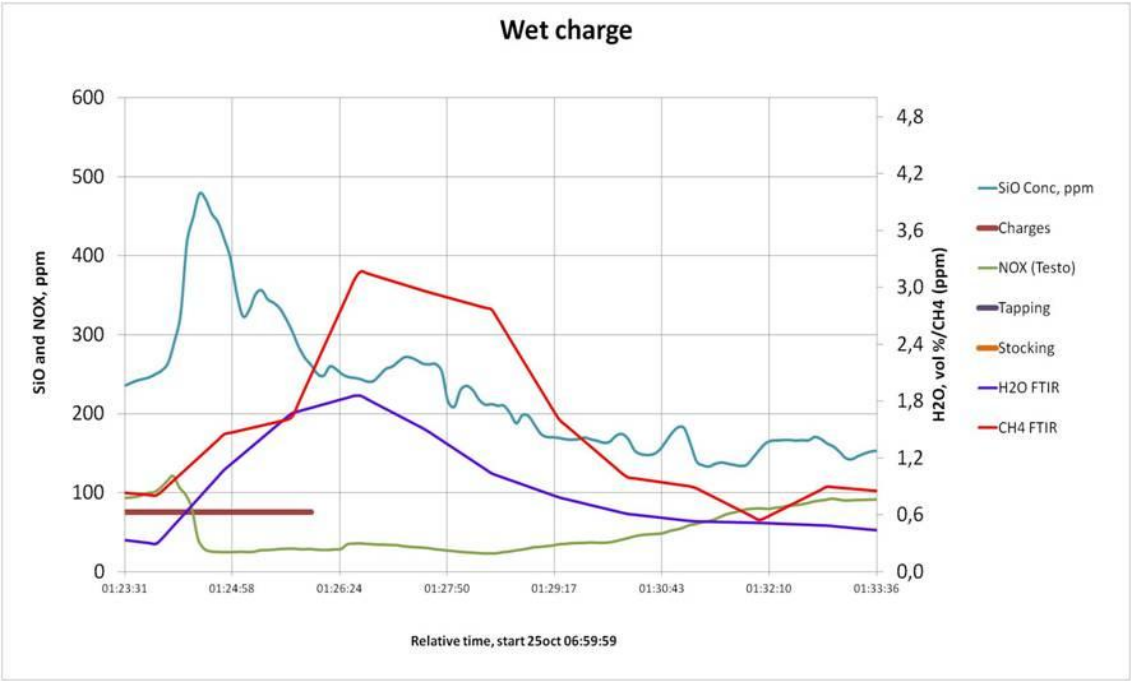

Fig. 5.18: The effect of charging on the silica formation and NO emissions.

For the wet charge it is likely that both the volatiles and the water have an effect on the emissions. The background for this assumption is because the dynamics show a clearer reduction of NO during the wet charge compared to the dry charge.

It is also worth mentioning that the inlet of air is close to the charge. The same graph is plotted for the dry charge, and that period is also characterized by an air flow close to the charge surface. The graphs are taken from this position so that the results can be compared.

5.2.3 Dry charge

In the dry charge the fixed carbon is the same as for the wet charge and is constant through the experiment. The coke contains 0.97 % humidity and 5.91 % volatiles. The woodchips has a humidity of 5.6 % and a volatile content of 72.9 %.

5.2.3.1 Water content and volatiles

Fig. 5.19 is an example of the dynamics when the charge is dry. In this case there is also a reduction in emissions during charging. The water increases in the same way as for the wet charge, but the volatiles do not seem to respond during charging. However, the content of volatiles in the coke is around 5.91 %, which is a small amount compared to the content in coal (39.8 %).

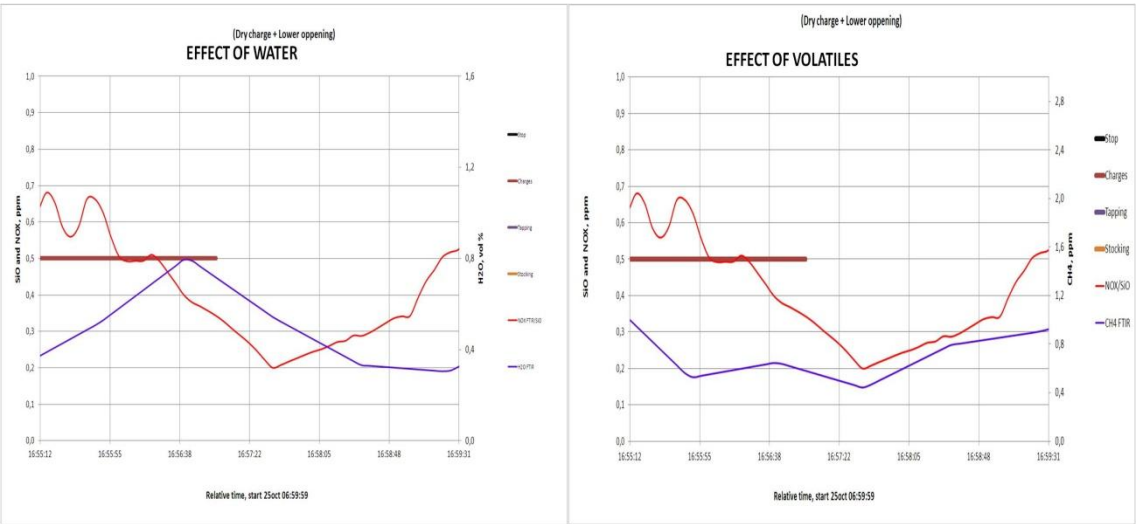

Fig. 5.19: Effect of water and volatiles for the dry charge.

Another example of the behavior of volatiles and water can be found in Fig. 5.19. The water behaves the same way both for the wet charge and the dry charge. During charging the content increases because the water evaporates. After all of the water has evaporated, the content begins to decrease. During charging there is a reduction of the emissions and the amount of silica that is produced. However, the emissions are only reduced for a short period of time. Most likely, the short period is due to a limited amount of moisture found in the coke. A deviation from the wet charge is the behavior

of the volatiles. In this case the content of volatiles increase after the charging process is done. However, this is not a trend that is found for every charging. The volatiles do increase to a certain level during charging, however not in the same scale as for the wet charge. The increase in volatiles is small due to the limited amount of volatiles in coke.

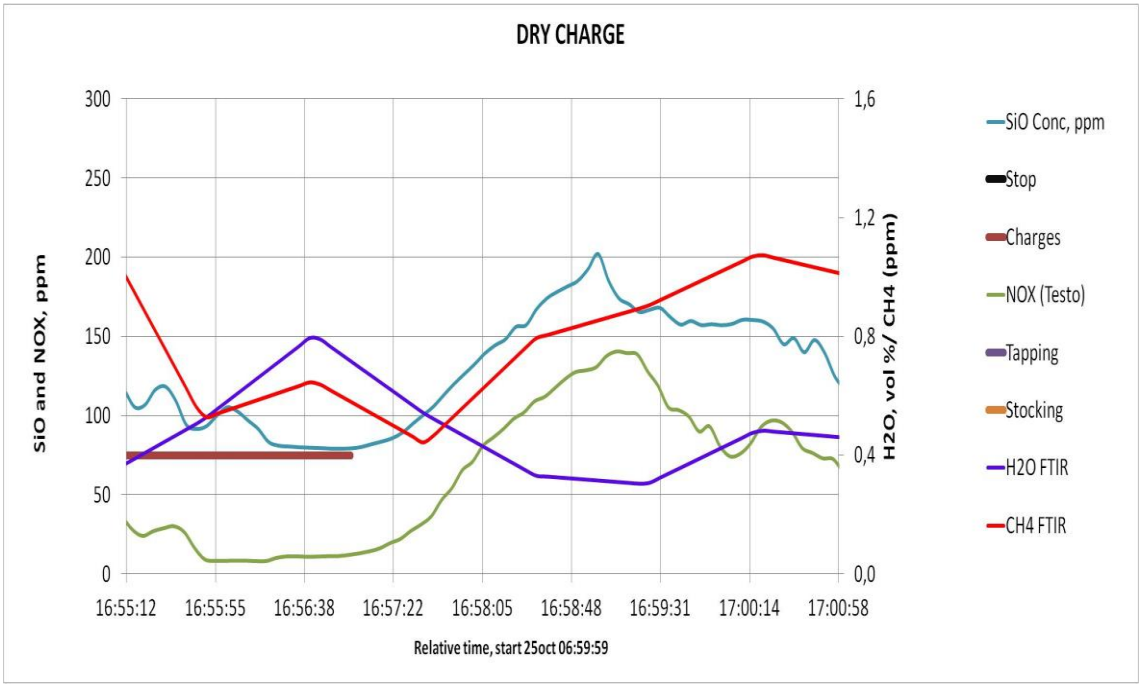

Fig. 5.20: The effect of charging when the charge is dry.

5.2.4 Summary

The wet charge and the dry charge are discussed above in two parts. To summarize these chapters the wet and dry charge is compared in Fig. 5.21. The graphs have the same time scale (10 minutes) and the axes are the same. The axes are not clear and are added to appendix A.7.

As mentioned before, the difference between the wet charge and the dry charge is the amount of volatiles and moisture. Fig. 5.21 illustrates what happens when the furnace is charged for both of the cases. When the furnace is charged there is a reduction in the silica fume. The volatile content and the moisture content increases during charging, and starts decreasing when all of the volatiles and water have evaporated. The deviation between the two graphs is that the furnace is charge two times in the 10 minute period. There is a peak of NO_x before every charging process for the dry charge. For the wet charge it is hard to observe a peak when both of the graphs are in the same scale.

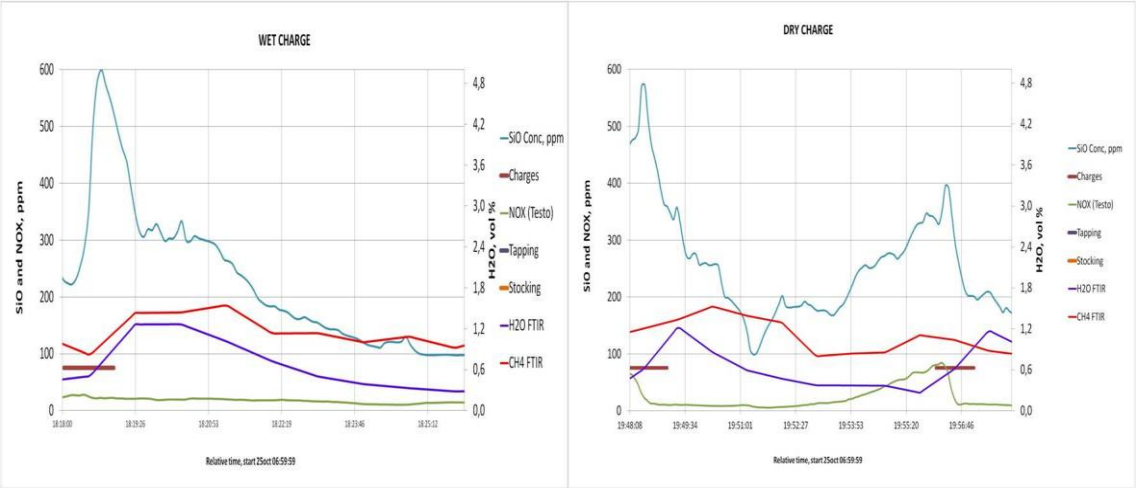

Fig. 5.21: Left: Wet Charge. Right: Dry Charge. The figure includes a comparison between the wet and dry charge where the inlet of air is close to the off-gas system (upper).

The observations made from these two graphs fit with the predicted theory. According to theory, it is predicted that the formation of NO would be lower for the wet charge compared to the dry charge. This is because the wet charge will lower the overall charge temperature. Also, the water and volatiles will have to combust or evaporate before SiO gas is allowed to combust and produce oxygen radicals.

In a period of ten minutes, the furnace with the dry charge is charged two times. In this period it is observed two peaks for the silica fume and two peaks for the emissions. Both of these peaks are right before charging, and during charging both the silica fume and the emissions decrease. The furnace is charged based on observation, which means that the operators charge the furnace when there are many blows or when the temperature is high. This could indicate that the water and volatiles have evaporated quickly. The fast evaporation can be related to the dry charge, because the moisture content and the volatile content are lower compared to the wet charge.

The conclusion of this discussion is that the raw material mixture does reduce the emissions during charging.

5.2.5 Other parameters

As mentioned in the experimental part and in the results the position of the inlet of air is also a changing parameter in this study. Earlier Kamfjord (Kamfjord) has stated that gas velocity has an impact on the formation of NO. This is because if the gas velocity is low, the gases combusting on the charge surface will have more time to heat up. The effect of this will be “hot spots”, which are areas in the furnace with high temperatures. In the results, there is also an indication that keeping the inlet of air higher towards the off-gas system produce less NO_x/SiO. This is valid for both the wet and dry charge. Fig. 5.22 is a confirmation of the results that is discussed here.

Fig. 5.22 illustrates that the average emissions found for the cases with the wet charge is lower compared to the periods with the dry charge. The deviation from theory is that the average emissions are higher for the case "Dry Charge + Upper Openings" compared to when the openings are close to the charge. However, the results are made by data collected for a short period of time. The point is that the average in this case does not give the information necessary to understand how these cases are different. In a complex system there will be periods with high emissions and low emissions and the results could be influenced by many parameters related to the conditions of the furnace. Average values give information about the trend to a certain extent; however the dynamics of the many parameters can be used to explain the trend.

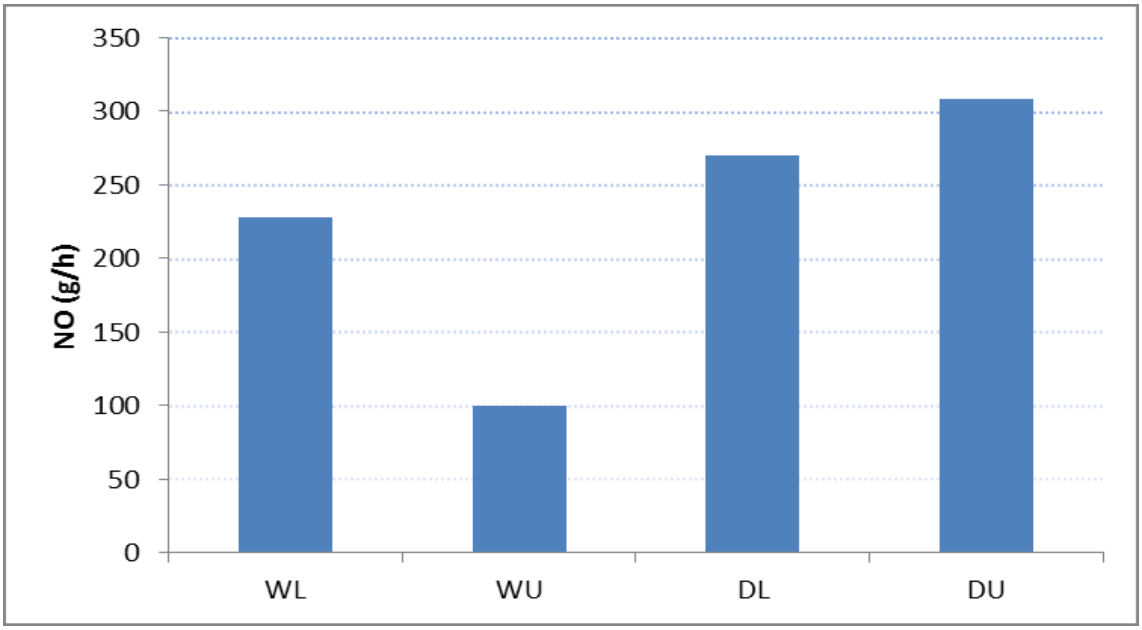

Fig. 5.22: This figure is taken from results made by SINTEF from the same experiment. The figure shows the average NOx emissions represented by four different combinations of parameters: "Dry + Lower" = DL, "Wet + Upper" = WU, "Dry + Upper" = DU and "Wet + Lower"= WL. These four combinations can be found also from the theory part and from other results in the thesis. (Olsen, Solheim, Panjwani, & Andersson, 2013)

5.2.6 Further work

This experiment shows trends of how the carbon materials can influence the formation of NO_x. However, it is difficult to get absolute values when running a furnace due to many parameters that can influence the results. In this experiment the plan was to get results from thirteen runs where the changing parameters are inlet of air and wet or dry carbon materials. Because of the open tapping hood and some issues with the measurement devices, only four periods are valid from this experiment.

To understand the mechanism of why the water and volatiles seem to influence the formation of NO, it might be an idea to try ten different carbon materials in an experimental set-up where the only parameter is the effect of carbon. It would be valuable to do a study of the basic combustion mechanisms. In addition to varying the carbon materials it can also be an idea to add water. It is difficult to understand if the water only reduces the overall temperature or if it takes part in some reaction.

6 Results and Discussion Charge Experiment Elkem Thamshavn

6.1 Results

The charge experiment done in Elkem Thamshavn is different from the pilot-scale experiment. In this case the furnace is tapped continuously and charged continuously. The raw material composition is constant, and it is a mixture between coke, coal and woodchips. From the pilot-scale experiment it is found that the carbon materials influence the emissions of NO_x. Indirectly this means that charging also influence the formation of NO and in this experiment the charging pattern is the parameter that is changed.

An important part of understanding how the change in charging frequency influences the emissions of NO_x, is studying the dynamics during the normal conditions. Fig. 6.1 illustrates the dynamics and from this graph it can be observed huge variations in the emissions. The variation of the emissions is related to the operational parameters of the furnace such as the silicon yield, temperature and the general condition of the furnace.

The data from Fig. 6.1 is taken from the plants measurement device, which is a NEO LASERGAS (see appendix A.3). The data was collected from a period when one furnace was running, so the data is precise and is not influenced by gas from the other furnace. The average from this period is 300 ppm.

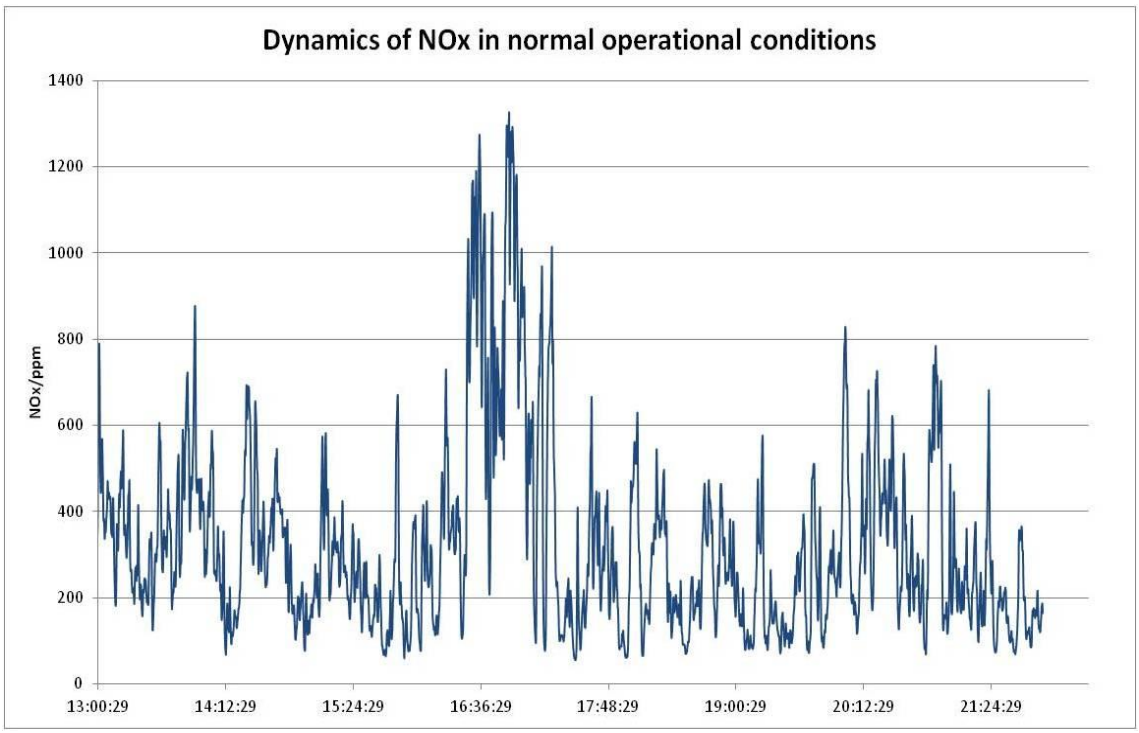

Fig. 6.1: Fig. 6.1 shows the dynamics of the NO_x emissions from one of the furnaces.

6.1.1 Average results from the time the FTIR was functioning.

Data from the experiment was transformed into one hour data by taking the average of the last hour. Based on these data, Fig. 6.2 is plotted from the day before the experiment and during the experiment. As mentioned before, the emissions are dependent on the furnace condition. Even when the average is plotted there will be periods when the emissions are high and low. However, Fig. 6.2 gives an overview of how the emissions behave, and the graph can be used as a tool for which periods are relevant to study further.

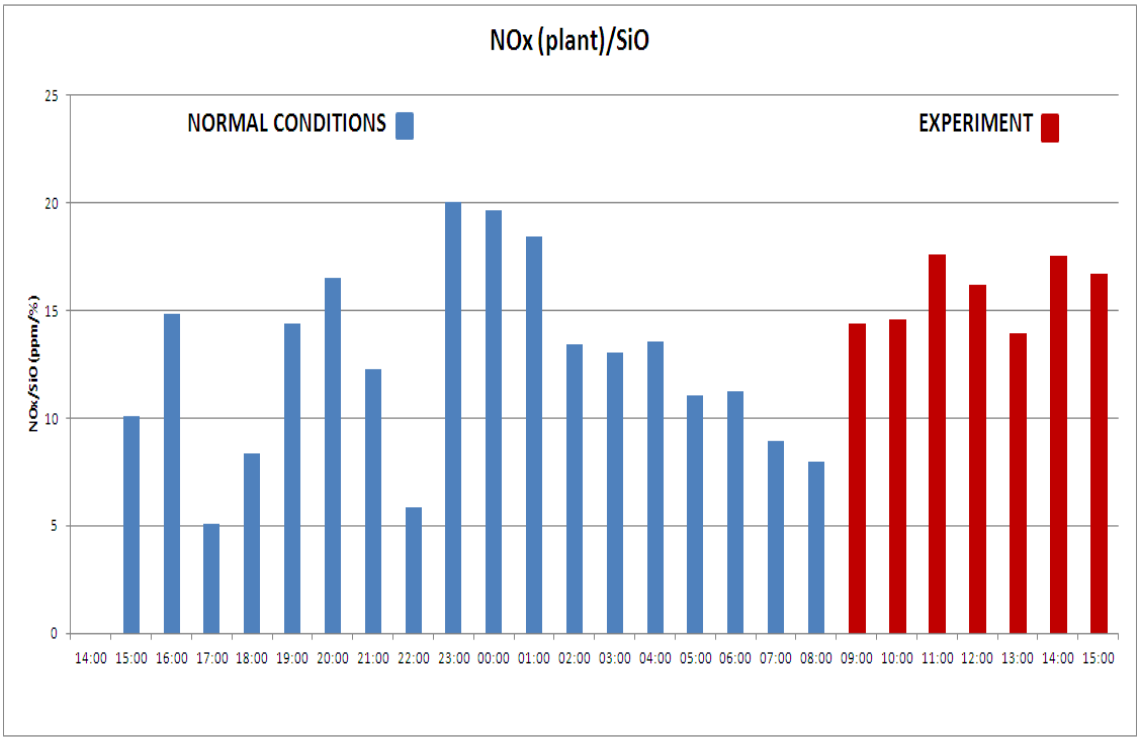

Fig. 6.2: This graph shows the average NOx/SiO from the day before the experiment and during the experiment.

6.1.2 Data divided into four periods.

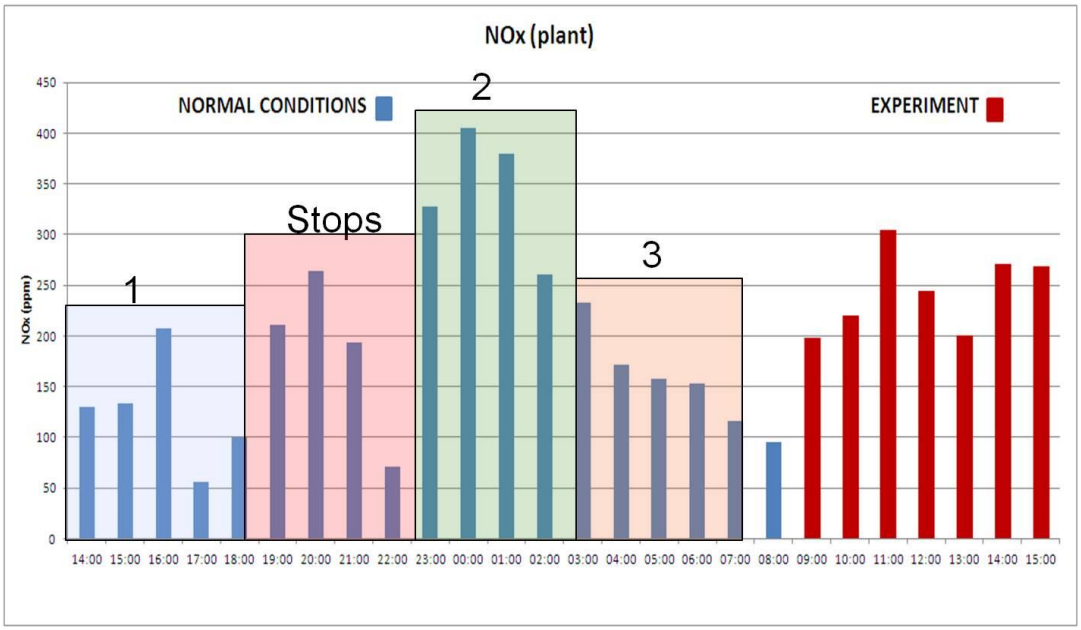

Fig. 6.3: The data is divided into four periods based on the emissions of NOx. The data from the experiment is used as an own period and is between 9:00-15:00. The experiment is one of the four periods.

Based on the average NO_x emissions from Fig. 6.3, the data was divided in to four periods. Three periods was taken from the normal conditions, and the experiment was taken as one period. The periods are selected during time-intervals when the emissions are either high or low. For the three cases from the normal conditions, data was collected for a time period of four hours. The experiment lasted for six hours. The purpose of looking into the results based on periods is to see if there is a trend when the emissions are high or if the emissions are low.

Fig. 6.4 shows a plot of how the average NO_x varies in the different periods. The FTIR was measuring for 25 hours, which makes it difficult to see if the experiment is a part of the normal variation or if there is an increase due to the experiment. To get the figure as correct as possible, the average from a period of five days is used to compare the results. The plot shows that period 2 is the case where the NO_x is highest, and it is 70 % higher than the “five day”- average emissions given as 100 %. The experiment is also higher than the total average. This graph is made in such a way that the average NO_x from the five last days is set as 100 % and the other periods is found in percent by comparing this average with the other cases.

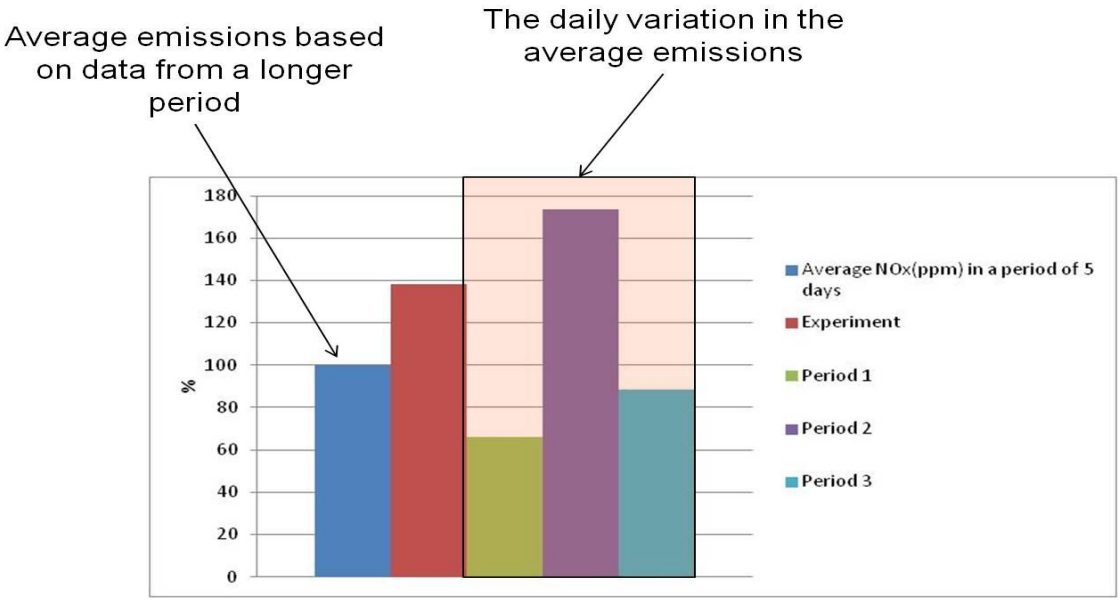

Fig. 6.4: Average data of NO_x (ppm) made in percent to see the difference between the periods. Included in this figure is the average emissions of NO_x for a time period of five days. This average is set as 100 % and the other periods are compared to this average. Period 1, 2 and 3 can be seen as the daily variation. It is natural that certain conditions influence the average and create the normal variation throughout a day.

While Fig. 6.4 is a general comparison of how the experiment could have influenced the emissions, Fig. 6.5 gives a comparison between the normal conditions and the experiment based on the four periods. The graph shows that the average NO_x/SiO_2 is also highest for period 2. The average from the experiment is in this case set as 100 % and has the value of 26 ppm/% SiO_2.

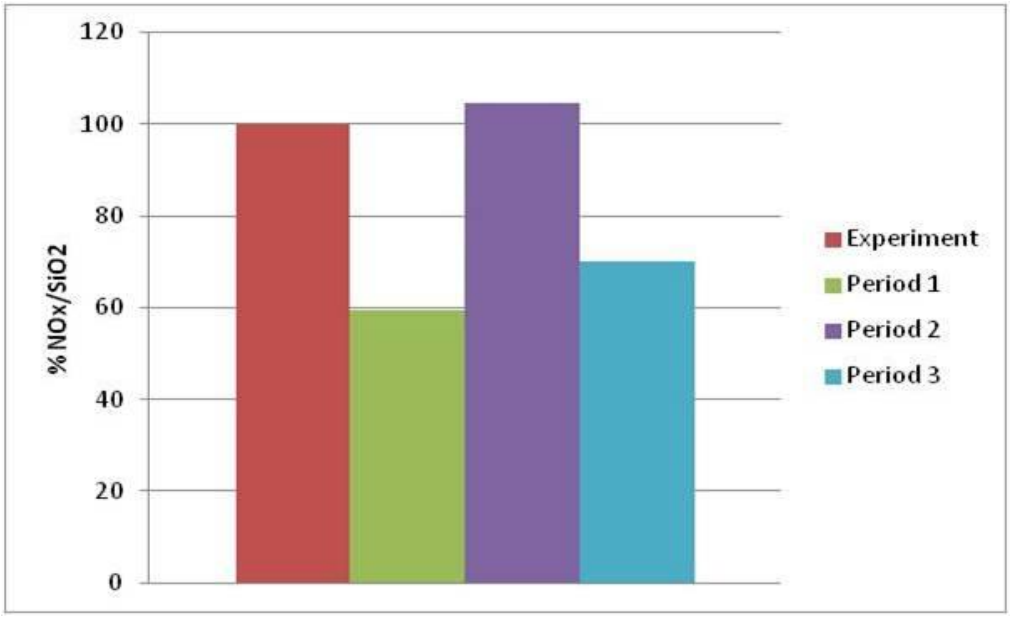

Fig. 6.5: NOx/SiO_2 for the three periods and the experiment is compared in this graph.

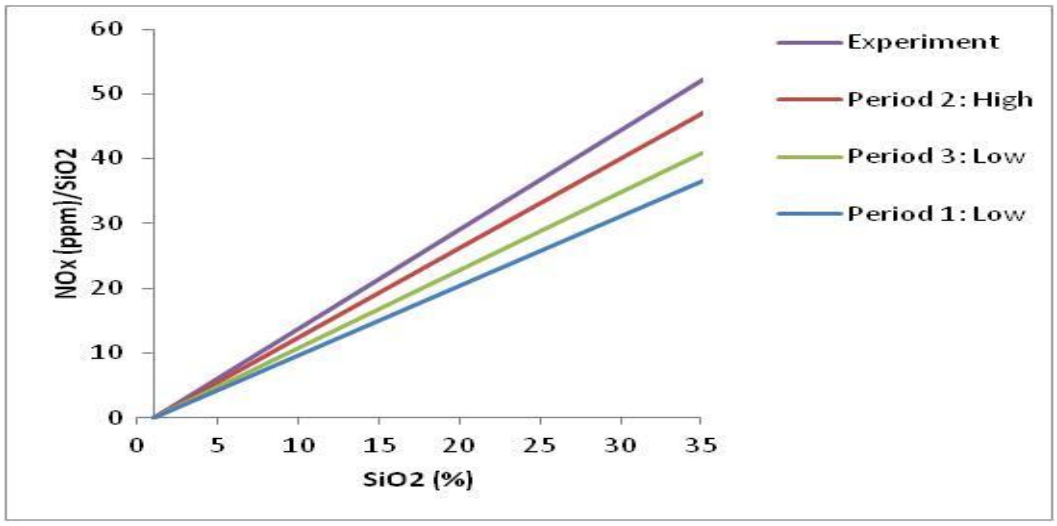

Fig. 6.6: This graph is made by plotting NOx/SiO_2 versus percent SiO_2 transmitted. Based on these plots the slope is found, and the slopes for the different periods are plotted in this graph.

In Fig. 6.6 the slope of NO_x/SiO_2 is found by making a scatter graph of NO_x/SiO_2 versus SiO_2 and adding a trend line. This shows that for the experiment the NO_x/SiO_2 increases more per unit SiO_2 than the periods from the normal conditions. In practice this means that the NO formation is higher for the experiment although the production of silica fume is high. These scatter graphs are shown from Fig. 6.7 to Fig. 6.10. These figures also reveal how the data is distributed. As an example, in Fig. 6.7, 38 % of the data was in the range of 0-10 NO_x/SiO (ppm/%).

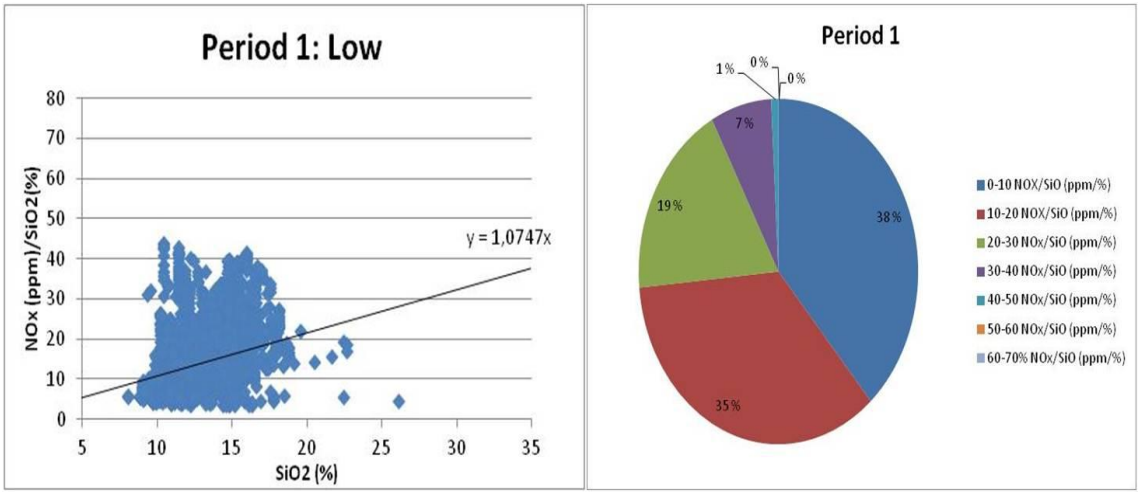

Fig. 6.7: The distribution of data from period 1 based on NO_x/SiO_2.

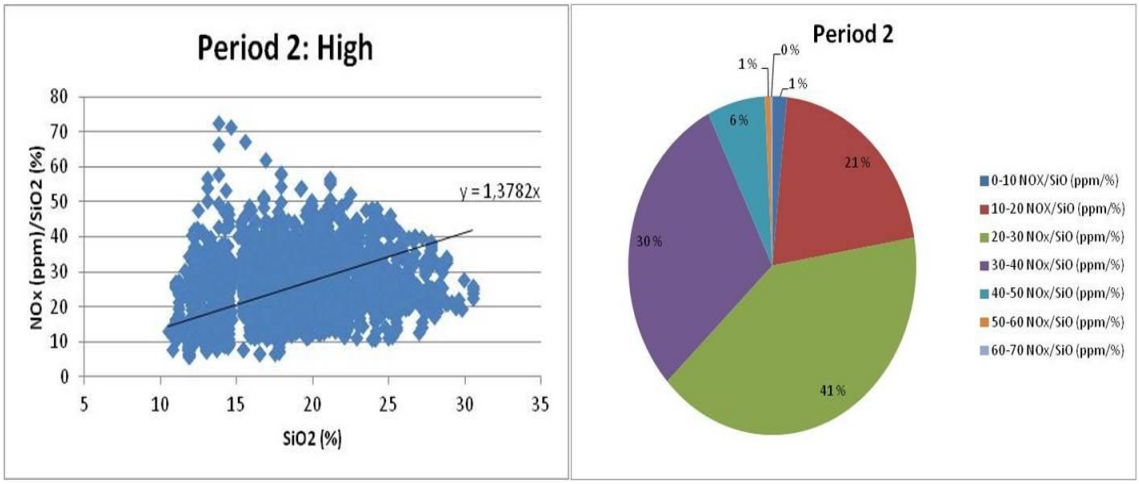

Fig. 6.8: The distribution of data from period 1 based on NO_x/SiO_2.

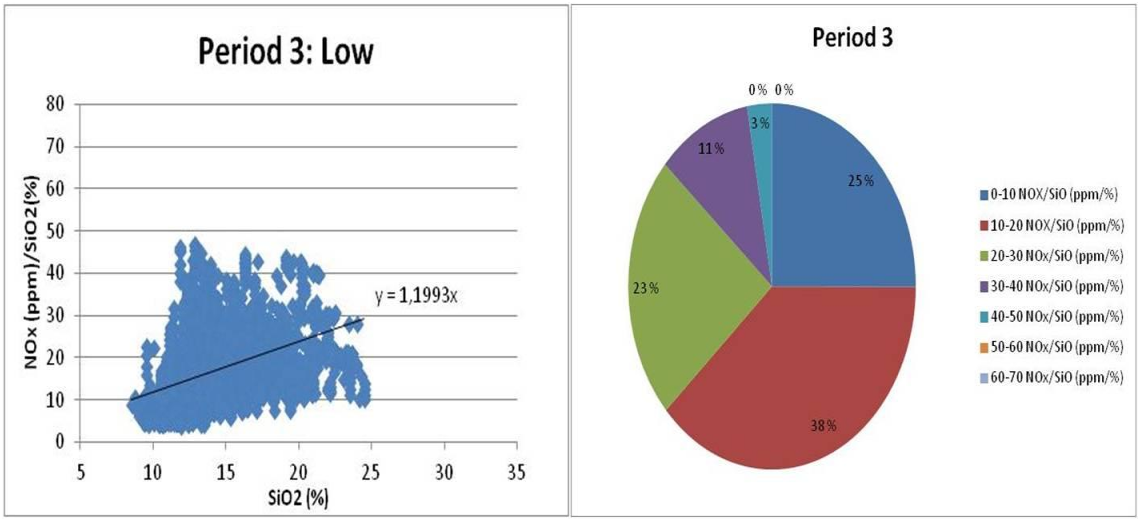

Fig. 6.9: The distribution of data from period 1 based on NO_x/SiO_2.

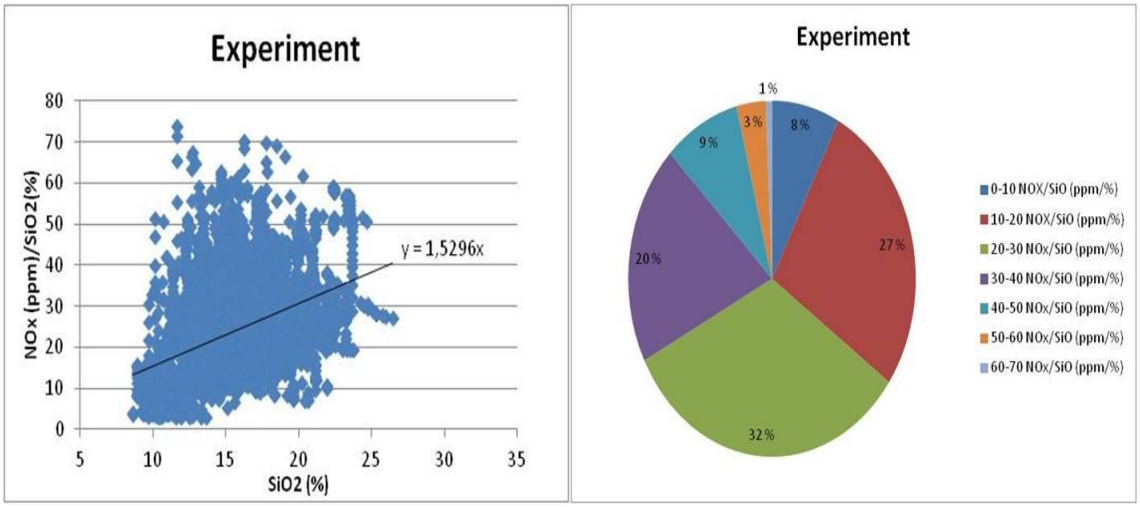

Fig. 6.10: The distribution of data from period 1 based on NO_x/SiO_2.

6.1.3 Effect of water

The response of water is clear for the pilot-scale experiment. Charging is linked to the water content because it is the process where the raw materials are fed to the furnace. Since there is a variation of NO_x for the normal conditions, it is natural to look into the four periods and how the water concentration behaves.

Fig. 6.11 to fig. Fig. 6.14 was plotted by taking sorting the data from the three periods and the experiment based on water content. It was natural to divide the data into the range from below 3.0 vol% H_2O to above 4.0 vol% H_2O. In practice slopes were found by plotting the NO_x/SiO_2 versus the SiO_2 that created scattered plots. From the scatter plots the trend lines intersecting zero is added to the plot, making it possible to compare the slopes based on water concentration. These slopes illustrate the trend, but it does not say anything about the distribution of the data. Every figure to the right show how the data is distributed. For period 1, which is a period of low emissions, 61 % of the data is in the range of 3.5-4.0 vol% H_2O. This means that the charge is more likely to have high water content, and this could explain why the NO_x is low during this period.

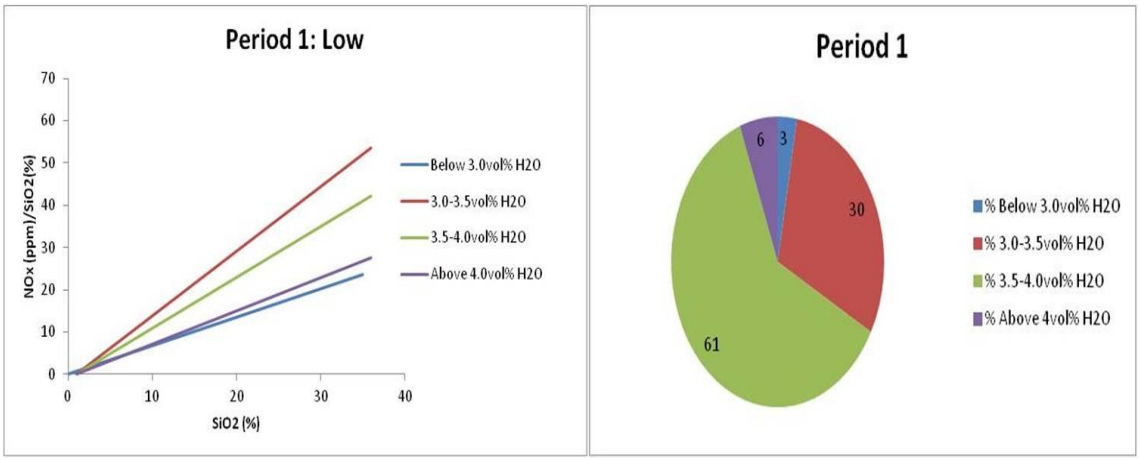

Fig. 6.11: This is a period with low NOx and the slopes of NO_x/SiO_2 versus SiO_2 based on water content are plotted together with the distribution of the data on the right.

In period 2, the NO_x-emissions were high. In the plot to the right in Fig. 6.12, 79 % of the data from this period is below 3.0 vol% H_2O, which indicates a dry charge. However, the slope to the left shows that less NO_x/SiO_2 is produced per percent SiO_2 when the water content is below 3.0 vol%. Based on the figures from the three cases during the normal conditions it can be noticed that the slopes based on the water content seems to have a random effect. For period 1 the slopes indicate that the NO_x/SiO_2 that is produced when the water content is below 3.0 vol% H_2O is lower than the water content above 4.0 vol% H_2O. This phenomenon will be discussed further in the discussion part. Most likely this is due to the amount of data. Statistically the data

should be more correct with a large amount of data. Seeing that only 3 percent of the data is found when the water content is from 3.5-4.0 vol% H_2O the results could be inaccurate.

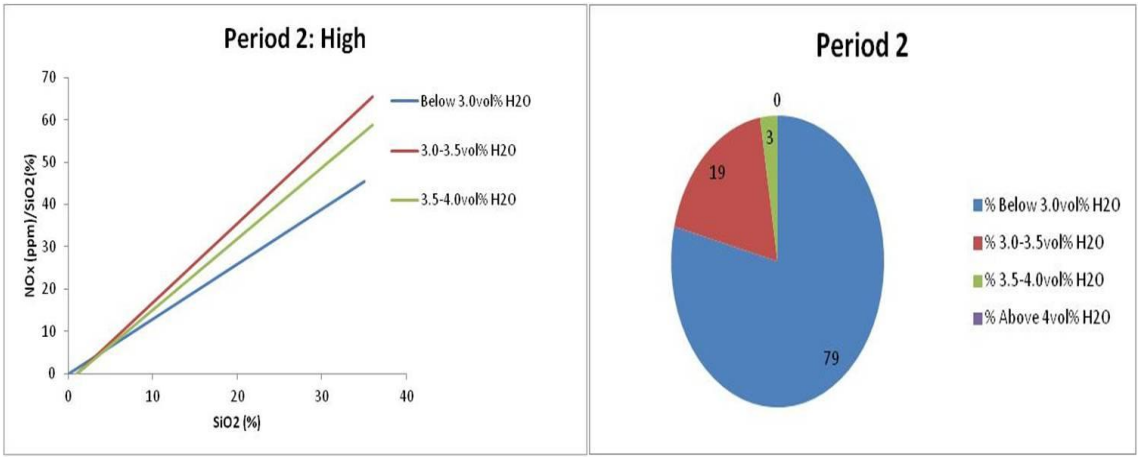

Fig. 6.12: This is a period with high NOx and the slopes of NO_x/SiO_2 versus SiO_2 based on water content are plotted together with the distribution of the data on the right.

Period 3 (Fig. 6.13) is characterized as a period with low emissions, and the data is more evenly distributed. This period is closer to the average NO_x of one of the furnaces at Elkem Thamshavn, which make this period interesting to discuss further.

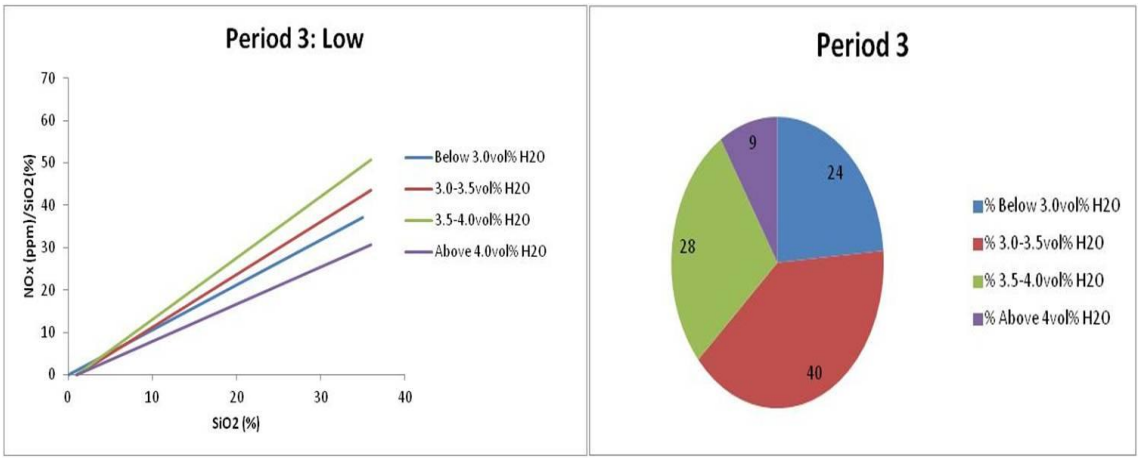

Fig. 6.13: This is a period with low NOx and the slopes of NO_x/SiO_2 versus SiO_2 are plotted together with the distribution of the data on the right.

This final plot based on the experiment (Fig. 6.14) is made to see the trend during the experiment. Noticeable from the figure to the left is that during the experiment the trend is according to theory regarding that for low concentrations of water the higher the formation of NO. From the figure to the right the data is also more evenly distributed. Another remark is that the furnace was charged less frequent during the experiment, which makes the batches of raw materials larger every time the furnace is

charged. In practice this gives the furnace more time to burn down and "dry" out, which can explain the large amount of data with values below 3.0 vol% H_2O. The amount of data was also larger compared to the other periods making the experiment more statistically accurate.

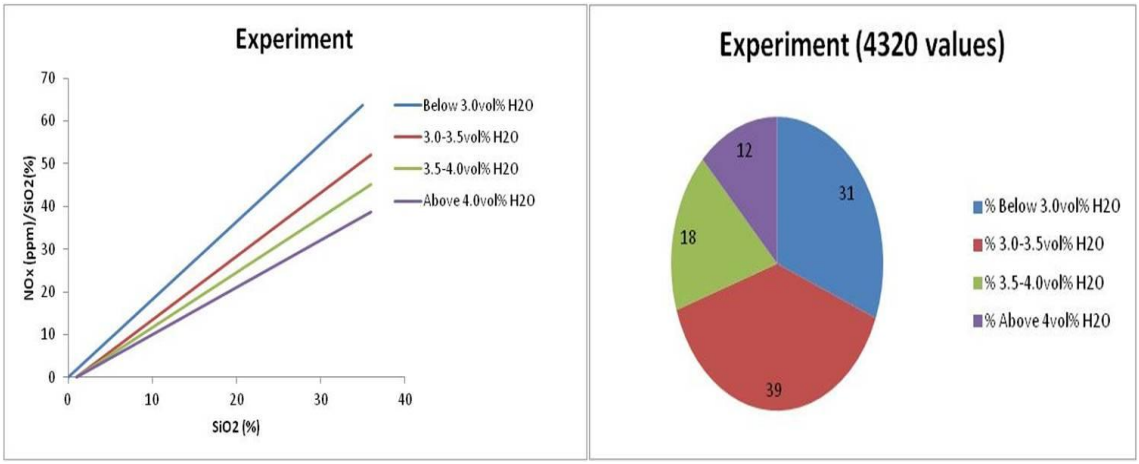

Fig. 6.14: This graph is taken from the experiment and the slopes of NO_x/SiO_2 versus SiO_2 are plotted together with the distribution of the data on the right.

6.1.3.1 Behavior of NO_x with the water content.

Based on the distribution figures of water it is possible to see the distribution of NO_x when the water content is at a specific range. From the four periods above, period 3 and the experiment are the cases when the water is more evenly distributed. A further investigation of these two periods has been done below.

Period 3 – A period with average emissions of NOx.

Fig. 6.15 illustrates the distribution of the data in different ranges of water content. From this graph the distribution of the values of NO_x can be investigated. This means that the data from for example below 3.0 vol% H_2O is set up in a table and sorted based on NO_x-emissions making new ranges. In this way it can be seen how the NO_x varies based on water content.

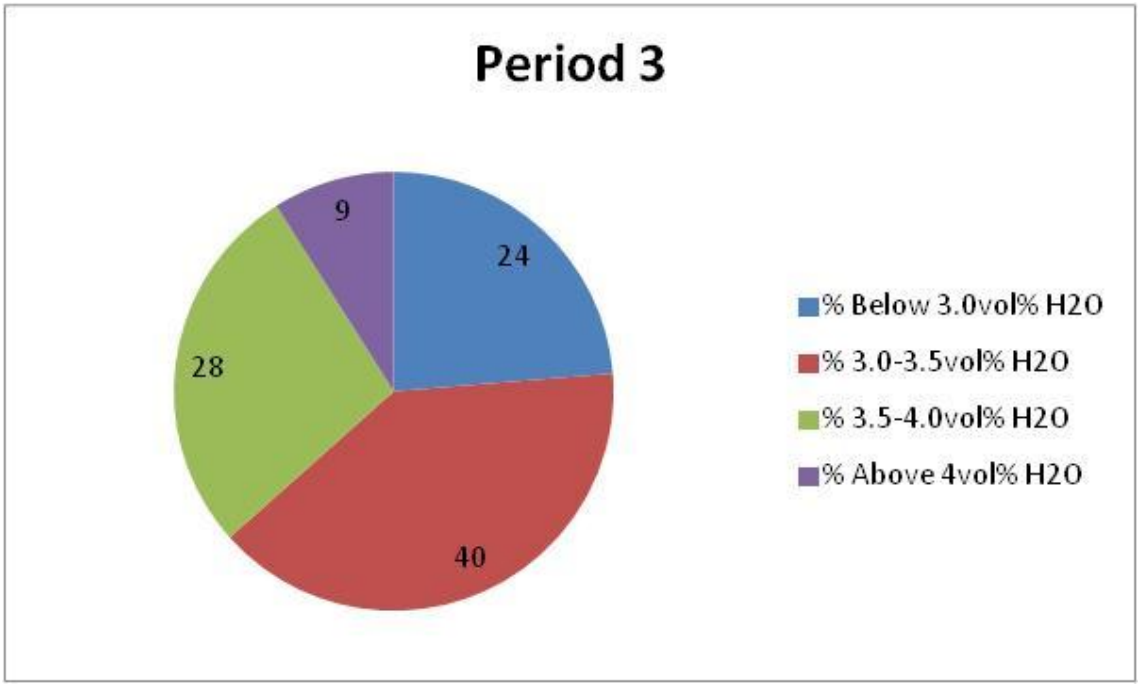

Fig. 6.15: This plot shows the distribution of data based on water content. As an example 40% of all the data is in the range 3.0-3.5 vol% H_2O.

Following there are four figures (Fig. 6.16 to Fig. 6.19) showing the distribution of NO_x based on the water content. The graphs below reveal how the higher ppm-levels of NO_x gradually decrease with increasing water content.

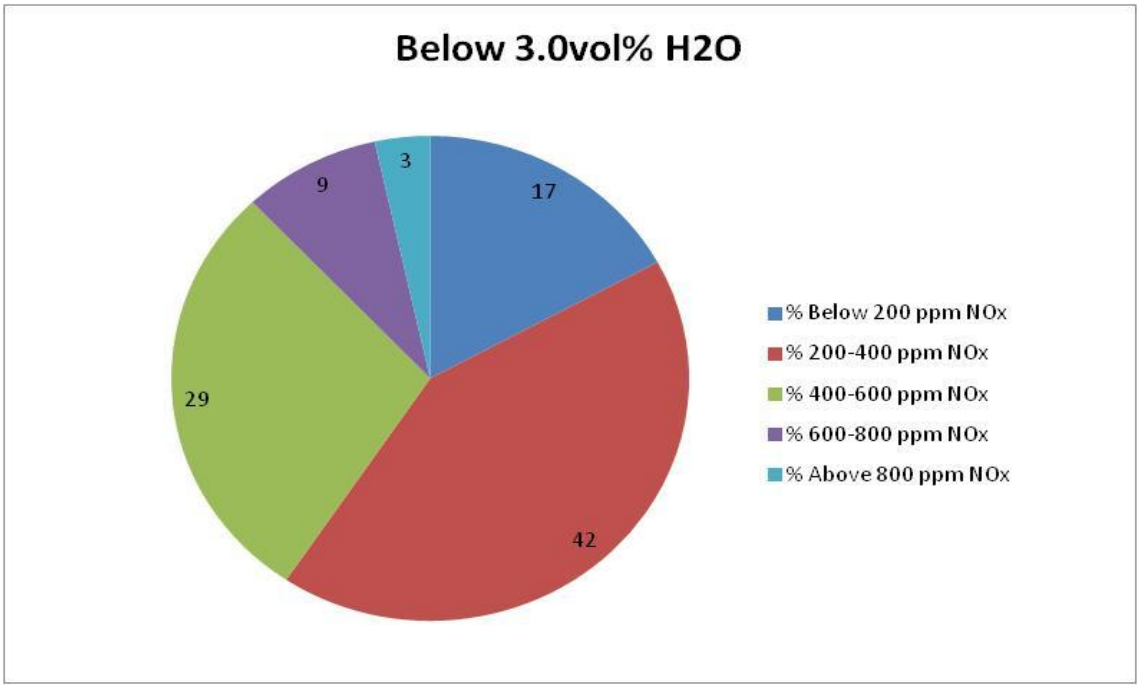

Fig. 6.16: Distribution of NO_x based on data with water content below 3.0 vol% H_2O. In this case there is data with both high and low ppm-levels of NO_x.

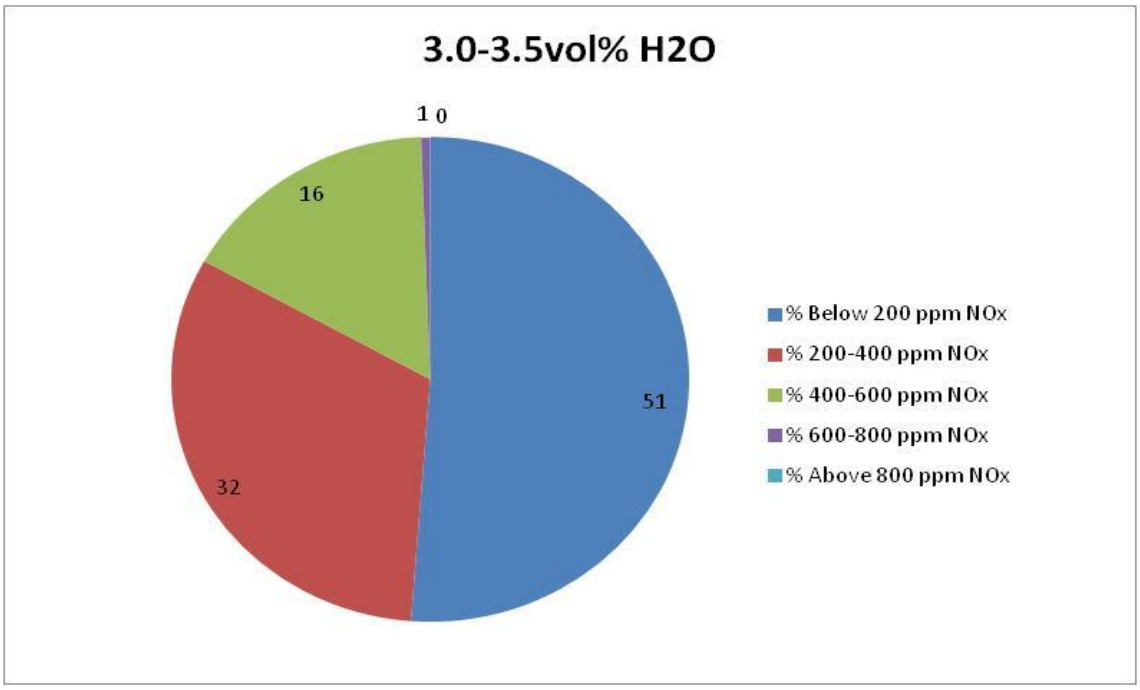

Fig. 6.17: Distribution of NO_x based on data with water content below 3.0-3.5 vol% H_2O.

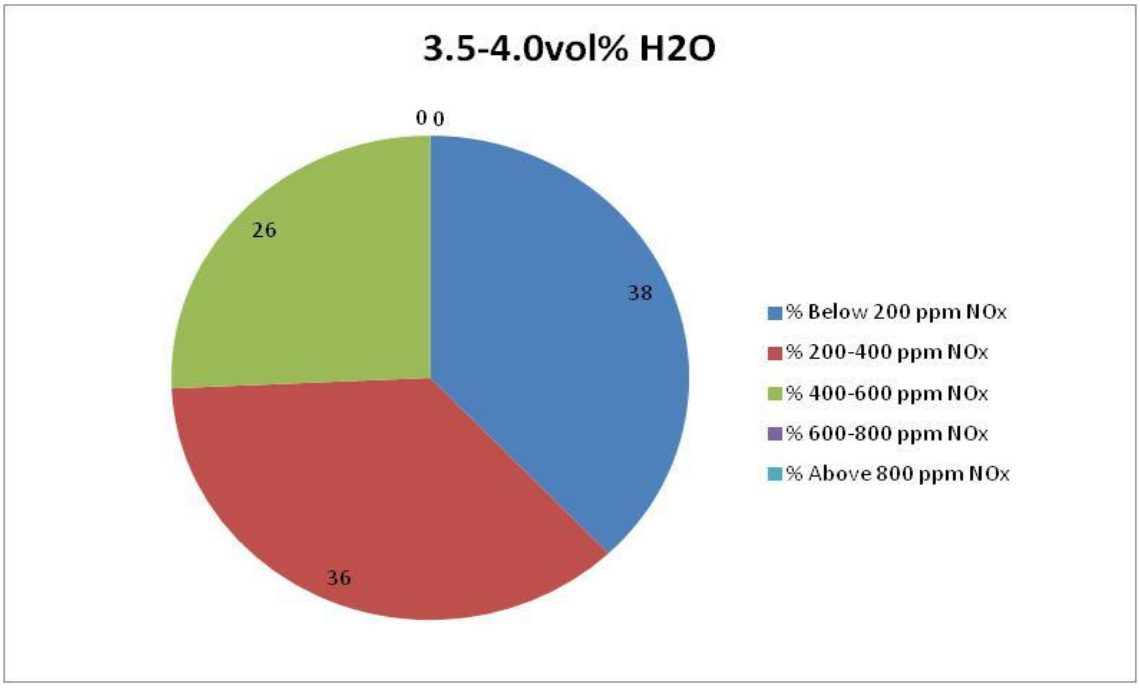

Fig. 6.18: Distribution of NO_x based on data with water content below 3.5-4.0 vol% H_2O. There is no NO_x above 600 ppm.

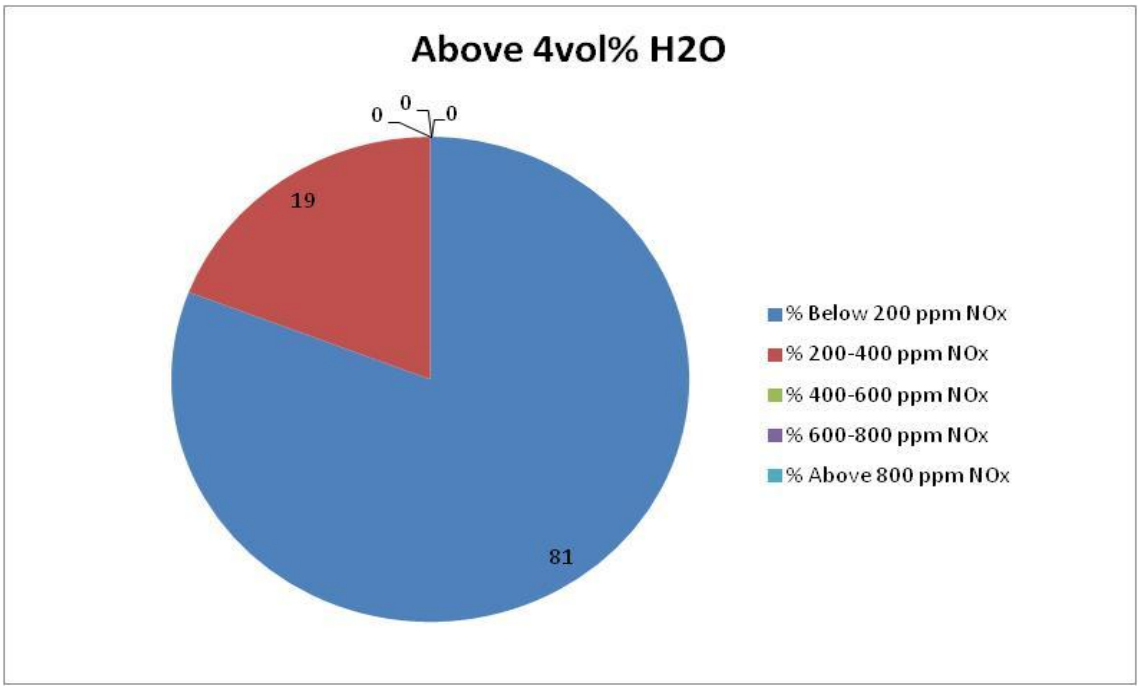

Fig. 6.19: Distribution of NO_x based on data with water content above 4.0 vol% H_2O. This graph shows that there is no NO_x above 400 ppm.

Experiment – A period with larger batches and a low charging frequency.

The same analysis of the results is done for the experiment as well as for period 3. A further comparison between these two cases will be analyzed further in the discussion part. The trend is however the same: higher values of NO_x are decreased with a higher amount of water.

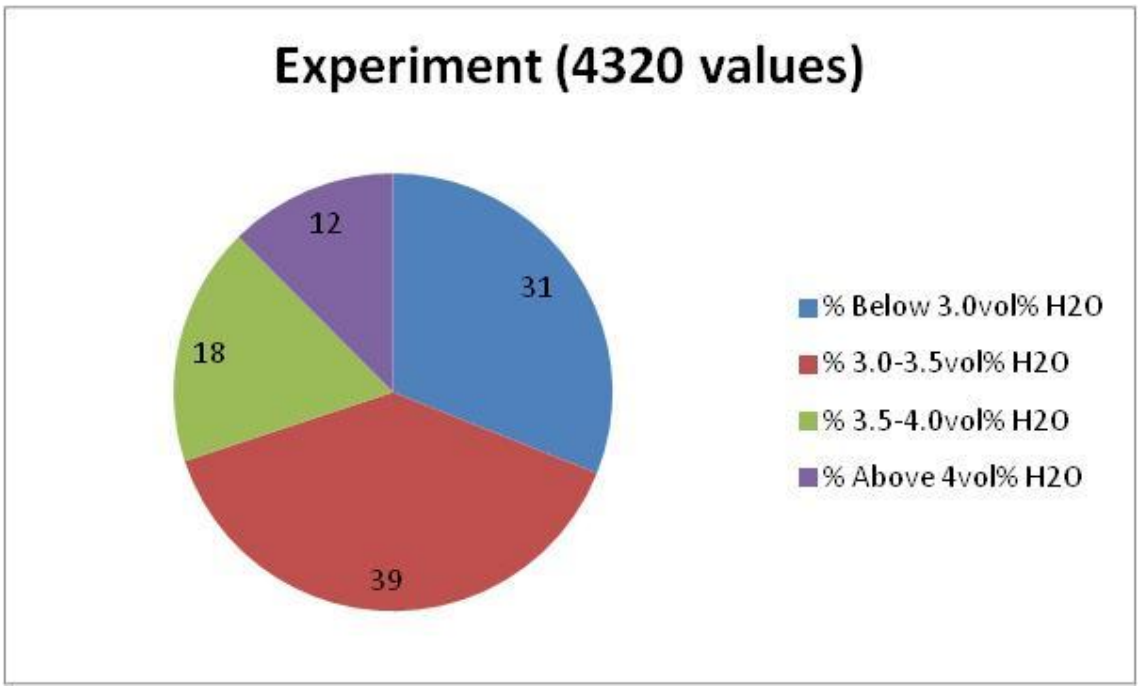

Fig. 6.20: This graph illustrates the distribution of the data from the experiments. The data is sorted based on water content and further the amount of data from a certain range is placed in the graph to see which range most of the data is found.

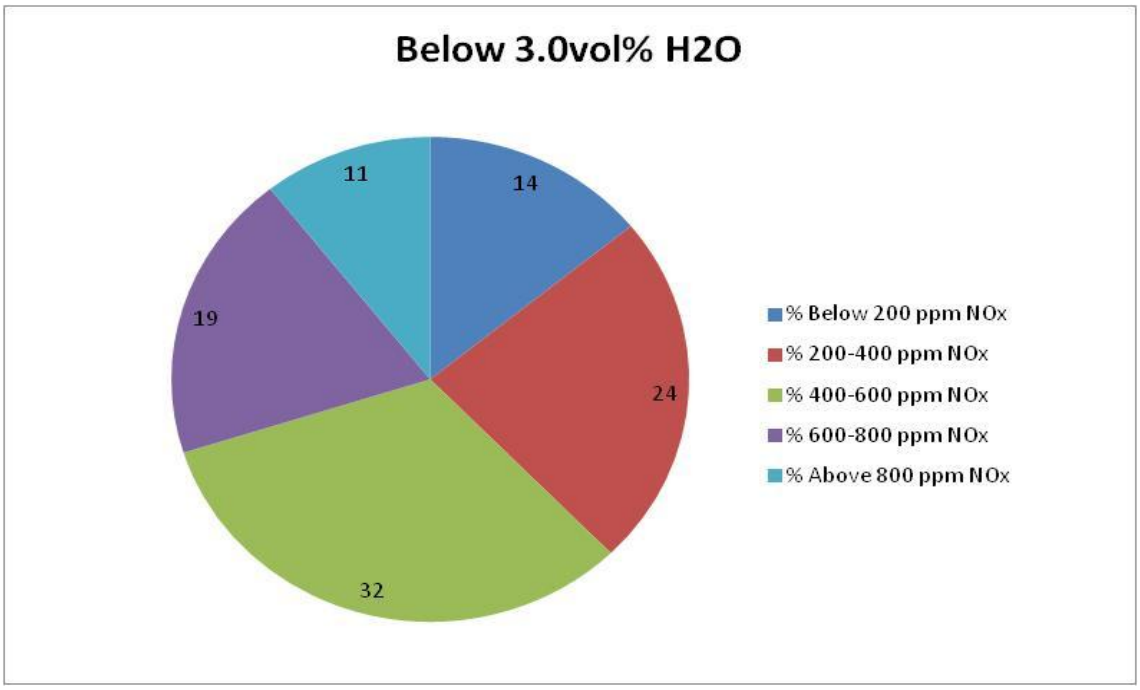

Fig. 6.21: The distribution of NO_x based on data with water content below 3.0 vol% H_2O. This graph shows that most of the NO_x is between 400 ppm-600 ppm

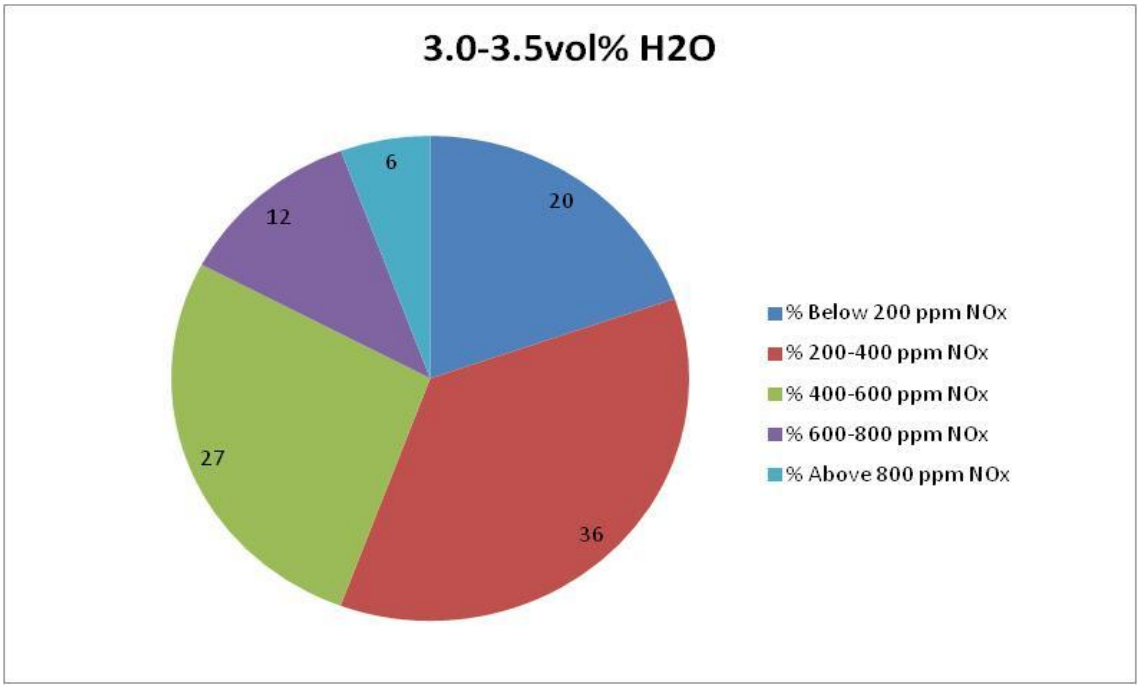

Fig. 6.22: The distribution of NO_x based on data with water content of 3.0-3.5 vol% H_2O. A higher amount of data is found when the NO_x-emissions are in the range 200 ppm-400 ppm.

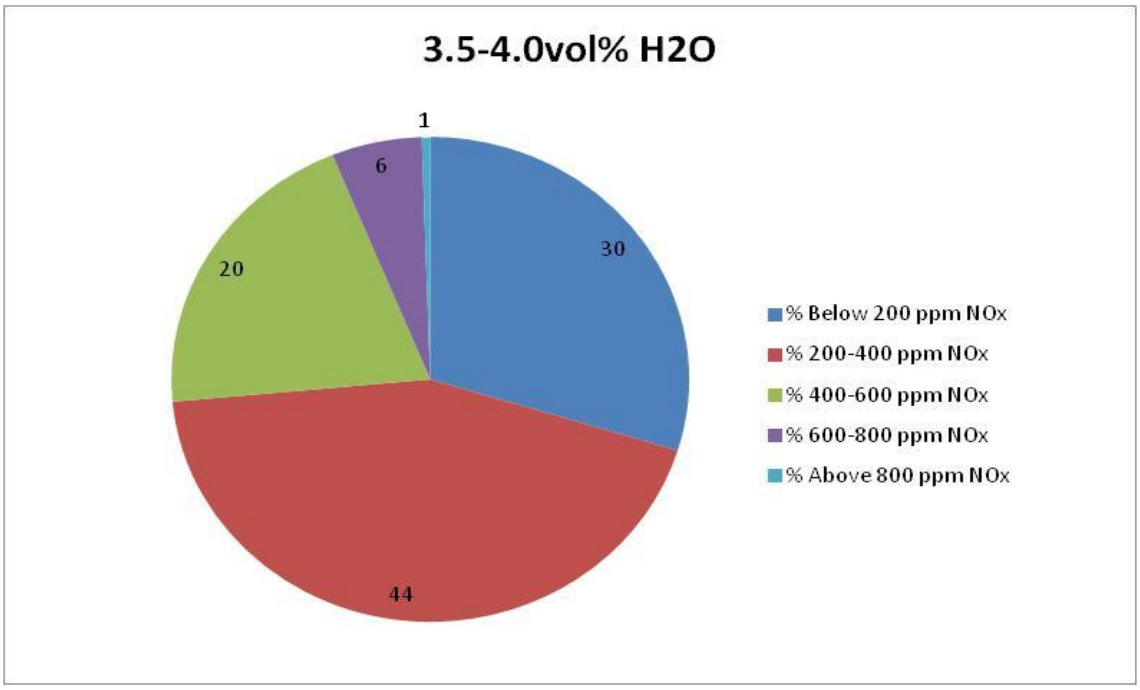

Fig. 6.23: The distribution of NO_x based on data with water content of 3.5-4.0 vol% H_2O. In this plot there is only 1 % of NO_x above 800 ppm. There is a general increase in NO_x with lower ppm-levels.

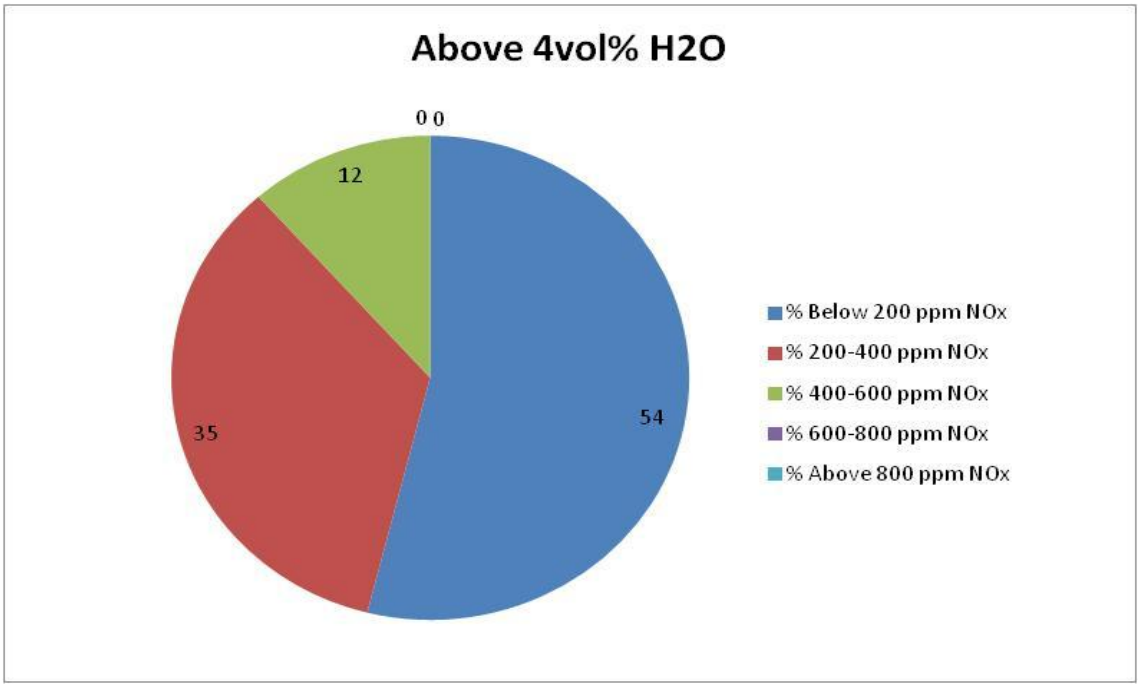

Fig. 6.24: The distribution of NO_x based on data with water content above 4.0 vol% H_2O. There is no NO_x above 600 ppm when the water content is above 4.0 vol%.

6.1.4 Dynamics during charging and stoking for the experiment

During the normal conditions the furnace is frequently charged. The feeder in the center charges the furnace about every minute, and with the other feeders working simultaneously it is difficult to see a reaction from the charging process. When the furnace is charged less frequent as in the experiment, it is easier to see the trend that has been found during the pilot-scale experiment and in furnaces with "batch-charging". During "batch-charging" the furnace is fed typically one time per hour with a large amount of raw materials (1000 kg). The trend regarding NO_x-emissions is that the water content increases creating a peak due to evaporation of water in the charge, at the same time the formation of NO decreases. The typical trend for a furnace that is continuously charged is that the water content is stabile with low variations.

To give an example of how the NO_x behaves during charging, Fig. 6.25 shows that during the normal conditions there is no clear peaks in the water content. Because of the stoking there is a small increase in water, while there is a low point for the NO_x. This example relates to theory since small frequent batches give almost a constant amount of water and volatiles to the charge surface. Before the water has the time to evaporate a new batch is fed to the furnace. The stoking will however have an impact since some of the gas channels will be covered with raw materials, preventing blows resulting in combustion of SiO.

The silicon furnace is a complicated system with many variables that can contribute to the formation of NO. The period for the normal conditions in Fig. 6.25 is taken in a period with low NO_x. In situations where the charge is "dry" and burned down, the dynamics will probably be different than the example in Fig. 6.25. High periods of NO_x-emissions are normally observed when the operational conditions of the furnace are unusual.

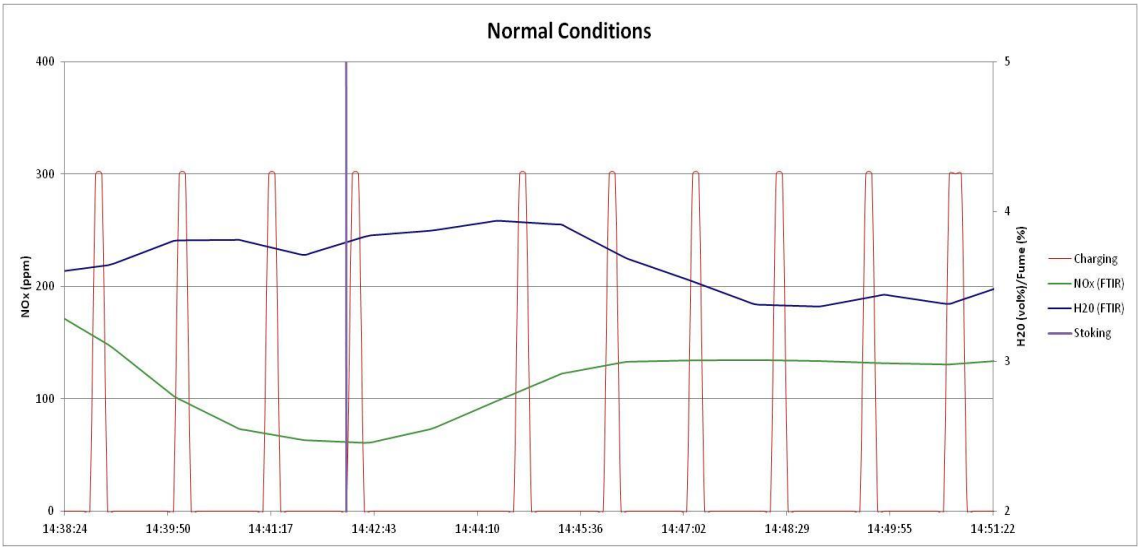

Fig. 6.25: An example of how the water behaves during charging and stoking. As it can be seen from the graph there are low variations in NO_x and in the water content. The furnace was stoked around 14:42 and the effect of this was a small increase in the water content.

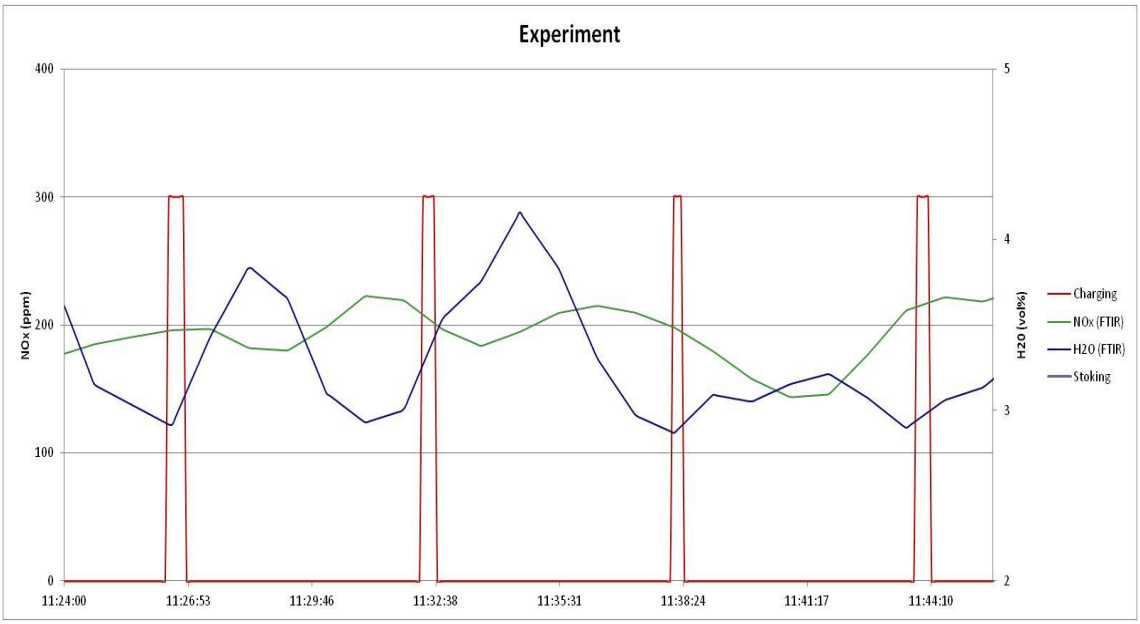

Fig. 6.26: This is an example of how the NO_x and water behaves during the experiment. Compared to the normal conditions there are clearly peaks of water resulting in a low point of NO_x.

In Fig. 6.26 there is a different dynamics, and this is similar to the behavior during "batch-charging" with typical peaks of water. In this case the center feeder charges around every five minutes, so this is not a condition that is close to "batch-charging", but compared to the normal conditions there is a difference in the dynamics.

6.2 Discussion

In the experiment there is only one parameter that is changed and that is the charging frequency. The center feeder is charged every five minutes instead of every minute, and from the theory involving charging it is expected that the average will increase. With the conclusion from the pilot-scale experiment being that water clearly reduces the emissions, the response of water is investigated in all of the results. Seeing the experiment is primarily about the effect of charging, it is natural to start the discussion with this parameter.

6.2.1 Effect of charging frequency

Nils Eivind Kamfjord (Kamfjord) did a parameter study in his PhD regarding the emissions of NO_x, stating that the primary formation mechanism of NO formation was related to the combustion mechanism that produces silica fume. He collected data from a furnace that was "batch-charged" and in Fig. 6.27 the typical dynamics of the behavior of NO_x is illustrated.

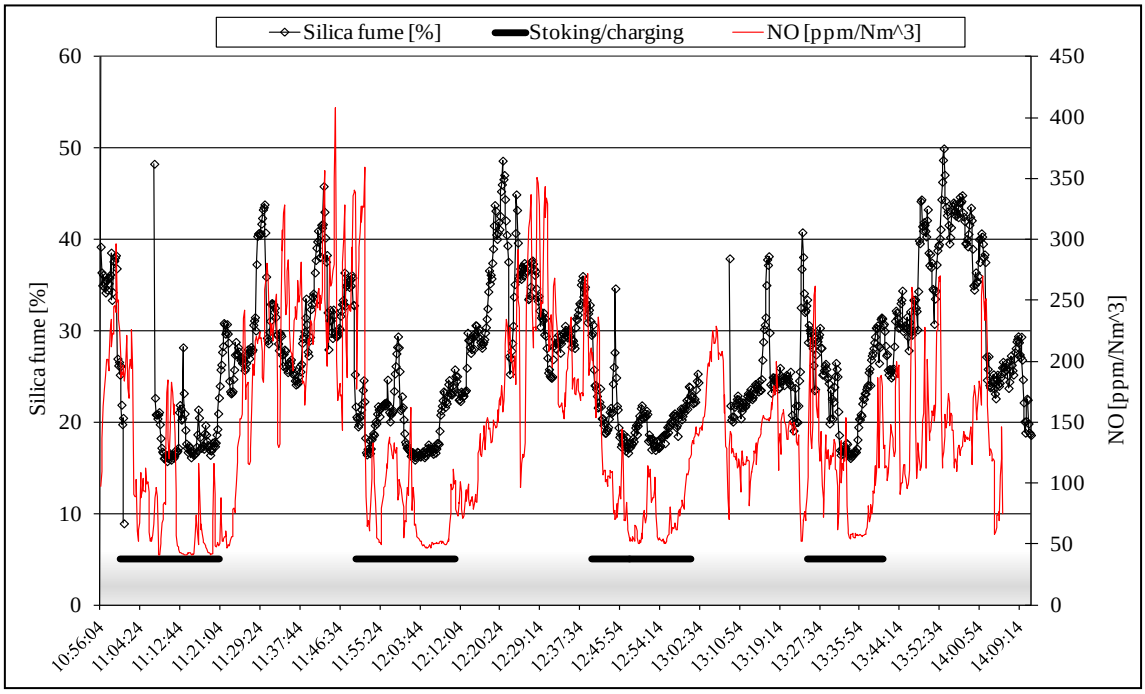

Fig. 6.27: This figure is taken from Kamfjords PhD (Kamfjord). The figure illustrates the effect of batch charging but also how the silica fume is related to NO_x-emissions.

The typical NO_x behavior for a furnace that is "batch-charged" is that a huge amount (1000 kg) of raw materials is fed to the furnace. After the charging process, the furnace is typically stoked to even out the raw materials and to fill gas-channels along the electrodes and the charge wall. The response of the charging process is a decrease in temperature at the charge furnace, evaporation of water from the raw materials and the combustion of volatiles. All of these reactions give low emissions of NO. After

these reactions take place the emissions and temperature gradually increase. The charge is burned down and reactions in the crater create gas-channels with SiO(g) that combusts at the surface.

In this experiment the furnace is continuously charged, which is the opposite from the type of charging that can be found in Fig. 6.27. This means that the typical trend that is found from "batch-charging" is more difficult to find because the time interval between every charging is every minute compared to every hour.

The easiest way to see if the charging frequency has an impact on emissions would be to compare data from a furnace with batch-charging and a furnace that is charged continuously. It is however difficult to compare data from two different furnaces due to that no furnace is similar geometrically and every furnace behaves differently. Using average values can also be misleading, because there are huge variations in emissions in such a huge and complex system.

In this experiment the furnace is continuously charged. However, a small change in batch-size and charging frequency will have an instant effect on dynamics of the emissions. The reason for the change in dynamics is that the batch-size goes from around 150 kg to 750 kg. In other words, the change in charging frequency creates a trend that is similar to the one for batch-charging. The results (Fig. 6.28) show that the average NO_x is higher for the experiment than the average during a period of five days. It is however difficult to say of this is due to some operational conditions giving a high period or if it is directly related to the experiment.

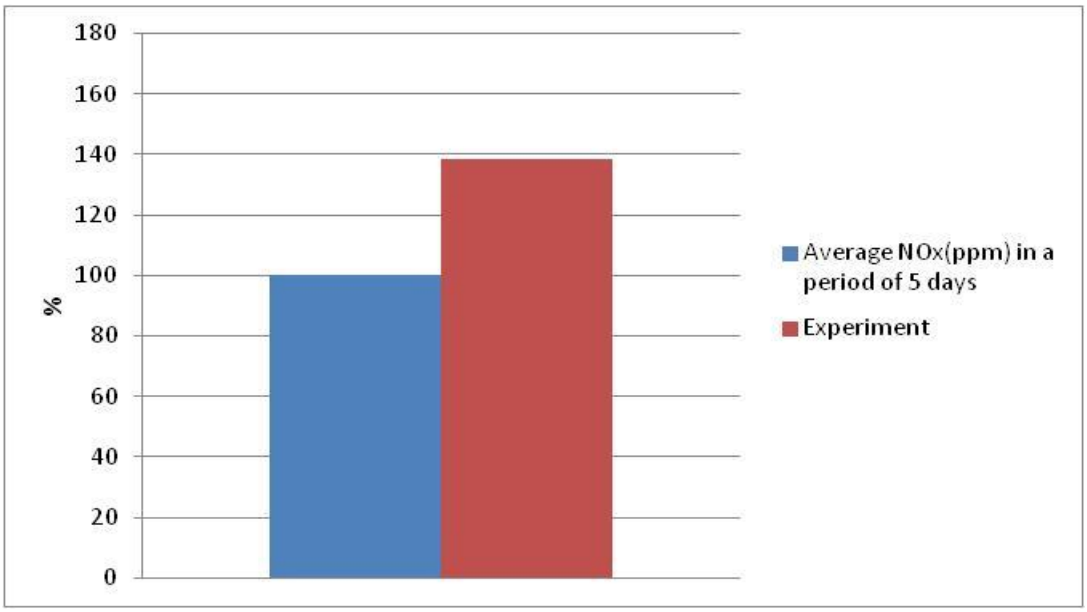

Fig. 6.28: Comparing the average from a longer period with the average during the experiment.

There are several indications that the average is higher due to the experiment rather than other operational parameters. The average silicon yield for the period during the five days is found to be 66.7 and for the experiment the silicon yield was found as 70.3. Knowing that the formation of NO is directly related to formation of silica fume, the average found in the “five day period” should in theory have been higher than for the experiment. This is however valid if the furnace is running 100 % every day, and this is not the case.

Another indication that the experiment influenced the increase in the emissions is the change in dynamics. Fig. 6.29 is an example of this change.

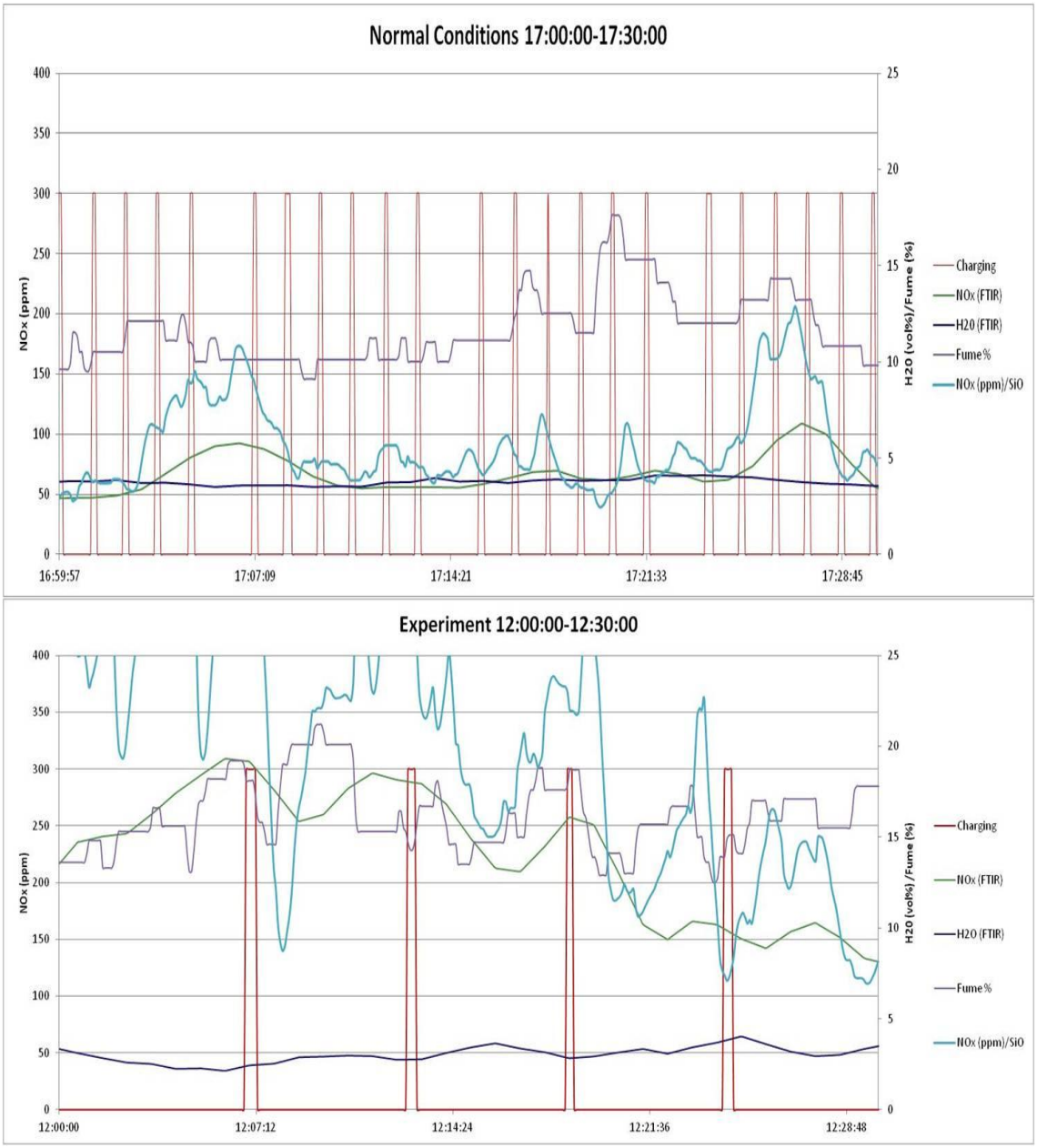

Fig. 6.29: A comparison between the dynamics for the normal conditions and the experiment. Both are taken from periods at times that are typical. The water content is seemingly constant for the normal conditions. For the experiment there are small variations. This is also the case with the NO_x-emissions, there are fewer variations for the normal conditions, but for the experiment it is observed more peaks in the emissions.

Fig. 6.29 included two graphs plotted in a time interval of 30 minutes. The graph plotted for the normal condition period is characterized by a low average in the NO_x-emissions. The average for this plot is 200 ppm and that average is below what is assumed to be the general average of 300 ppm. However, the graph from the normal period and the graph from the experiment are representative if the purpose is to show the trend in the dynamics. For the graph showing the normal conditions, the dynamics of NO_x, silica fume and water behaves according to the theory that is related to continuously charging. The water content is stabile, the silica fume variations are small and the emissions of NO are low. With a lower charging frequency the peaks of NO_x is seemingly more frequent due to larger batches, more blows and a higher overall temperature. The dynamics of the experiment is similar to the trend of batch charging. The experiment is charged every five minutes and a batch charged furnace is charged every hour. Although the experiment is not exactly batch-charging, the dynamics show that changing the charging frequency does create peaks in the emissions due to larger batches.

The results in Fig. 6.30 show how much NO_x is produced per percent produced silica fume. The figure indicates that more NO is formed for the experiment compared to the normal conditions when a certain amount of silica is produced. These results can be related to theory because it gives an indication that the temperature must have been higher seeing that the formation mechanism of thermal NO_x is dependent on temperature. The SiO(g) will combust when reaching the charge surface and give produce heat that is sufficient enough to form NO. The NO-forming reaction is the reaction between the oxygen radicals and nitrogen in the air. Since the average emissions are higher for the experiment it means that more oxygen radicals, formed by the combustion of SiO(g), have reacted with nitrogen in the air and produced NO. When the temperature is higher, the reaction rate between the oxygen radicals and the nitrogen in the air is also higher, due to that the reaction rate is dependent on temperature.

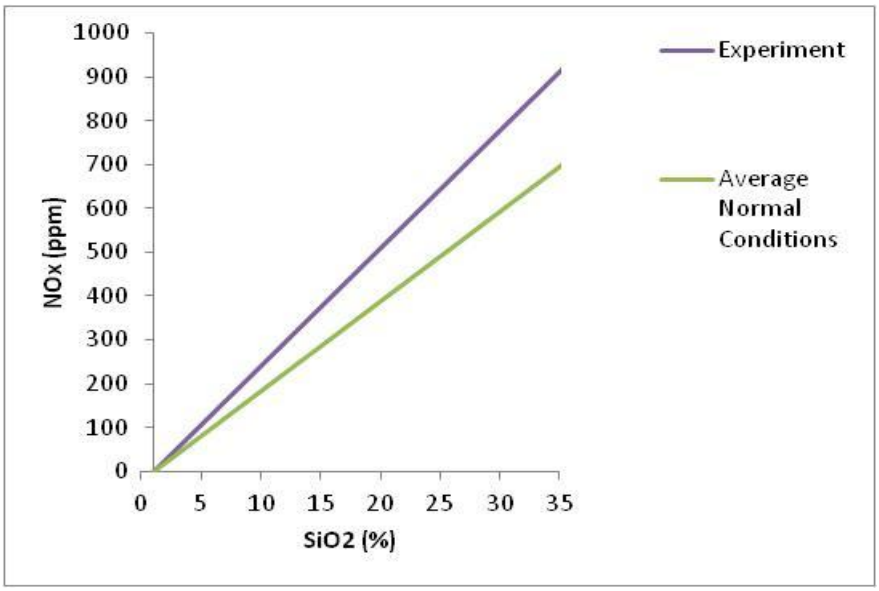

Fig. 6.30: For the experiment there is more NO_x produced per unit SiO_2 compared to the normal conditions.

6.2.2 Effect of water

An important part of this study is the effect of water on the emissions of NO. The results from the pilot scale experiment indicate a correlation between water and the emissions, which is the background for studying the effect of water. Although the mechanism is not fully understood in the literature, there are several findings that show that the water reduces the overall temperature of the flame and there is also found a decrease in oxygen atoms. (Bhargava, Sowa, Casleton, & Maloney, 2000) (Guo, Neill, & Smallwood, 2008).

As mentioned in the results-chapter, the normal conditions are divided into three different periods based on NO_x-concentration. The background for choosing these periods is due to an observation of the dynamics of the NO-emissions. The dynamics of the emissions show that there can be periods with either high or low concentrations of NO. Fig. 6.31 is plotted to see the trend during periods when the condition of the furnace is considered to be normal, but the average of NO is different (200 ppm and 500 ppm).

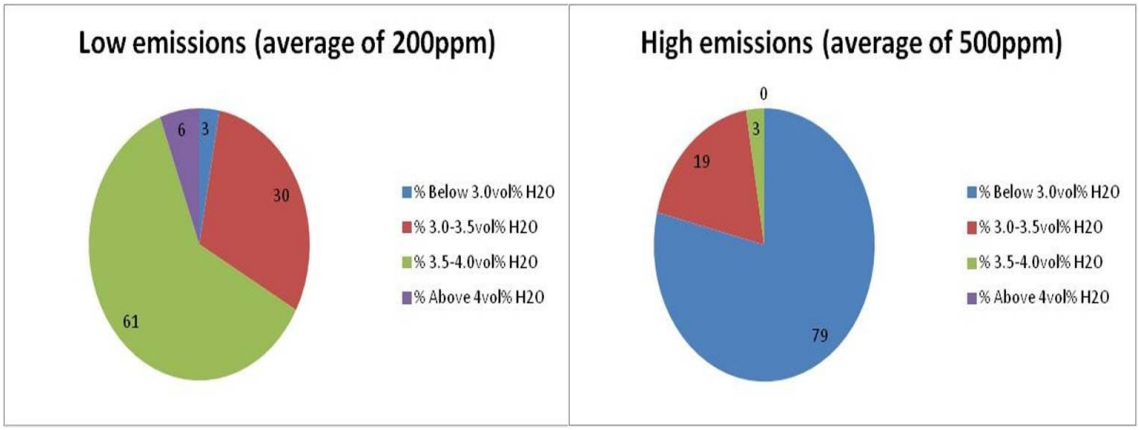

Fig. 6.31: An example of how the water is varies during low and high emissions of NO_x.

The two graphs in Fig. 6.31 are showing the distribution of data at different water concentrations. In the plot to the right the emissions of NO_x are high with an average of 500 ppm. The plots are based on data measuring every five seconds for four hours. The relevant part is that the data is distributed differently although the averages are different. For the high emissions 79 % of all the data is below 3.0 vol% H_2O, and this clearly indicates a dry charge that in theory should give high emissions. For the figure to the left with the low emissions 61 % of the data from this period is between 3.5-4.0 vol% H_2O. The conclusion from this figure is that high water content seemingly reduces the emissions.

Although the trend is clear, these data are collected from a limited time in selected periods. The plant does not measure water content in the off-gas system, so the only measurements of the water concentration are from the FTIR measuring device that measured for 25 hours. The lack of measurements of the water concentration makes it difficult to investigate other relevant periods from the furnace.

For period 2, the average NO-emission is around 500 ppm, and the explanation of the high average can be related to the condition of the furnace. Before this high emission period there furnace was stopped twice due to that the electrodes were not in suitable position. This problem can be solved by adding quartz around the electrodes. When reducing the power load of the furnace the temperature automatically decreases and the charging is stopped due to safety reasons. The observation of low levels of evaporated water strengthens this theory. The uneven charging and the stops contributed to a dry charge and influenced the emissions.

The distribution of the data is dependent on what period the data is collected from. If the data is collected from a period with high average emissions it is likely that there is a small amount of data with a water-concentration above 4.0 vol%. The plots that are interesting to study are the graphs where the data is distributed evenly, because they

are more statistically accurate. The period that is most evenly distributed is period 3. The data is also evenly distributed for the experiment, but the furnace is not in a normal operational condition when the charging frequency is changed. By studying a case where the emissions are assumed to be close to the average it is more likely to get information about how the water content influences the emissions during the normal conditions.

Fig. 6.32 is complicated, but the figure shows how the data is distributed for period 3 and the figure also shows the distribution of NO_x at a specific water concentration. As it can be seen from the figure, 40 % of all the data is in the range 3.0-3.5 vol% H_2O. From this plot, the behavior of NO_x can be understood further by showing the distribution of NO_x. The bar-plot illustrates that 50 % of the data is below 200 ppm when the water concentration is between 3.0 vol% H_2O to 3.5 vol% H_2O.

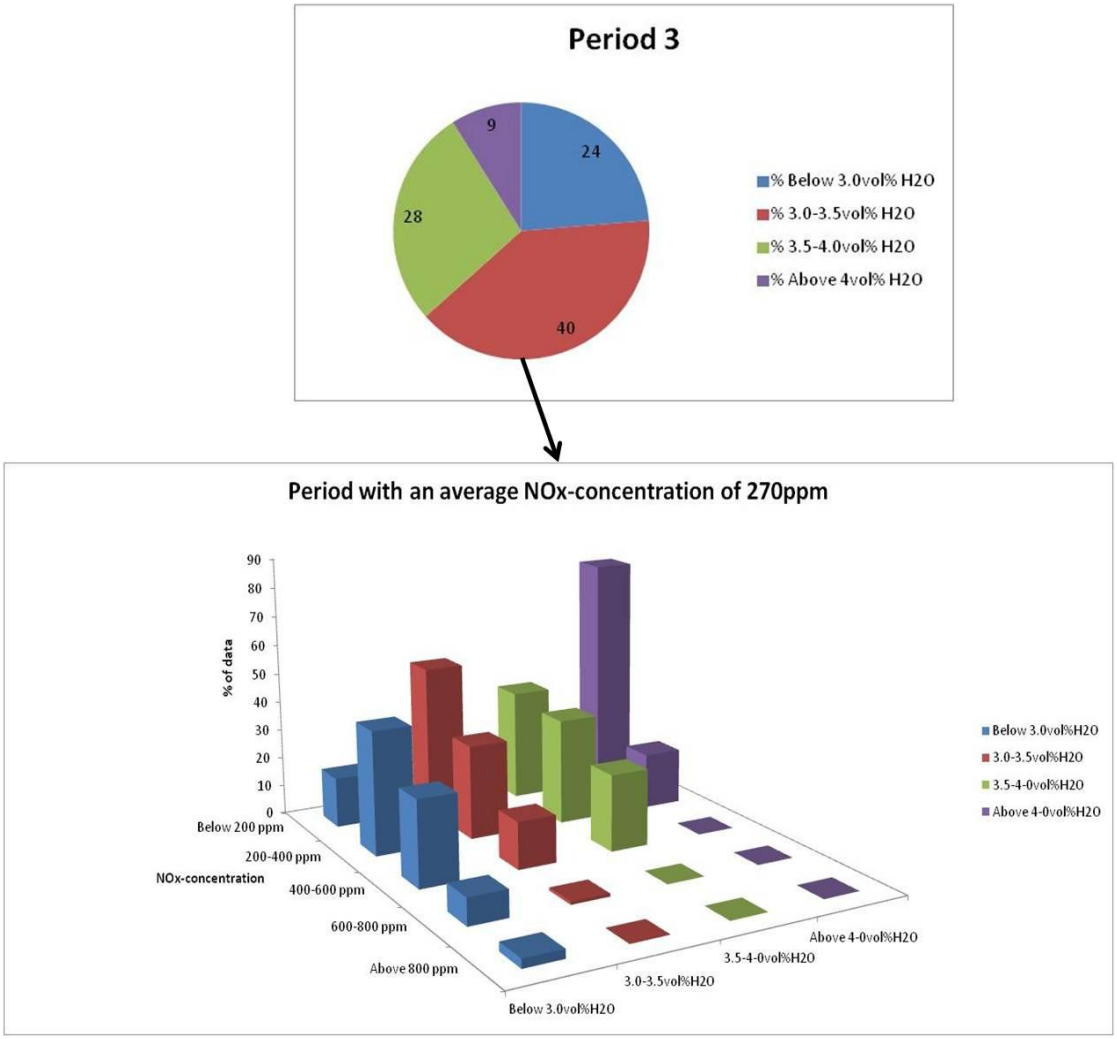

Fig. 6.32: This figure shows the distribution of NO_x when the water content is in the range 3.0-3.5 vol% H_2O. Observing the graph further, the conclusion is that there is no amount of NO_x above 800 ppm when the water content is in the given range.

Fig. 6.32 can be used to show how much water is needed to keep the amount of NO_x at a certain level. However, these data are not absolute; meaning that for other cases there can be NO_x-levels above 800 ppm when the water content is between 3.0-3.5 vol%. Also, the data are limited since it is only 40 % of data collected from four hours. The trend is the same for the experiment and the other periods with a decreasing amount of NO_x with increasing water content. If the same figure was to be made for the experiment, 6 % of the data would be above 800 ppm. For the experiment the data is taken from a time period of six hours and statistically this implies that the results are more correct. This difference could also be due to a higher overall temperature in the charge due to the change in charging frequency. This theory could be supported by a general higher average in the NO_x-concentration during the period.

Further, increasing the water amount from 3.0-3.5 vol% to 3.5-4.0 vol% there is no levels of NO_x above 600 ppm for the period described above in Fig. 6.32. The average NO_x during this water level is likely to be around 200 ppm, and this can be compared to the case with the low emissions where the emissions were 200 ppm.

As a conclusion, the emissions are low (around 200 ppm) when the water content, measured in the off-gas system, is above 3.5 vol% H_2O. The only background for this statement is the trends found in the 25 hours when the FTIR was measuring the water content. The theory behind this statement can only be related to that the water reduces the overall equilibrium temperature leading to a low reaction rate between oxygen radicals and nitrogen in the air. It is clear that this mechanism have to be studied further.

6.2.3 Theoretical calculations: water and silica amount in the furnace

The total amount of water added to the furnace per day is approximately 35 tons. This number is taken from the industry and is calculated based on the raw material mixture. The amount of water is 14 % of the total amount of raw materials.

The mass balance for the system is the same, which means that the amount of silicon that goes into the system needs to either go to the metal or to the silica in the off-gas system. During this day the silicon yield was 70.4 %, which means that 70.4 % of the silicondioxide put into the system is recovered in the metal.

The amount of SiO_2 that goes into the system (from all raw materials) is 124 tons, and from this amount 41 tons silicon is tapped from the system.

$$(x+1)SiO_2 + (x+2)C = Si + x\,SiO + (x+2)CO \qquad (6.1)$$

Reaction (6.1) can be used to calculate the theoretical amount of silicon metal and silica produced from the process. In the reaction equation, x is found from the silicon

yield. Calculations show that theoretically 40.95 tons of Si is supposed to be produced from the process, which is close to the 41 tons Si that actually is produced. However, the amount of dust measured during this date is 89 tons and the theoretical data shows that the amount of silica should be 83 tons. The dust that is measured is a combination between carbon and other particles, which can explain the deviation of 6 tons.

6.2.4 Further work

In the industrial experiment the emissions of NO_x are found to be low in periods where the water-concentration is high. The mechanism for this reduction is related to a decrease in temperature and oxygen radicals, but the reaction mechanisms are not understood. It is necessary with a basic study related to this subject. There is some uncertainty to if the water somehow reacts with the oxygen radicals seeing that in theory the OH-concentration increases when water is submitted to the experiments with premixed flames. An idea could be to do experiments with different raw materials while measuring the water and NO_x to see how different raw materials behave during combustion of SiO(g).

7 General discussion: Comparing the pilot-scale experiment and the industrial experiment.

Chapter 5 and chapter 6 include the results for from the pilot scale experiment and the industrial experiment. In every chapter the results have been followed by a discussion, but there are some trends that are clear for both experiments although the purposes of the experiments are not the same.

A pilot scale furnace and an industrial furnace are difficult to compare seeing the power load and the overall temperature is higher for the industrial furnace. Basically the industrial furnace is larger with a system that is complex and more difficult to control. Because of the scale difference between the industry and the small furnace, the data is not compared directly due to that the emissions from the industry much larger.

There are other differences in addition to the size and geometry. The industrial furnace has a constant inlet of air, meaning that the amount of air is not controlled in the same way as for the pilot scale furnace where the air came through open rings surrounding the furnace. The inlet of air will control the gas velocities on the charge surface and this will also influence the emissions.

The raw material mixture will also be different for these two cases. For the pilot scale experiment the mixture is set up to create a wet and dry charge. In the industry the mixture of raw materials are set up to achieve high silicon yield. The mixture is a combination of quartz, woodchips, charcoal and coke based on with beneficial contaminations and the carbon source is normally selected based on reactivity and fixed carbon. The charge will in this case consist of both wet and dry carbon.

The charging and stoking pattern is another important difference. In the pilot scale experiment the furnace was charged based on observation. Charging the pilot scale furnace can be compared to a combination of charging and stoking the industrial furnace. When charging the pilot scale furnace the raw materials were added manually and the furnace was fed by adding raw materials to the positions where it was needed. In the industrial furnace used in this experiment the furnace was charged automatically and continuously followed by stoking the furnace with a lance. During stoking the industrial furnace can be manually charged by the operators if it is necessary. As a conclusion it can be stated that the pilot scale furnace is charged by “batch-charging” and the industrial furnace is charged continuously as mentioned before.

The differences are relevant when comparing the results. The focus of this discussion will be the mechanisms during charging and how the water behaves similar for both the experiments.

7.1 Charging

When comparing the charging pattern the raw material mixture has to be taken into consideration. Although the mixture consists of several carbon sources for the industrial case the charge is considered to be wet. Although it is not accurate, the dynamics is of higher importance than the absolute values.

Fig. 7.1 is an example of the difference between batch charging and continuous charging. The data used for to plot the batch charging is taken from the pilot scale experiment and for the plot showing continuous charging the graph shows how the center feeder charges in the industrial furnace. Looking besides that the two plots is in a completely different scale, both the cases are taken in a time period of around 45 minutes. While the batch charging clearly reduces the emissions, the trend is more difficult to see for the continuous charging. One similarity is that there are peaks of NO_x, but it is difficult to relate them to charging. This is because the water does not have time to fully evaporate and the volatiles will not have time to combust on the surface.

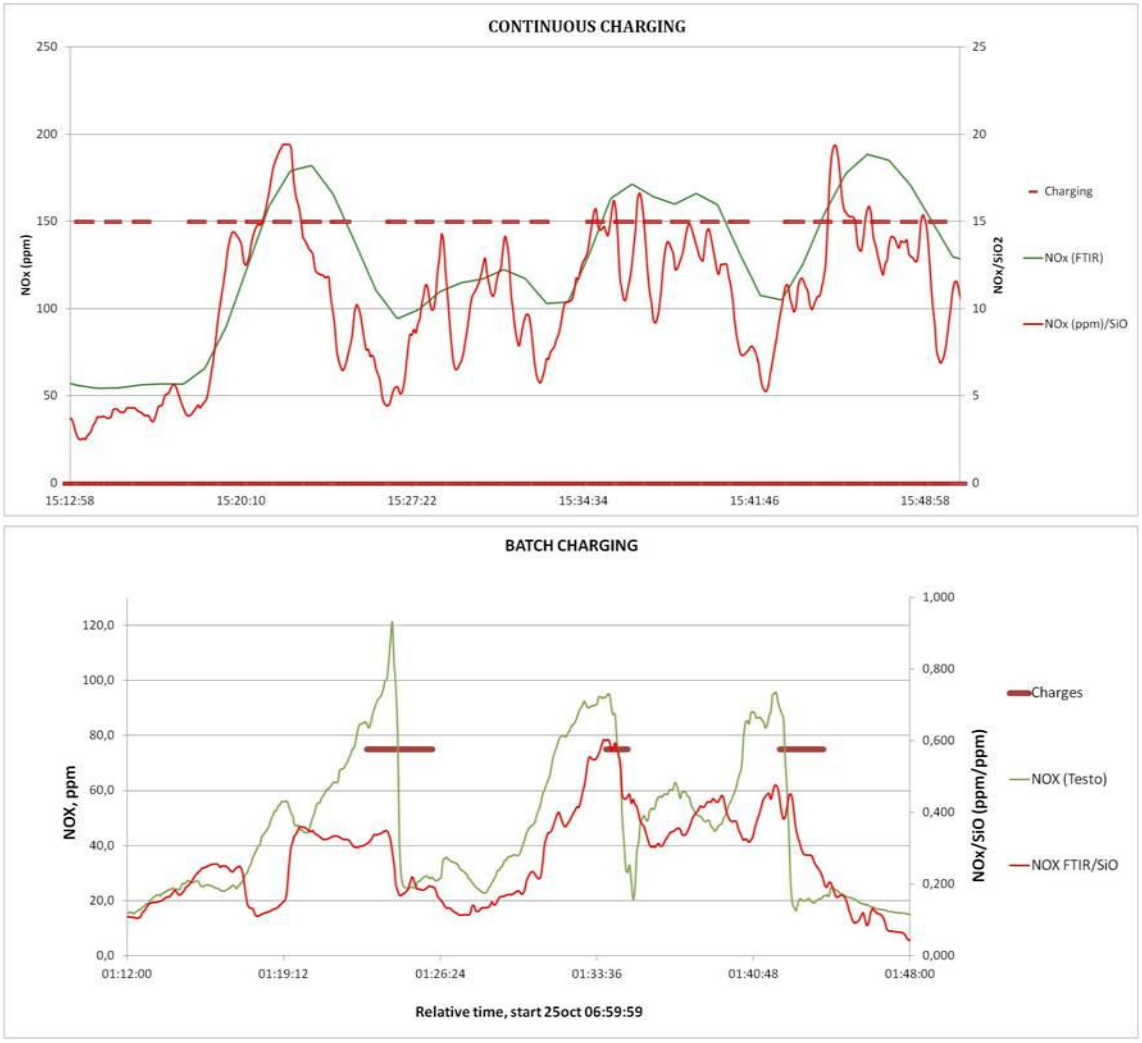

Fig. 7.1: The difference between batch charging and continuous charging is illustrated in this figure.

7.2 Water and volatiles: The reaction mechanism.

From both experiments it is clear that increasing water-concentration reduces the NO_x when the furnace is charged. Instead of repeating the results it is valuable to discuss this mechanism further.

As mentioned several times in the theory part the formation of NO is a result of that nitrogen from the air reacts with oxygen radicals formed by the combustion of SiO at a high temperature. The combustion of SiO(g) is repeated in reaction (7.1). This combustion is exothermic producing temperatures up to 2000 °C.

$$SiO(g) + O_2(g) = SiO_2(g) + O \text{ (radical)} \qquad (7.1)$$

The oxygen radical further reacts with nitrogen from the air and is given as reaction (7.2). This reaction forms NO at high temperatures.

$$N_2 + O = NO + N \qquad (7.2)$$

However, when adding moisture to the charge the water reduces the emissions and in the literature review this is primary due to a temperature drop, but it can also be due to a chemical effect. The OH-concentration is found to increase, and the amount of oxygen and hydrogen radicals are found to decrease. The OH-concentration can increase by reaction (7.3) and reaction (7.4). Reaction states that oxygen radicals are consumed, which could explain the decrease in the oxygen radical concentration. Reaction (7.4) produces OH and hydrogen radicals by the decomposition of water. However, reaction (7.4) does not explain the decrease in hydrogen radicals for the system.

$$H_2O + O = 2OH \qquad (7.3)$$

$$H_2O = OH + H \qquad (7.4)$$

Most recently SINTEF (Olsen, Solheim, Panjwani, & Andersson, 2013) has completed a report from the results of the pilot scale experiment. The report states that the gas temperature is reduced from 1000 °C to 800 °C when the moisture content is increased. It is assumed that water increase the heat capacity and reduce the gas temperature. They have included a new reaction, which could explain how the water can influence the emissions chemically. The reaction is given below as (7.5).

$$SiO + H_2O = SiO_2 + H_2 \qquad (7.5)$$

When the water is included in a chemical reaction for the process, the OH-concentration naturally decreases. There is a lower OH concentration in the system because water is consumed in the reaction with SiO gas. Reaction (7.5) means that SiO(g) competes with the combustion of volatiles and in addition the SiO gas reacts

with water. The process produces hydrogen instead of oxygen radicals, and that leads to that less NO is formed. This reaction together with the physical properties leading to a decrease in the gas temperature, contributes to decreasing the NO_x emissions.

By commenting on the reactions in the process it is natural to study the reactions and the kinetics. SINTEF concludes in their report that the kinetics needs to be studied further but they have made some thoughts about which reactions that could take place in the process. Fig. 7.2 shows the reactions and their kinetic parameters.

Reactions	A_r	n	E_r
1. $O_2+CO \rightleftarrows O+CO_2$	2.50E+12	0.00	47800
2. $2OH \rightleftarrows O+H_2O$	3.57E+04	2.40	-2110
3. $OH+CO \rightleftarrows H+CO_2$	4.76E+07	1.23	70
4. $H+O_2 \rightleftarrows O+OH$	2.65E+16	-0.67	17041
5. $O+H+M \rightleftarrows OH+M$	5.00E+17	-1.00	0
6. $2O+M \rightleftarrows O_2+M$	1.20E+17	-1.00	0
7. $O+CO \rightleftarrows CO_2$	1.80E+10	0.00	2385
8. $H+OH+M \rightleftarrows H_2O+M$	2.20E+22	-2.00	0
9. $N+NO \rightleftarrows N_2+O$	2.70E+13	0.00	355
10. $N+O_2 \rightleftarrows NO+O$	9.00E+09	1.00	6500
11. $N+OH \rightleftarrows NO+H$	3.36E+13	0.00	385
12. $SiO+O_2 \rightleftarrows SiO_2+O$	2.31E+13	0.00	26016
13. $SiO+OH \rightleftarrows SiO_2+H$	1.80E+10	0.78	1218
14. $SiO_2 \longrightarrow SiO_2(s)$	2.00E+15	0.00	0

Fig. 7.2: The reactions that could take place in the process. The figure shows the kinetic parameters given in Kelvin, cal/mol and cm^3 (Olsen, Solheim, Panjwani, & Andersson, 2013).

Reaction (7.5), which is the reaction between SiO(g) and H_2O is found to be endothermic. An endothermic reaction consumes energy. It is also concluded in the report that the activation energy is found to be high, and that the reaction probably happens in several steps. A part of the further work should be to do a kinetic study of this reaction.

Another explanation of this could be that the charging covers the blows that are due to the combustion of SiO. With a lower amount of SiO reaching the surface there will be a lower concentration of oxygen radicals. This will also cover areas that have a high local temperature reducing the overall temperature at the charge surface. In this explanation the SiO never reaches the surface, hence never gets the chance to react with oxygen. In this case it can be assumed that the water only has a cooling effect on the temperature rather than participating in the reactions.

8 Concluding remarks

This report is based on two experiments with the main purpose of investigating the effect of raw materials and the importance of charging on the formation of NO. It is natural to divide the conclusion into three parts: Effect of charging, effect of raw material mixture and experiences done during the experimental work.

Experimental work

The experimental work that is summarized in this thesis has mostly been the data analysis based on data from a pilot scale furnace and an industrial furnace. Some of the experiences that have been done regarding this work are summarized below:

- When collecting data from different measurement devices it is important to understand how often the device collects data and how the device measures different gases and species. This is because the data are often logged in different units and at different time intervals. Sometimes there can be a delay in the measurements. When comparing data from different devices it is necessary to transform the data so that the time interval is the same for all of the data. This has been done here where the data from the FTIR was transformed from 54 second data into 5 second data by interpolation and the NEO LASERGAS was transformed from 1 second data into 5 second data. This way it is easier to compare the results.
- A huge part of the work is to validate the data and see that the results are in the range that is expected. However, the dynamics are often as important as absolute values when investigating emissions. This is because this study has the focus on understanding the mechanism of how NO forms.
- Another important aspect of the experimental work done in this thesis is that a pilot scale furnace can simulate an industrial furnace. The trends that are found regarding the water content can be compared with actual data from the industry. This can confirm the work of Nils Eivind Kamfjord, who studied the emissions of NO from the industry and from the small pilot furnace.

The effect of charging

The effect of charging is studied both in the pilot scale experiment and in the industrial experiment. The conclusions of the results are given below:

- The formation of NO_x is reduced when the furnace is charged. This is due to a decrease in the overall surface temperature of the charge.
- The pilot scale experiment has a charging pattern equal to batch charging. In this case the volatiles and moisture in the charge has the time to combust and

evaporate and the carbon is given the time to react. This leads to that the charge level is burned down creating peaks in the emissions.

- When the furnace is charged continuously the volatile and water levels are kept constant creating where the variation in NO is not due to charging but rather other parameters.
- By changing the charging frequency in the industrial furnace to a lower frequency giving larger batches of raw materials the dynamics of the emissions changes and becomes more similar to the dynamics for batch charging.
- It is likely that continuous charging is more beneficial than batch charging regarding emission of NO_x and this is confirmed by an increase in the average of 40 %.

Effect of the raw material mixture

For the industrial experiment the raw material mixture was kept constant during the experiment. In the pilot scale experiment the raw material composition changed between wet and dry carbon, which means that the carbon contains a different amount of volatiles and moisture.

- Adding a carbon source that contains moisture reduce the silica formation and NO formation during charging. The water content along with the volatile content reduce the overall temperature and react with oxygen hindering the combustion of SiO(g).
- The wet charge contributes more to the reduction of emissions during charging than the dry charge. With increasing water content and volatile content there is a decrease in formation of NO and formation of SiO_2.
- The effect of water could be a combination between a chemical reaction and the physical reaction of decreasing the gas temperature. The SiO gas could potentially react with SiO gas and form hydrogen. This means that the process will consume water instead of oxygen. The decrease in oxygen radicals due to this reaction can explain why the emissions decrease.
- For the industrial experiment the moisture content is also found to have an effect. Above 3.5 vol% H_2O the emissions of NO_x above 600 ppm are less frequent compared to if the water content is below 3.5 vol%.
- A part of the further work should be to do a kinetic study of the reactions that could participate in the process. It should be relevant to understand the thermodynamics and kinetics of the reactions between water and SiO gas.

References

Bhargava, M. C., Sowa, W., Casleton, K., & Maloney, D. (2000). An Experimental and Modeling Study of Humid Air Premixed Flames. *Journal of Engineering for Gas Turbines and Power* .

Bireswar, P., & Amitava, D. (2008). Burner Development for the Reduction of NOx Emissions from Coal Fired Electric Utilities. *Recent Patents on Mechanical Engineering* , ss. 175-189.

Britten, J. A., Tong, J., & Westbrook, C. K. (1990). A Numerical Study of Silane Combustion. *Twenty-Sixth Symposium (international) on Combustion, The Combustion Insitute* .

De Nevers, N. (2000). *Air Pollution Control Engineering.* Boston: McGraw-Hill.

ELKEM (Åslaug Grøvlen). *Local Report.*

Elkem. (u.d.). *Fibre Cement*. Hentet fra http://elkem.com/en/Silicon-materials/Products/Fibrecement/

Fagerlund, G. (u.d.). *Determination of Specific Surface by the BET-method.* Hentet fra http://link.springer.com/article/10.1007%2FBF02479039#page-2

FTIR. (u.d.). *Product controlling emissions*. Hentet April 16, 2013 fra http://sxsmedioambiente.com/?lang=es&seccion=productos&cat=10000&catend=19999

Guo, H., Neill, W. S., & Smallwood, G. J. (2008). A numerical study on the effect of water addition on NO formation in counterflow CH4/air premixed flames. *Journal of Engineering for Gas Turbines and Power* (5), ss. 054502-05405.

Jachimowski, C. J., & McLain, A. G. (1983). A Chemical Kinetic Mechanism for the Ignition of Silane/Hydrogen Mixtures. *NASA Technical Paper* .

Kamfjord, N. E. *Mass and Energy Balances of the Silicon Process.*

Klif. (u.d.). *Norwegian Climate and Pollution Agency*. Hentet fra klif.no

NEO MONITORS. (u.d.). *LASERDUST*. Hentet fra http://www.neomonitors.com/products/dust-cross-stack/laserdust/

NEO MONITORS. (u.d.). *LASERGAS II SP*. Hentet fra http://www.neomonitors.com/products/gas-in-situ/lasergas-ii-sp/

Norske Utslipp. (2012, 10). Hentet fra www.norskeutslipp.no

Olsen, J.-E., Solheim, I., Panjwani, B., & Andersson, S. (2013). *Combustion and NOx formation in silicon pilot furnace.* Trondheim: SINTEF.

Raaschou-Nielsen, & Andersen, Z. (2000). Lung Cancer Incidence and Long-Term Exposure to Air Pollution from Traffic. *Environmental Health Perspectives* (6), p. 860.

Schei, A., Tuset, J., & H.Tveit. (1998). *Production of High Silicon Alloys.* Tapir Forlag.

TESTO. (2012). *cleanair*. Hentet fra TESTO 350XL Portable Combustion Analyzer Specifications: www.cleanair.com

Tranell, G., Ringdalen, E., Ostrovski, O., & Steinmo, J. J. REACTION ZONES IN A FeSi75 FURNACE - RESULTS FROM AN INDUSTRIAL EXCAVATION. *FERROSILICON SMELTING.* NTNU.

Turns, S. R. *An introduction to Combustion: Concepts and Applications* (2. utg.). McGraw-Hill Science Engineering.

Tveit, H., & Kadkhodabeigi, M. (n.d.). CFD Modeling of the Effect of the Furnace Crater Pressure on the Melt and Gas Flows in the Submerged Arc Furnace. *Journal of Progress in Computional Fluid Dynamics* (5/6), pp. 374-383.

UNECE. (u.d.). Hentet fra (http://www.unece.org/env/lrtap/multi_h1.html)

WHO. (u.d.). *World Health Organization*. Hentet fra http://www.euro.who.int/__data/assets/pdf_file/0005/112199/E79097.pdf

Zeldovich, J. B. (u.d.). Oxydation of Nitrogen in Combustion and Explotion. *Comtes Rendus (Doklady) de L`Acadèmie des Sciences de l'URSS Li* (3), ss. 217-220.

A.1 NEO Lasergas

neo monitors
Experience - the Difference

LaserGas™ II Single Path Monitor

- Data sheet

Key Features

- Response time down to one second
- No gas sampling: IN-SITU measurement
- No interference from background gases
- Stable calibration, no zero drift
- Applicable for many process conditions: High temperature, high dust, corrosive gases
- Line measurement, integral concentration over the full stack diameter
- No moving parts, no consumables
- ATEX and CSA certified
- TÜV approved technology

NEO Monitors LaserGas II Single Path (SP) Monitor is a highly reliable gas analyser for true continuous in-situ monitoring. Single Path Monitors are designed for measurements across stacks, ducts, and reactors with typical path lengths of 0.5 – 20 m. By-pass and extractive configurations are also possible. The SP Monitor utilizes a transmitter / receiver configuration to measure the average gas concentration along the optical line-of-sight.

State of the Art Technology

NEO Monitors LaserGas is using Tuneable Diode Laser Absorption Spectroscopy (TDLAS) i.e. a non-contact optical measurement method employing solid-state laser sources. Therefore, the sensor remains unaffected by contaminants and corrosives and does not require regular maintenance. The absence of extractive conditioning systems further improves availability of the measurement and eliminates errors related to sample handling.

Easy Installation

The monitor is mounted directly onto DN50 or ANSI 2" flanges, which include purge gas connections and a tilting mechanism for easy alignment. A continuous purge flow will prevent dust and other contamination from settling on the optical windows. Once power and data lines are connected, measurements are performed in real-time.

Key Application Areas

With **market experience since 1995** and an installed base of more than 3000 LaserGas analysers, we offer our customers a long-term experience from many challenging applications:

- Chemical industry (inertisation control of reactors, Vinyl Chloride or PVC, Acrylic acid, solvent acid recovery, carbon black etc.)
- Petrochemical industry (FCC Units, tail gas treatment, flare gas monitoring, sulphur recovery, vent headers of incinerators etc.)
- Steel industry (Coke oven gas, converter coal gas, reheating furnaces)
- Power plants (boiler control, DeNOx - ammonia slip control, economiser)
- Waste incineration, cement plants, aluminium smelters (emission monitoring)

Technical Data LaserGas™ II SP

neomonitors.com

Table of Principal Gases

Gas	Detection limit [ppm]	Max temp. [°C]	Max pressure [bar abs]
NH_3	0.15	600	2
HCl	0.05	600	2
HF	0.015	400	2
H_2S	3	300	2
O_2	100	1500	20
% H_2O	50	1500	2
ppm H_2O	0.1	400	2
% CO	30	1500	2
% CO_2	30	1200	2
ppm CO	0.3	1500	2
ppm CO_2	0.2	300	2
NO	10	300	2
N_2O	1	200	2
CH_4	0.2	300	3

NOTE: Detection limits are specified as the 95% confidence interval for 1 m optical path and gas temperature / pressure = 25 °C / 1 bar abs.
Also available are HCN, NO_2, C_2H_2, $C2H_4$, C_3H_6, CH_3I, CH_2O, CH_2CHCl (VCM), $C2H_4O$ (EtO), CH_2Cl_2 (DCM), HBr, and HI.
Dual Gas: NH_3+H_2O, HCl+H_2O, HF+H_2O, CO+CO_2, CO+H_2O, CO+CH_4, O_2+temp, CO+temp
Higher pressures may be available on request for certain gases. Please contact us!

Instrument data

Specifications	
Optical path length	typically 0.5 – 20 m
Response time	1 – 2 sec
Averaging time	Rolling average from 2 seconds to 24 hours (exp. decay)
Repeatability	+/- Detection limit or +/- 1% of reading, whichever is greater
Linearity	< 1%
Environmental conditions	
Operating temperature	-20 °C to +55 °C (special version up to +65 °C on request)
Storage temperature	-20 °C to +55 °C
Protection classification	IP66
Inputs / Outputs	
Analogue output (3)	4 – 20 mA current loop
Digital output	RS – 232 format, Optional 10 or 10/100 Base T Ethernet, Optional fibre optic (ASCII – format)
Relay output (3)	High gas-, Maintenance-, Warning - and Fault relays (normally closed-circuit relays)
Analogue input	4 – 20 mA process temperature and pressure reading
Ratings	
Input power supply unit	100 – 240 VAC, 50/60 Hz, 0.36 – 0.26 A
Output power supply unit	24 VDC, 900 – 1000 mA
Input transmitter unit	18 – 36 VDC, max. 20 W
4 – 20 mA output	500 Ohm max. isolated
Relay output	1 A at 30 V DC/AC
Installation and Operation	
Flange dimension	DN50/PN10 or ANSI 2"/150lbs (other dimensions on request)
Alignment tolerances	Flanges parallel within 1.5°
Purging of windows	Dry and oil-free pressurised air or gas, or by fan
Purge flow	10 – 50 l/min per flange (application dependent)
Maintenance	
Visual inspection	Recommended every 6 – 12 months (no consumables needed) Remote instrument check by Ethernet connection or external modem possible
Calibration	Check recommended every 12 months
Validation	In-situ span and zero check with optional internal cell (EN 14181 compliant)
Security	
Laser class	Class 1 according to IEC 60825-1
CE	Certified, conformant with LVD 73/23/EEC, including 93/68/EEC
EMC	Conformant with directive 2004/108/EC
Explosion protection (optional)	
ATEX zone 1	II 2 G Ex px op is Gb II T4, II 2 D Ex pD 21 IP 66 T64°C
ATEX zone 2	II 3 G Ex nA nC op is Gc IIC T4, II 3 D Ex td A22 IP65 T100°C
CSA	Class I, Div. 2, Groups A, B, C and D; Temp. Code T4; non-incendive
Dimension and weight	
Transmitter unit	405 (plus 65 for purge unit) x 270 x 170 mm, 6.2 kg
Transmitter unit (Ex version)	405 (plus 65 for purge unit) x 270 x 310 mm, 7.9 kg
Receiver unit	355 (plus 65 for purge unit) x 125 x 125 mm, 3.9 kg
Power supply unit	180 x 85 x 70 mm, 1.6 kg

neo monitors as
A subsidiary of Norsk Elektro Optikk

Solheimveien 62A, P.O.Box 384
N-1471 Lørenskog, Norway
Phone +47 67974700. Fax +47 67974900

Your local distributor:

A.2 NEO Laserdust

neo monitors
Experience - the Difference

LaserDust™ MP, LP and XLP Monitors

- Data sheet

Key Features

- Response time down to one second
- Suitable for high gas temperatures
- Cross stack measurement up to 10 m
- High dynamic range (mg or g with one instrument)
- Scattered light detection for high sensitivity
- Non-contact measurement (no probes)

NEO Monitors LaserDust Medium Path (MP), Long Path (LP), and Extra Long Path (XLP) Monitors are compact, optical dust monitors for true continuous in-situ measurement of dust concentration or opacity. The monitors are designed for measurement across pipes, stacks, and ducts with typical path lengths of 0.5 – 10 m. LaserDust Monitors use a transmitter / receiver configuration to probe the dust concentration along the optical line-of-sight. Our true non-contact approach (no probes) is superior to point type dust meters.

State of the Art Technology

With innovative laser technology the LaserDust combines two measurement principles in one instrument. At low dust levels it operates with forward scattered light technology: The incident laser light is scattered by dust particles and collected onto a solid-state sensor for dust quantification. This highly sensible mode enables detection limits of < 0.5 mg/Nm^3 and is unaffected by dust depositing on the windows. At high dust levels the LaserDust will measure transmittance or opacity: Light absorption by dust particles is captured by a 2nd sensor. The operation mode is user selectable and can be changed on site.

Installation

Transmitter and receiver are mounted opposite each other onto DN or ANSI flanges, which include purge gas connections and a tilting mechanism for easy alignment. A continuous purge flow will prevent dust and other contamination from settling on the optical windows. Once power and data lines are connected, measurements are performed in real-time.

Main Applications

The LaserDust monitors are suitable for measuring particles after baghouse filters and electrostatic precipitators even at elevated gas temperatures. Their response is unaffected by charged particles and changes in velocity, making them the choice for obtaining robust and reliable emissions data. Some of the typical applications:

- Emission monitoring in Aluminium smelters and steel works
- Emission monitoring in waste incinerators, power plants, cement kilns
- Scrubber and filter optimisation, bag house filter surveillance
- Dust explosion prevention (e.g. in silos or bins)

Technical Data LaserDust MP, LP and XLP

neomonitors.com

Instrument data

Specifications	
Process temperature	Above dew point up to 700 °C
Process pressure	0.1 – 1.5 bar abs (optional windows for up to 5 bar)
Detection limit	< 0.5 mg/Nm^3 (in scattered mode)
Measurement range	min. 0 – 15 mg/Nm^3 (scattered mode) max. 0 – 10.000 mg/Nm^3 (transmission mode)
Resolution	0.05 mg/Nm^3
Optical path length	Medium Path: 0.5 – 3 m Long Path: 3 – 6 m Extra Long Path: 6 – 10 m
Response time	1 – 2 sec Pulse mode: 50 ms
Environmental conditions	
Operating temperature	-20 °C to +55 °C
Storage temperature	-20 °C to +55 °C
Protection classification	IP66
Inputs / Outputs	
Analogue output (3)	4 – 20 mA current loop
Digital output	RS – 232 format Optional 10 or 10/100 Base T Ethernet, optional fibre optic (ASCII – format)
Relay output (3)	High dust -, Warning - and Fault relays (normally closed-circuit relays)
Analogue input	Optional 4 – 20 mA process temperature and pressure reading
Ratings	
Input power supply unit	100 – 240 VAC, 50/60 Hz, 0.36 – 0.26 A
Output power supply unit	24 VDC, 900 – 1000 mA
Input transmitter unit	18 – 36 VDC, max. 20 W
4 – 20 mA output	500 Ohm max. isolated
Relay output	1 A at 30 V DC/AC
Installation and Operation	
Flange dimension	Medium Path: DN50/PN10 Long Path: DN80/PN10 Extra Long Path: DN150/PN10 Optional ANSI or other on request
Alignment tolerances	Flanges parallel within 1.5°
Purging of windows	Dry and oil-free pressurised air or gas, or by fan
Purge flow	50 – 100 l/min (application dependent)
Maintenance	
Visual inspection	Recommended every 6 – 12 months (no consumables needed) Remote instrument check by Ethernet connection or external modem possible
Calibration	Recommended every year (against gravimetric analysis)
Validation	Integrated zero and span check (EN 14181 compliant)
Security	
Laser class	Class IIIb according to IEC 60825-1
CE	Certified, conformant with LVD 73/23/EEC, including 93/68/EEC
EMC	Conformant with directive 2004/108/EC
Explosion protection (optional)	
ATEX Cat 3 (zone 2)	II 3 GD T100 °C Ex nA nC II T5
CSA	Class I, Div. 2 on request
Dimension and weight	
Transmitter unit (MP, LP, XLP)	200 (plus 100 for purge unit) x 270 x 170 mm, 6.2 kg
Transmitter unit (Ex version)	200 (plus 100 for purge unit) x 270 x 310 mm, 7.9 kg
Receiver unit (MP)	300 (plus 100 for purge unit) x 120 x 120 mm, 3.9 kg
Receiver unit (LP)	380 (plus 100 for purge unit) x 120 x 120 mm, 5 kg
Receiver unit (XLP)	410 (plus 100 for purge unit) x 270 x 170 mm, 8 kg
Power supply unit	180 x 85 x 70 mm, 1.6 kg

neo monitors as
A subsidiary of Norsk Elektro Optikk

Solheimveien 62A, P.O.Box 384
N-1471 Lørenskog, Norway
Phone +47 67974700. Fax +47 67974900

Your local distributor:

A.3 TESTO MX/L

CleanAir.

CleanAir Instrument Rental
500 W. Wood Street
Palatine, IL 60067-4975
800-553-5511
www.cleanair.com

Testo 350XL Portable Combustion Analyzer

The 350XL Includes:

- 350XL Analyzer
- 454 Control Unit
- Extra Printer Paper
- Probe and Umbilical
- Shoulder Strap
- Spare Filters
- Power Cord
- Data Cable
- Comsoft 3 Software
- Manual (CD ROM & Print)
- Instrument Rental Shipping Carton

Specifications:

- Approximate Shipping Weight: 30 lbs.
- Dimensions: 16" x 11" x 4" (actual)
- Probe: Standard size 15" length (1000°C max temp), 8mm external diameter, 5mm internal, w/90" umbilical (longer probes and umbilicals may be available)
- Detection Method: Electrochemical Sensors for O2, CO, SO2 , NO, NO2, H2S, CO2 calculated unless the infrared CO2 cell is , CxHy- pellistor
- Electrical requirements: 110-230, 90-260V, or rechargeable battery
- Battery Life: Analyzer Box is NiMH 2-3 hrs, Control Unit is 4AA batteries 8 hrs
- Operating Temperature: -20 to +115°F
- Material: ABS
- Memory: 250,000 readings
- Max. Pos. Pressure: 20" H2O
- Max. Neg. Pressure: 80" H2O
- Pump Draw: 0.8 to 1.2 LPM (results can vary depending on duct pressure)
- CO Dilution: Factors- 0, 2, 5, 10, 20, 40; Accuracy- Readings +2%; Gas- Fresh Air or N2
- Data Transfer: RS232 Interface (Optional 4-20mA available)

Rental/Application Notes:

- This unit has temperature-controlled sensors.
- A CO dilution system is available upon request
- It can be operated remotely from 150' away.
- The sample conditioner has a built in chiller.
- CO2 is a calculated value on most of our units. An infrared cell is available that can read from 0- 50 Vol. % CO2. Accuracy: +/-0.3 Vol.% + 1% of mv (0 to 25Vol.%CO2), +/-0.5 Vol.% CO2 + 1.5 Vol.% CO2 (>25 to 50 Vol.% CO2). Resolution: 0.01 Vol.% (0-25 Vol.%). Units with this option rent for more than the calculated CO2 Testo 350XL's.
- The NO low and NO cells can not be combined on the same unit. If the maximum value of 300ppm is exceeded on the NO low cell it will shut down flow to the entire unit.
- If you need a pitot with umbilical please request one when placing your order.
- The cells for this unit can be swapped/replaced for different configurations. Please call with specific cell requirements. Our standard unit comes equipped with O2, CO, NO, NO2, & SO2 cells.
- A 4-20mA output adapter can be rented for an additional price if specified.
- Equipment must be returned in its original packaging.

1/2

CleanAir.

CleanAir Instrument Rental
500 W. Wood Street
Palatine, IL 60067-4975
800-553-5511
www.cleanair.com

Testo 350XL Portable Combustion Analyzer

	O_2	CO	CO-low	NO	NO-low	NO_2	SO_2	H_2S	C_xH_y
Range	0-25%vol	0-10,000 H2 comp	0-500ppm H2 comp	0-3000 ppm	0-300ppm	0-500 ppm	0-5000 ppm	0-300 ppm	0-4%
Accuracy	<0.8% of f.v	<5ppm 0-99 ppm <5% of m.v. 100-2000 ppm <10% of m.v. 2001-10000 ppm	<2 ppm 0-39.9 ppm <5% of m.v. 40-500 ppm	<5 ppm 0-99 ppm <5% of m.v. 100-2000 ppm <10% of m.v. 2001-3000 ppm	<2 ppm 0-39.9ppm <5% of m.v. 300 ppm	<5 ppm 0-99 ppm <5% of m.v. 500 ppm	<5 ppm 0-99 ppm <5% of m.v. 100-2000 ppm <10% of m.v. 2001-5000 ppm	<2 ppm 0-39.9 ppm <5% of m.v. 40-300 ppm	<0.04% vol. 0-0.4% vol. <10% of m.v. 0.41 - 4% vol.
Resolution	0.1% vol	1 ppm	0.1 ppm	1 ppm	0.1 ppm	0.1 ppm	1 ppm	0.1 ppm	0.01 vol%
Resp. Time	20s (t95)	40s (t90)	40s (t90)	30s (t90)	30s (t90)	40s (t90)	30s (t90)	35s (t90)	40s (t90)

Our Standard cell configuration is NO (0-3000ppm), NO2, CO (0-10,000ppm), O2, & SO2. Advanced notification is necessary for alternative cell requirements.

A.4 FTIR

Protea
advanced monitoring
process improvement
pollution prevention

PROTEA APPLICATION SHEET: *Protir 204M*

ProtIR 204M

With a proven track record and full mCerts certification, the ProtIR 204M FTIR gas analyser is the tool of choice for environmental stack emissions testing. In use for Waste Incineration and other combustion process, the 204M has shown, with its powerful high resolution spectrometer, on-board sampling system (including mCerts approved O2 sensor) and easy to use software, that accurate multi-component gas measurement with FTIR does not have to be the realm of the expert spectroscopist.

The ProtIR 204M is based upon a high-resolution, robust and proven FTIR spectrometer that offers high signal throughput and low-noise measurements. The 204M has been developed **by stack testing professionals, for stack testing professionals** incorporating hardware and software features to make deployment of this FTIR as straight forward as possible, including:

- On-board sampling system - N_2 purge, MFC for dilution/analyte spiking, inlet filtration
- Standard Analysis Mode - fixed, controlled acquisition and analysis procedure without the need for complex set-up
- Powerful chemometric modelling - Standard Analysis Model providing measurement for 30 gases "out-of-the-box"
- True multi-range analysis with FTIR - software selects best model (analysis band) for each measurement
- Software reporting features - mean/max/min, LDL and drift calculations

These advantages come with the benefit of Protea's UK-based, training and support, so that the user is able to achieve the best performance out of the product.

Hardware Specifications

Resolution:	1cm^{-1} (Standard) 2cm^{-1}, 4cm^{-1}, 8cm^{-1}, 16cm^{-1}, 64cm^{-1}, 128cm^{-1}
Optics:	Zinc Selenide beam splitter (non-hygroscopic)
Spectral Range:	700 – 5000cm^{-1} (variable with optics)
Reference laser:	Long-life HeNe
Source:	Mid-IR source, ceramic Globar
Detector:	DTGS offering wide range Mid-IR measurement with excellent linearity
Cell material	Nickel-plated Aluminium
Cell volume	2.7 litre
Pathlength	6.4m (standard) Variable from 1m to 9.6m for custom applications
Sampling system:	Flow Control Automated Nitrogen Purge Valve Mass Flow Control for dilution and/or analyte spiking Cell and Venturi pressure sensors Cell inlet filter No need for separate pre-analyser sample conditioning box
Pump	Post-analyser vacuum sample pump with PTFE wetted parts
On-board IO	16 4-20mA output channels; 9 4-20mA input channels 5 Digital input; 2 Digital output
Ethernet	OPC Server and Client
Operating environment	5°C – 40 °C
Weight	71kg, mounted on trolley for transport
Dimensions	117 x 66.5 x 43cm

Multi-component, multi-range FTIR gas analyser

Standard Analysis Mode – simple but complete multi-gas analysis

Measure 1000's of gases with single unit

PAS software offers no-limit on number of gas measurements at once

Data can be re-analysed offline for new gases

Specific Applications for ProtIR 204M:

Stack Emission Testing

Back-up to Continuous Emission Monitoring Systems

Combustion gases under WID, LCPD

*Real*TOC™ measurement

Speciated VOC with benefit of high resolution

www.protea.ltd.uk

Call us on: +44(0)1270 256 256

Protea Limited. First Avenue, Crewe, Cheshire, CW1 6BG

Protea
advanced monitoring
process improvement
pollution prevention

PROTEA APPLICATION SHEET: *Protir 204M*

Component	Standard Range / mg/m3	Extended Range / mg/m3*	Lower Detection Limit
CO	0 - 75 mCerts	0 – 18750	0.2
NO	0 - 200 mCerts	0 – 2000	0.9
NO_2	0 – 200	0 – 2000	0.3
N_2O	0 – 100	0 – 1000	0.2
SO_2	0 - 75 mCerts	0 – 30000	0.8
NH_3	0 - 15 mCerts	-	0.1
HCl	0 - 15 mCerts	0 – 4000	0.3
HF	0 – 15	0 – 70	0.1
HBr	0 – 200	-	1.8
CH_4 (Methane)	0 – 70	0 – 700	0.2
C_2H_6 (Ethane)	0 – 50	0 – 1400	0.4
C_3H_8 (Propane)	0 – 50	0 – 2000	0.3
C_4H_{10} (n-Butane)	0 – 50	0 – 300	0.9
C_6H_{14} (n-Hexane)	0 – 50	0 – 400	0.9
C_2H_4 (Ethene)	0 – 25	0 – 1250	0.3
CH_3OH (Methanol)	0 – 70	-	0.4
HCHO (Formaldehyde)	0 – 20	-	0.3
C_6H_6 (Benzene)	0 – 250	-	3.4
C_6H_6O (Phenol)	0 – 100	-	0.4
HCN	0 – 15	0 – 600	0.2
CCl_4	0 – 200	0 – 1400	3.0
CS_2	0 – 100	0 – 400	0.4
COS	0 – 50	-	0.05
CF_4	0 – 40	0 – 600	0.05
SF_6	0 – 65	-	0.05
TOC (Indication only)	0 – 50	0 – 2000	0.4
H_2O	0 - 40%mCerts	-	<1000ppm
CO_2	0 - 20%	0 - 60%	<2 ppm
O_2 (via zirconia sensor)	0 - 20.9%mCerts	N/A	<0.4%

The ProtIR 204M and PAS software have been designed to allow stack emission monitoring to be carried out to the **Environment Agency's Technical Guidance Note M22 Measuring Stack Gas Emissions Using FTIR Instruments (TGN M22)** as simply and quickly as possible. With the built-in Standard Analysis Model for common gases there is no complex set-up of analysis required. The software has built-in calculations for drift and residual analysis, following the methods described in TGN M22. The 204M analyser is also equally suitable for deployment in US procedures Method 320 and ASTM 6348.

Skilled users of the FTIR can use the chemometric building routines of the PAS software to build analytical methods for specific applications. Set up this way, the 204M can measure thousands of possible gas species over ranges from ppm to %Vol in applications such as speciated VOC measurements.

The only FTIR gas analyser specifically tested as a transportable CEM, the 204M has passed the Environment Agencies MCERTS test programme for use on waste incineration processes. This allows the instrument to be used by stack testing organisations with guarantees on quality of product build and on analytical accuracy.

The possibilities with the ProtIR 204M do not stop with combustion stack emissions testing. With variable resolution ($1cm^{-1}$ to $128cm^{-1}$) and a gas cell with variable pathlength up to 9.6m Protea can tailor the 204M to meet many niche applications such as process control and ambient air measurements.

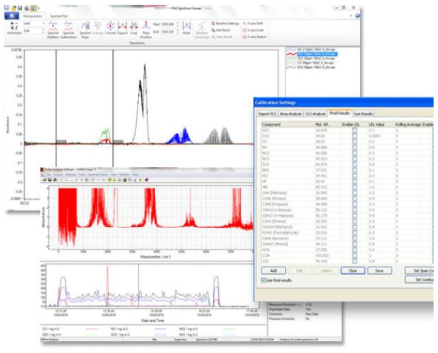

SIRA Certificate No. MC090142/00

A.5 BET-Analysis

micromeritics®

TriStar 3000 V6.05 A | Unit 1 Port 1 | Serial #: 1514 | Page 1

Sample: Silica Tap 1
Operator: Ingeborg Brede
Submitter:
File: C:\...\INGEBO~1\TAP1.SMP

Started: 01.02.2013 11:14:17
Completed: 01.02.2013 12:22:01
Report Time: 01.02.2013 13:07:03
Warm Free Space: 11.5439 cm³ Measured
Equilibration Interval: 5 s
Sample Density: 1.000 g/cm³

Analysis Adsorptive: N2
Analysis Bath Temp.: -195.850 °C
Sample Mass: 0.1730 g
Cold Free Space: 34.1848 cm³ Measured
Low Pressure Dose: None
Automatic Degas: No

Comments: 01.02.2013: prve 1,2,3. opplring

Isotherm Tabular Report

Relative Pressure (p/p°)	Absolute Pressure (mmHg)	Quantity Adsorbed (cm³/g STP)	Elapsed Time (h:min)	Saturation Pressure (mmHg)
			00:52	746.90436
0.066956423	50.01004	8.6572	00:58	
0.076634798	57.23886	8.9518	01:00	
0.117874551	88.04102	9.9652	01:02	
0.158133719	118.11076	10.7806	01:04	
0.198426125	148.20534	11.5018	01:06	

Sample: Silica Tap 1
Operator: Ingeborg Brede
Submitter:
File: C:\...\INGEBO~1\TAP1.SMP

Started:	01.02.2013 11:14:17	Analysis Adsorptive:	N2
Completed:	01.02.2013 12:22:01	Analysis Bath Temp.:	-195.850 °C
Report Time:	01.02.2013 13:07:03	Sample Mass:	0.1730 g
Warm Free Space:	11.5439 cm³ Measured	Cold Free Space:	34.1848 cm³ Measured
Equilibration Interval:	5 s	Low Pressure Dose:	None
Sample Density:	1.000 g/cm³	Automatic Degas:	No

Comments: 01.02.2013: prve 1,2,3. opplring

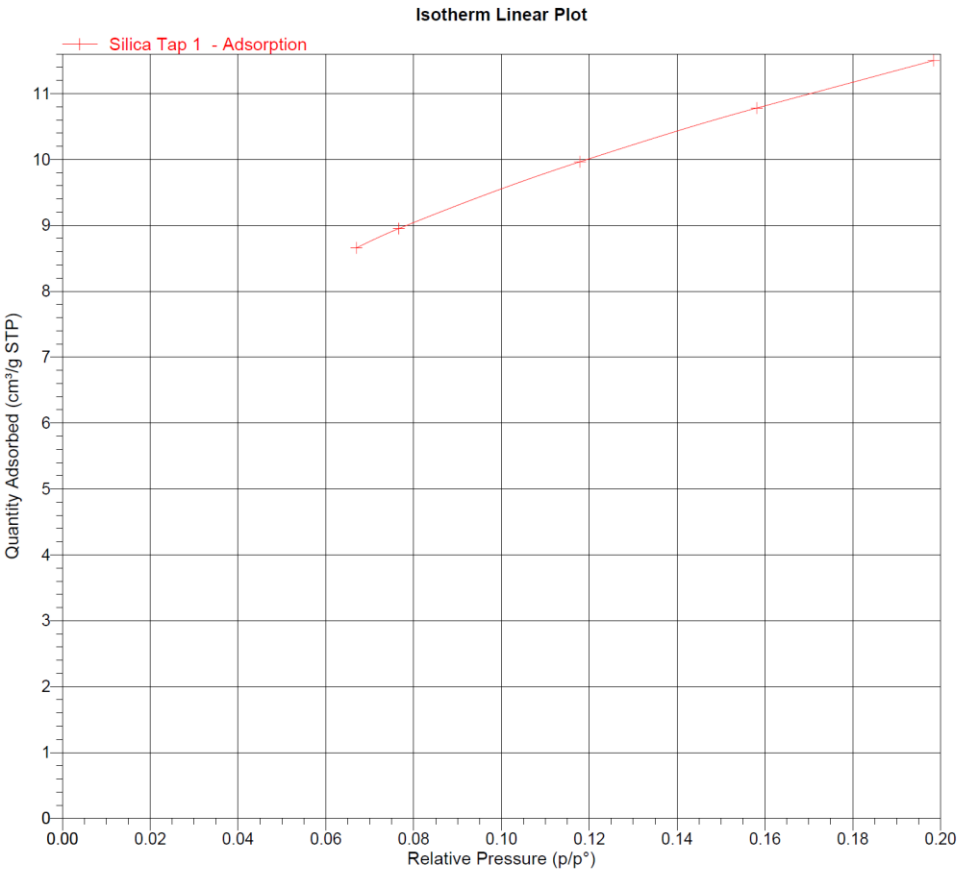

micromeritics®

Sample: Silica Tap 1
Operator: Ingeborg Brede
Submitter:
File: C:\...\INGEBO~1\TAP1.SMP

Started: 01.02.2013 11:14:17
Completed: 01.02.2013 12:22:01
Report Time: 01.02.2013 13:07:03
Warm Free Space: 11.5439 cm³ Measured
Equilibration Interval: 5 s
Sample Density: 1.000 g/cm³

Analysis Adsorptive: N2
Analysis Bath Temp.: -195.850 °C
Sample Mass: 0.1730 g
Cold Free Space: 34.1848 cm³ Measured
Low Pressure Dose: None
Automatic Degas: No

Comments: 01.02.2013: prve 1,2,3. opplring

BET Surface Area Report

BET Surface Area: 42.6510 ± 0.0809 m²/g
Slope: 0.100506 ± 0.000192 g/cm³ STP
Y-Intercept: 0.001560 ± 0.000026 g/cm³ STP
C: 65.421048
Qm: 9.7976 cm³/g STP
Correlation Coefficient: 0.9999945
Molecular Cross-Sectional Area: 0.1620 nm²

Relative Pressure (p/p°)	Quantity Adsorbed (cm³/g STP)	1/[Q(p°/p - 1)]
0.066956423	8.6572	0.008289
0.076634798	8.9518	0.009271
0.117874551	9.9652	0.013409
0.158133719	10.7806	0.017424
0.198426125	11.5018	0.021522

A.6 Data processing of the pilot scale experiment and the industrial experiment.

An important part of the study has been to analyze the data and do a data validation. This is because different measurement devices are used with different time intervals. Below are some figures showing that the data fit.

Pilot scale experiment

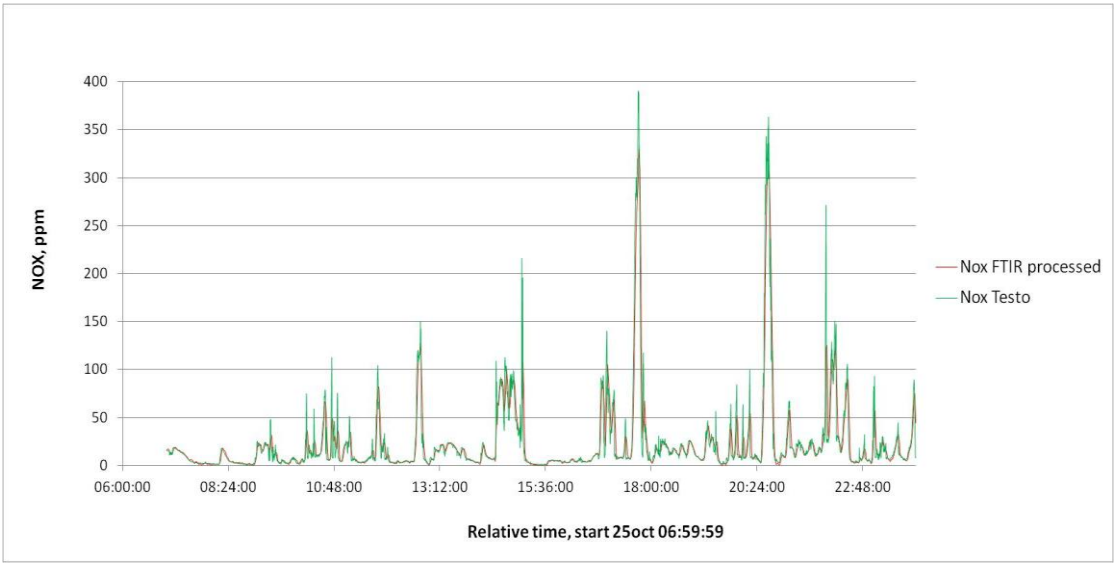

Fig. A.6.1: Measurements from the FTIR and TESTO fit with time and scale.

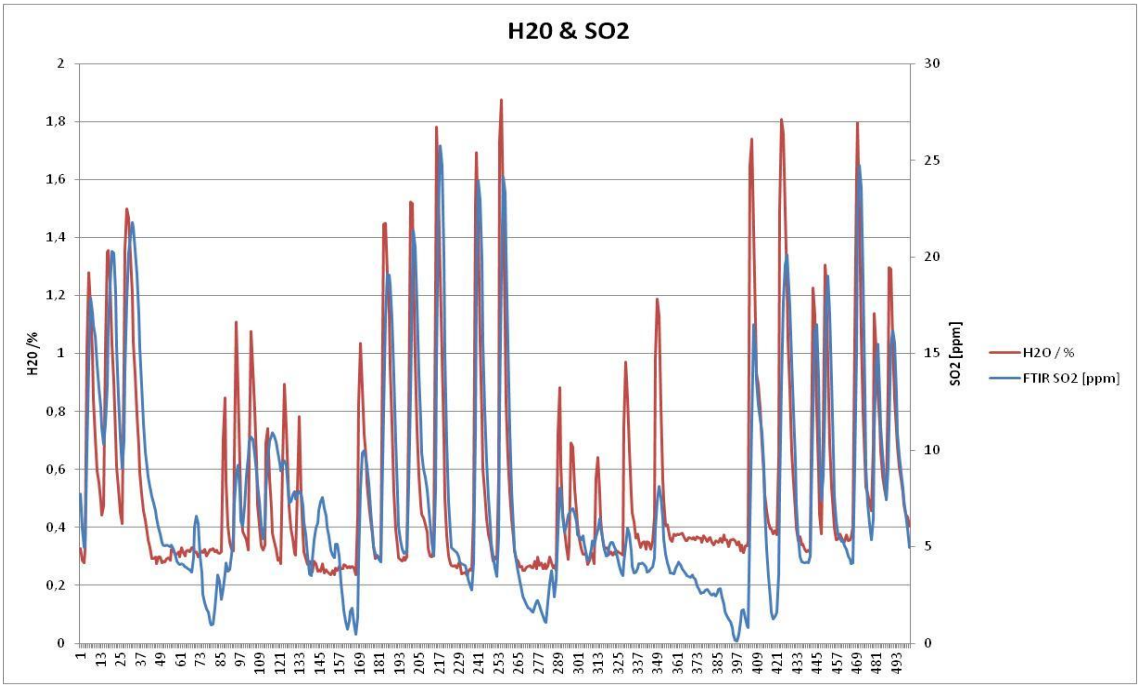

Fig. A.6.2: The volatiles and water correlate by looking at SO_2 and water.

Industrial Experiment

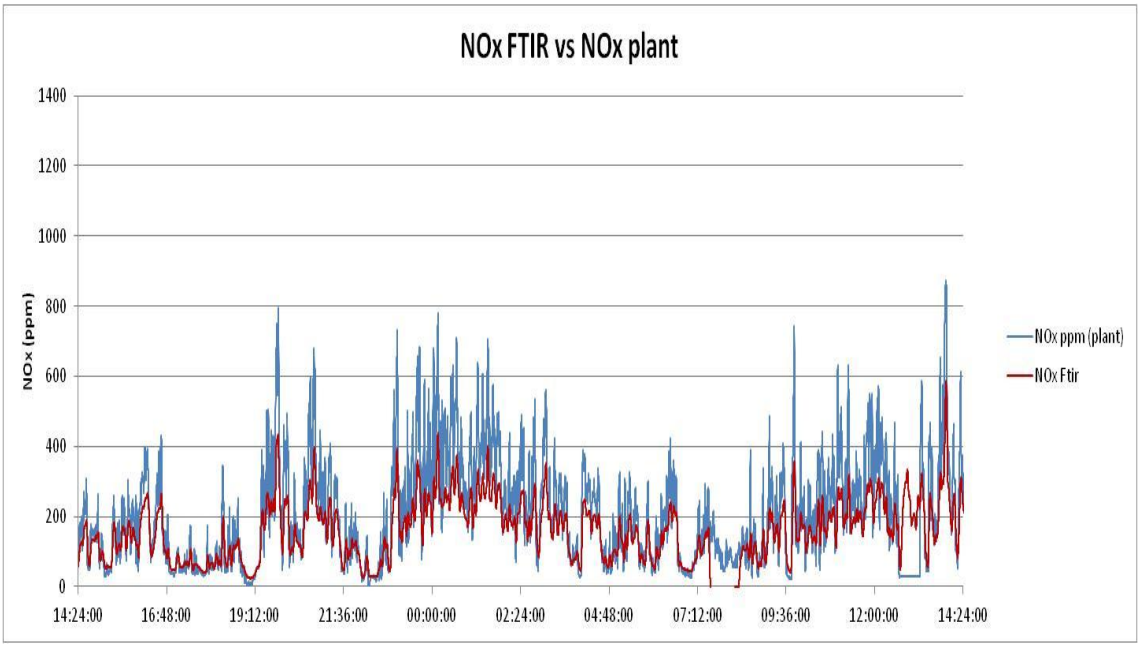

Fig. A.6.3: Here is an example of how the NO_x for the FTIR and NO_x from the plant fit together with the time scale. The emissions are given in ppm.

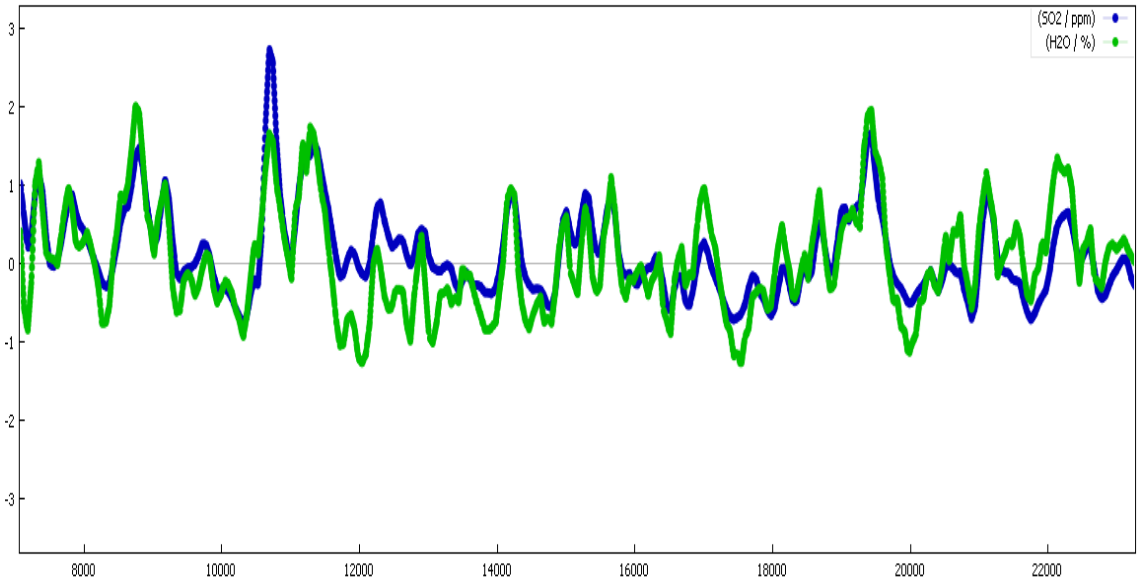

Fig. A.6.4: This shows how the water content and the SO_2 content fit together. This is important because it gives information about the validation of the data. SO_2 can be related to the volatiles and the water can be related to the moisture level of the carbon materials.

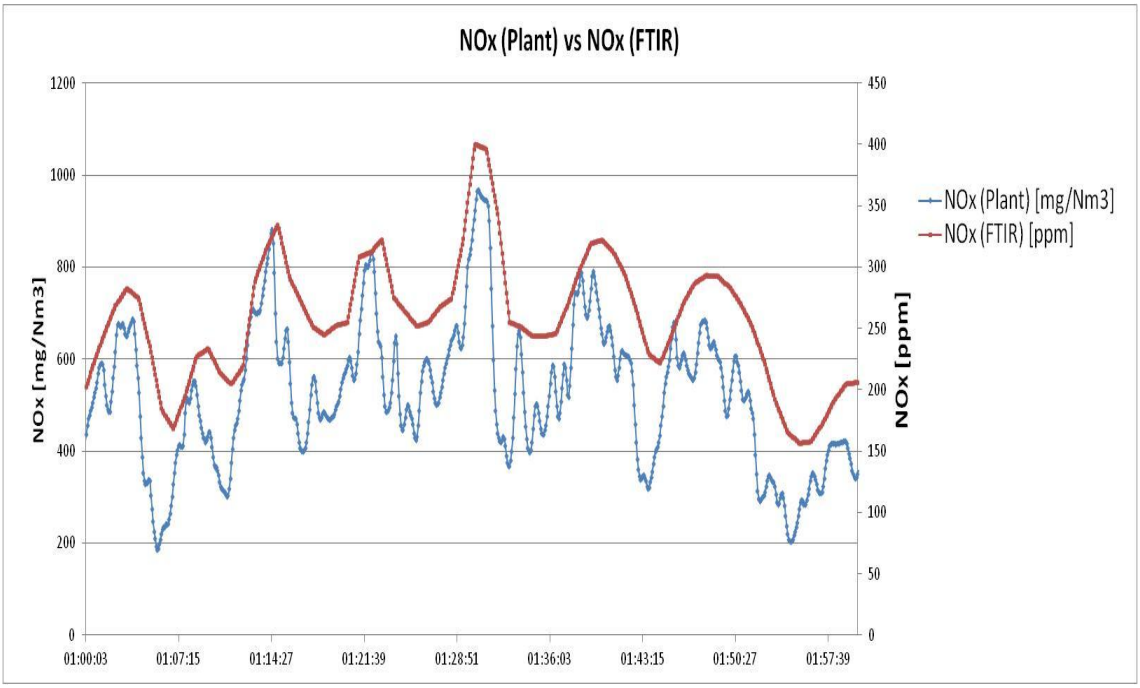

Fig. A.6.5: Another comparison of the emissions measured at the plant and measured by the FTIR.

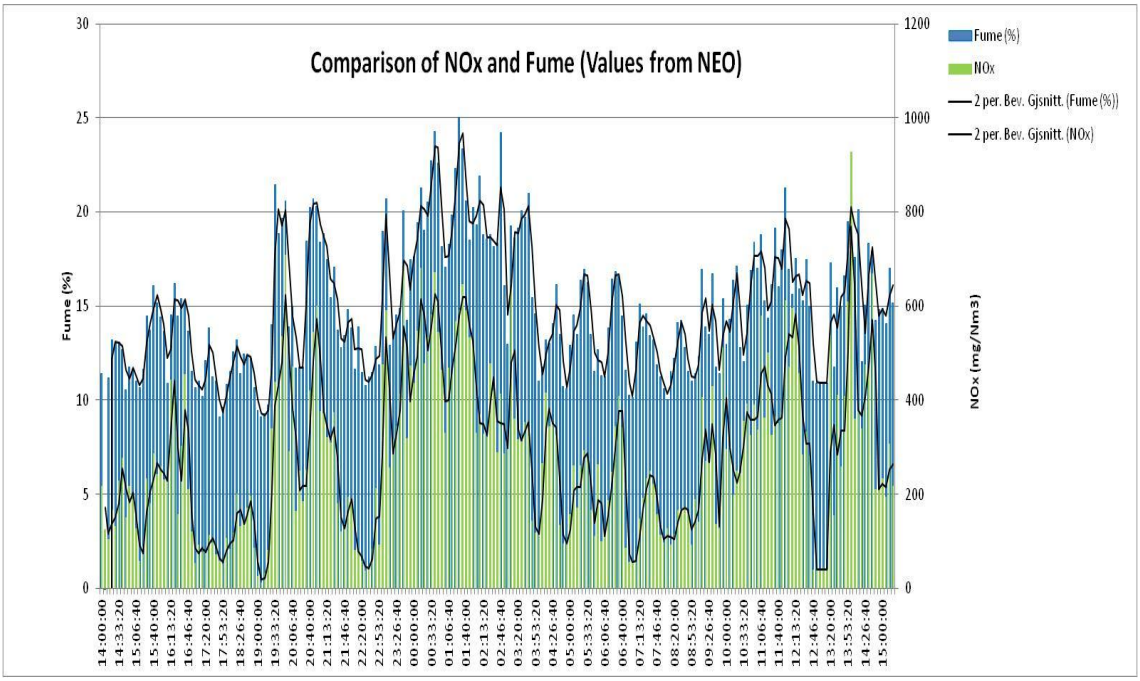

Fig. A.6.6: The correlation between NO and silica fume.

A.7 Pilot-Scale Experiment

The graphs below show the four cases for the pilot scale experiment.

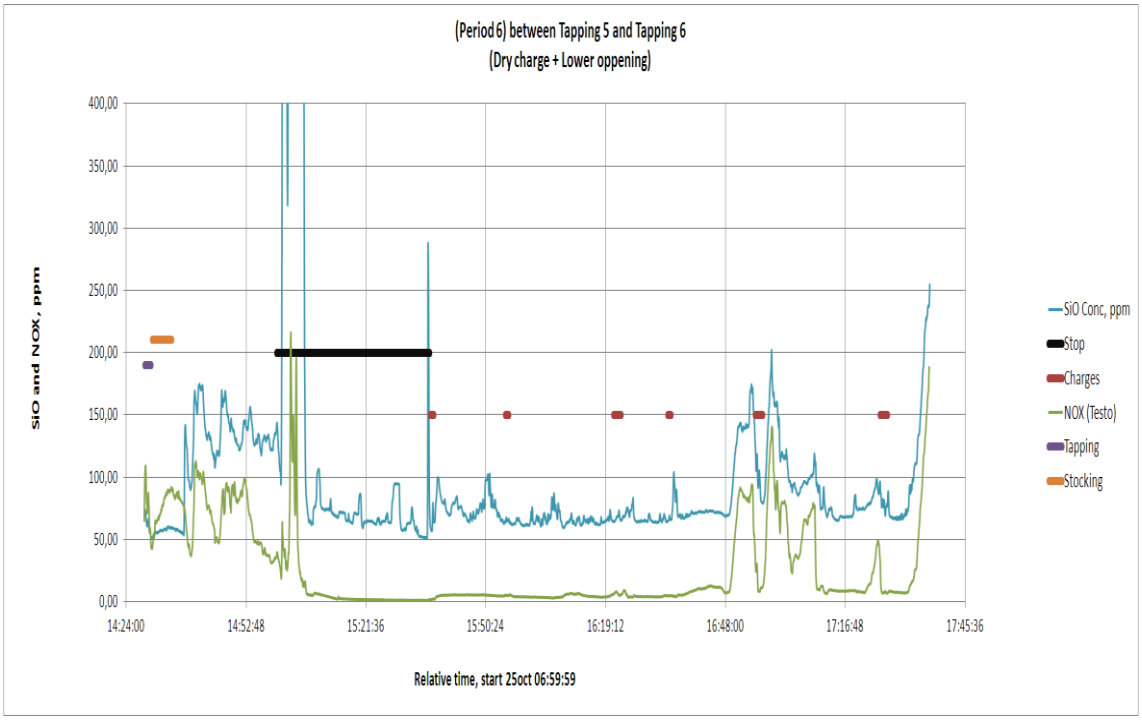

Fig. A.7.1: This graph shows the dynamics of the Dry charge + lower openings.

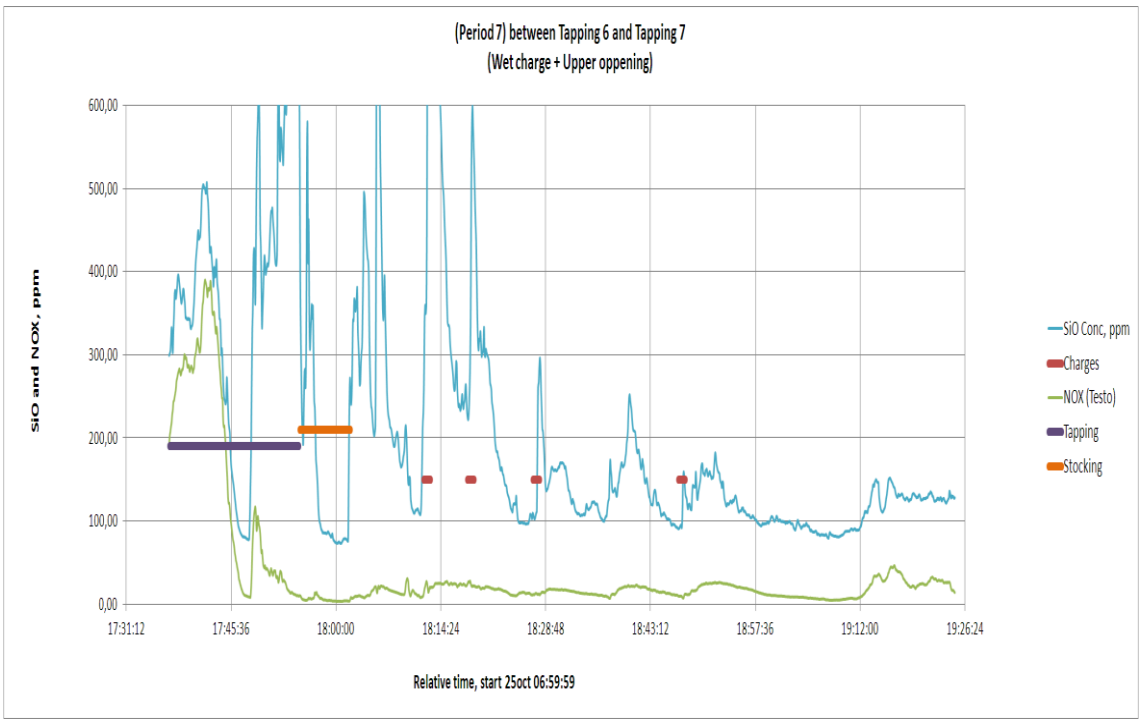

Fig. A.7.2: This graph shows the dynamics of the Wet charge + Upper openings.

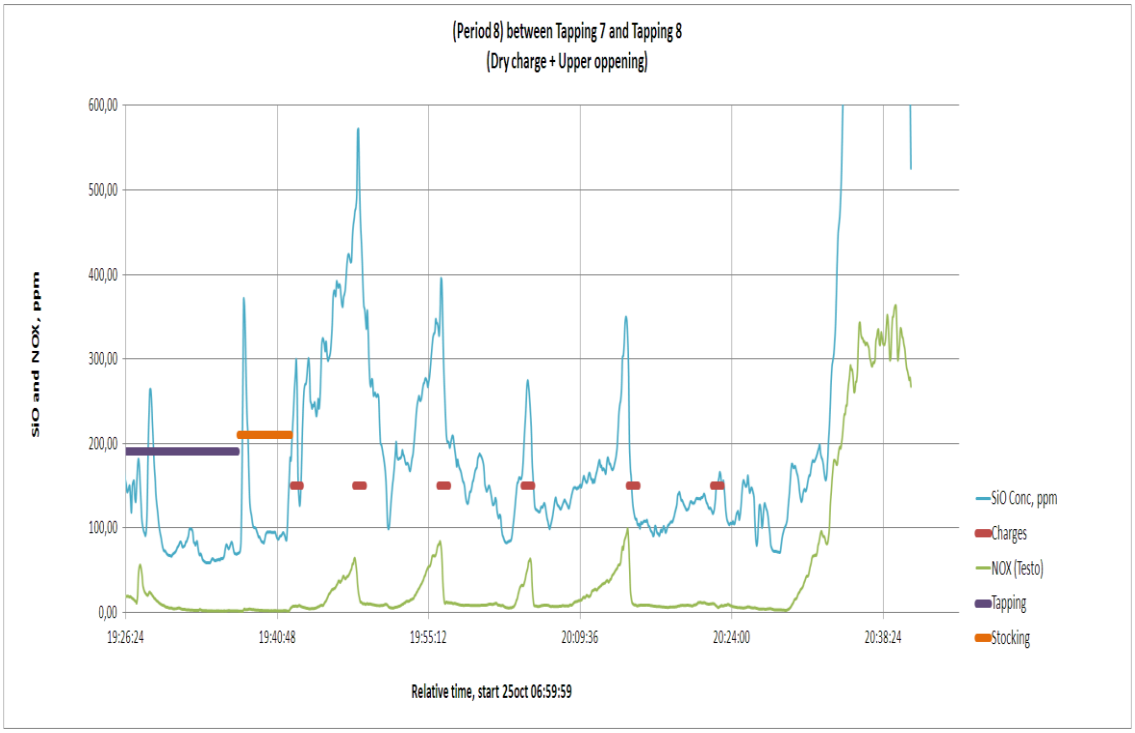

Fig. A.7.3: This graph shows the dynamics of the Dry charge + Upper openings.

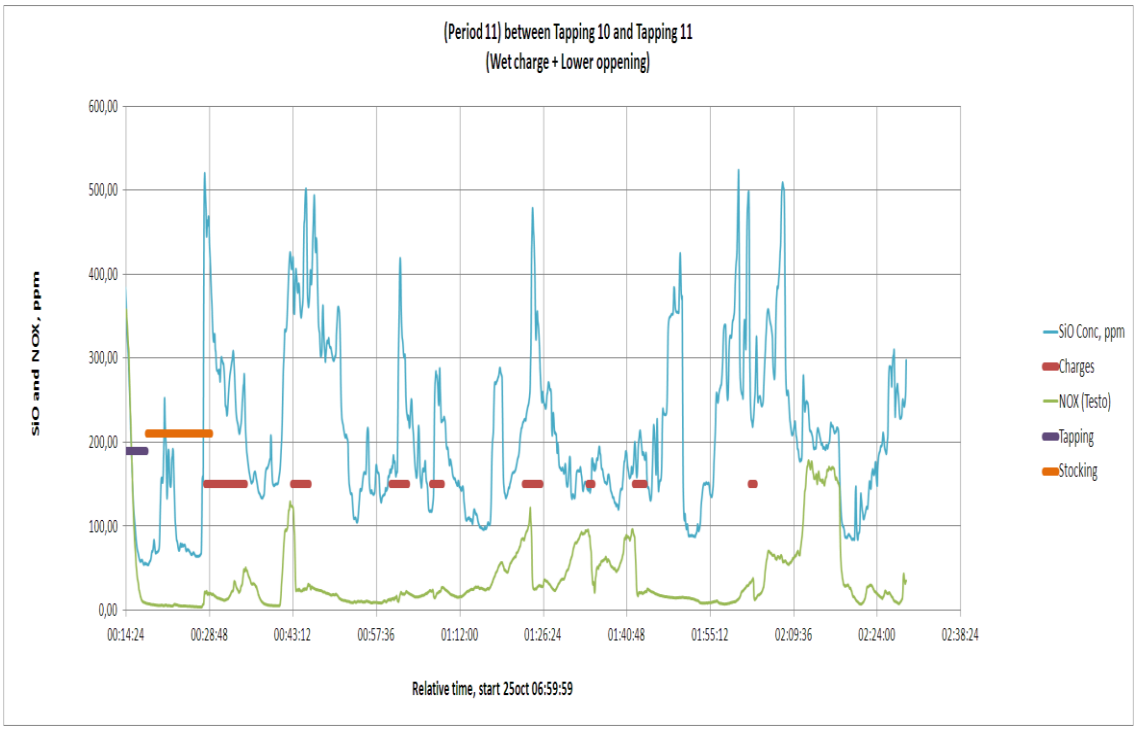

Fig. A.7.4: This graph shows the dynamics of the Wet charge + lower openings.

Water-contents from 0.5-0.6 vol%.

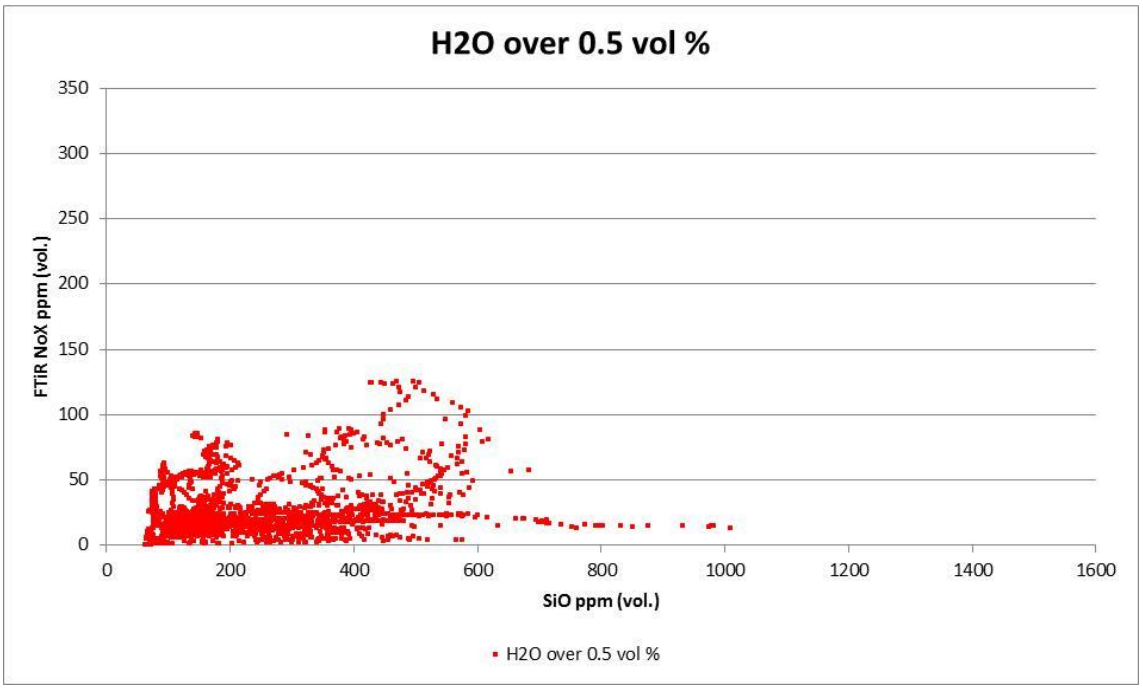

Fig. A.7.5: This figure shows the values of NO_x from the FTIR above 0.5 vol%.

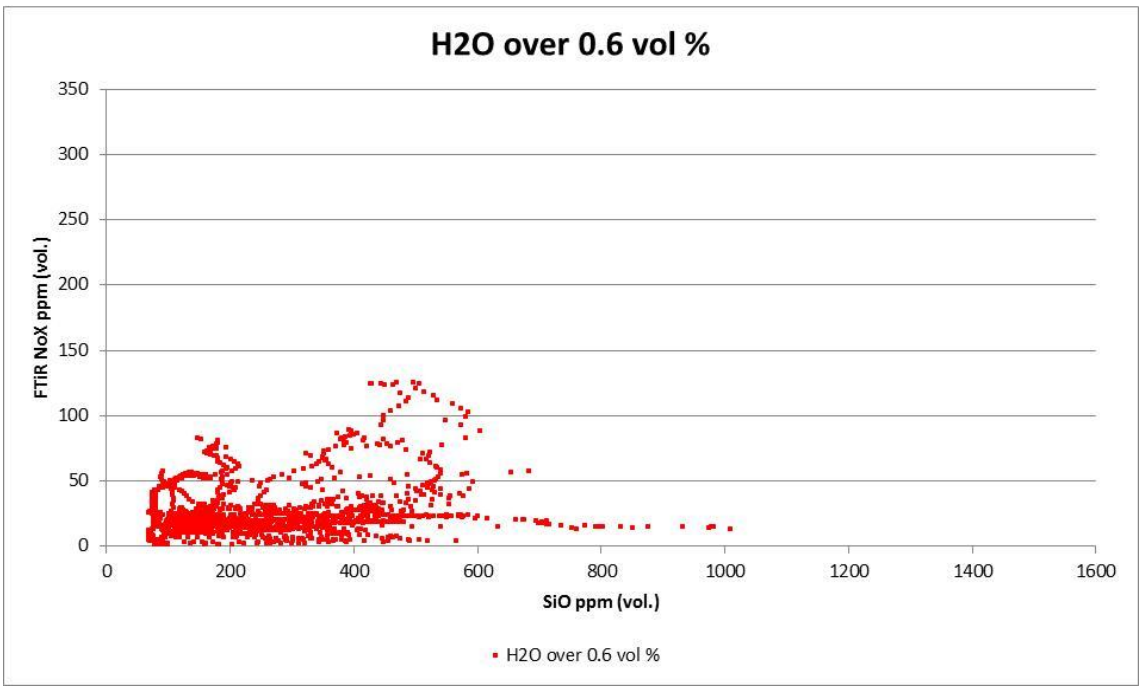

Fig. A.7.6: This figure shows the values of NO_x from the FTIR above 0.6 vol%.

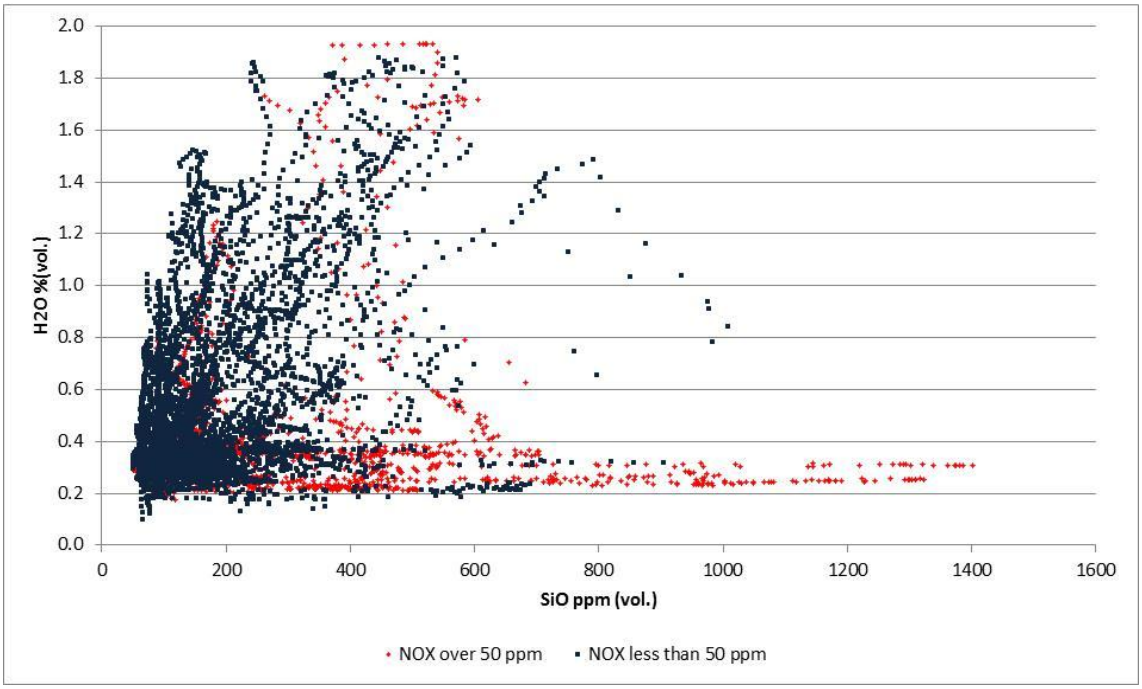

Fig. A.7.7: Here the distribution of NO_x below and above 50 ppm is given. The trend shows that most of the low emissions can be found in the area with low water content and low levels of silica fume.

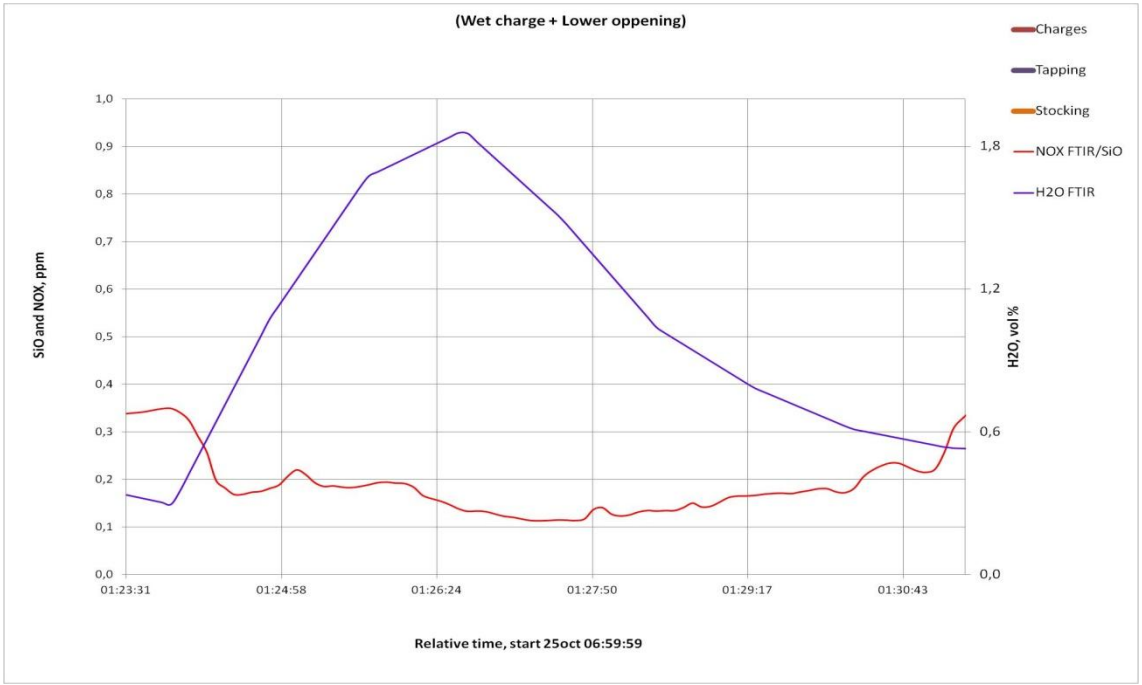

Fig. A.7.8: Effect of water for the wet charge.

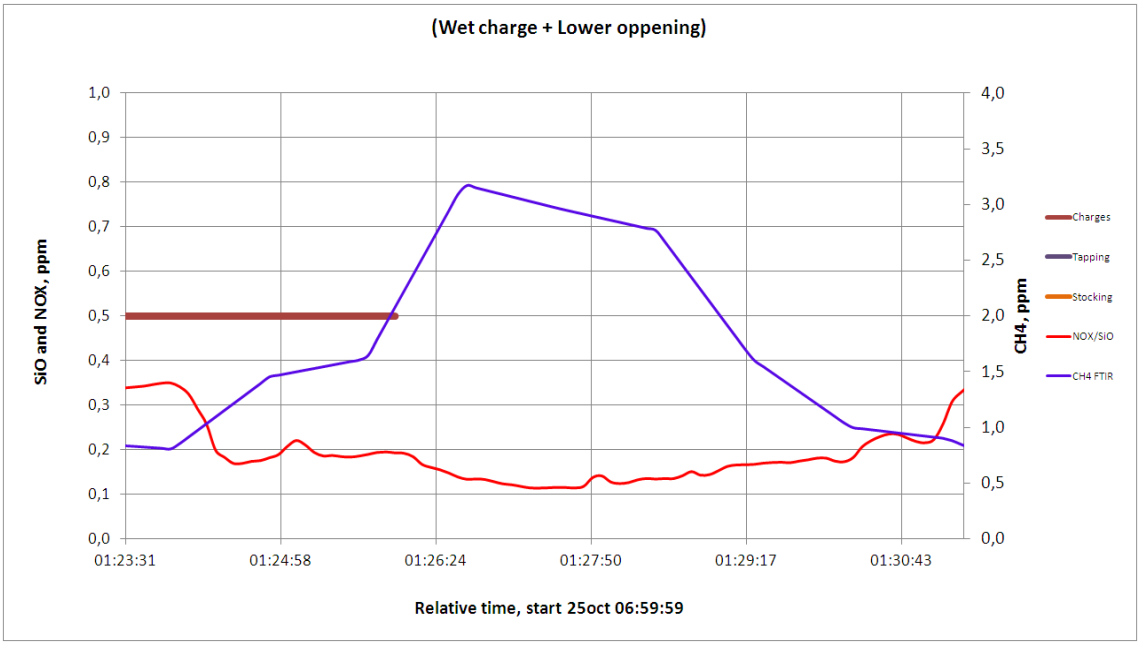

Fig. A.7.9: Effect of volatiles for the wet charge.

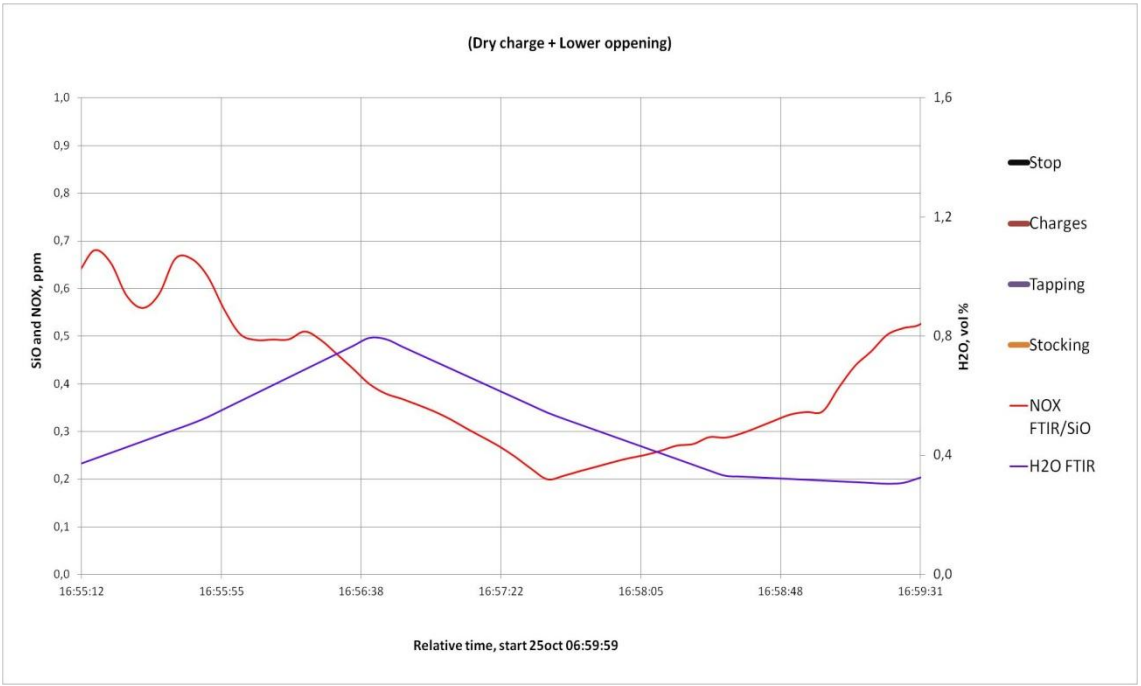

Fig. A.7.10: Effect of water for the dry charge.

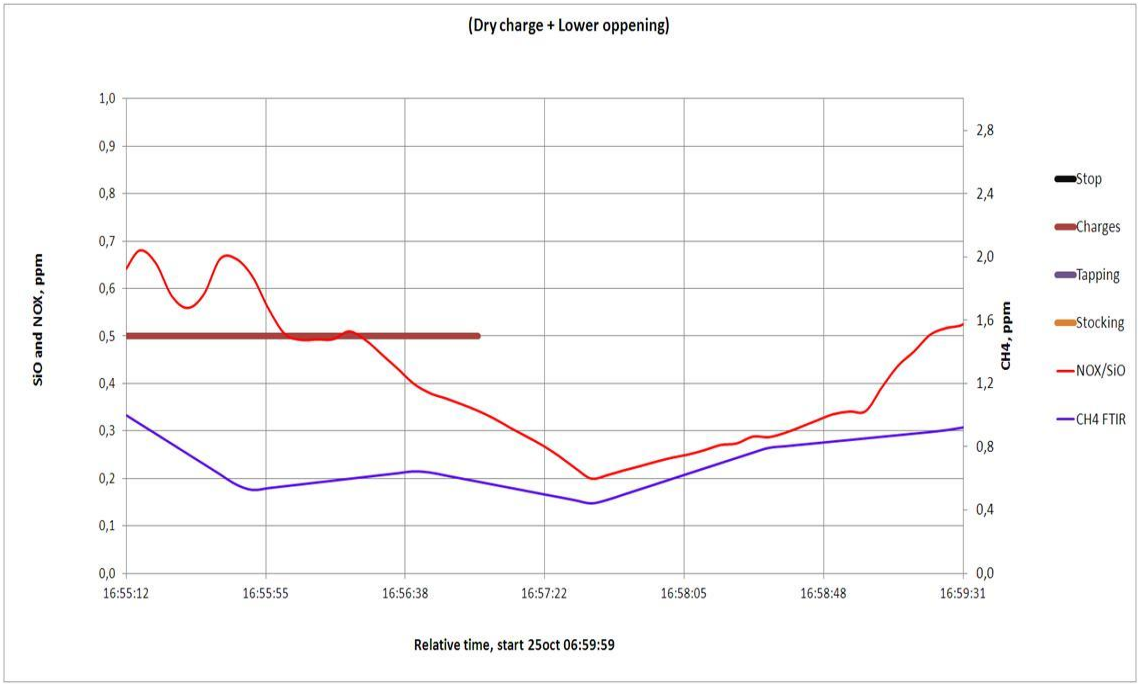

Fig. A.7.11: Effect of volatiles on the dry charge.

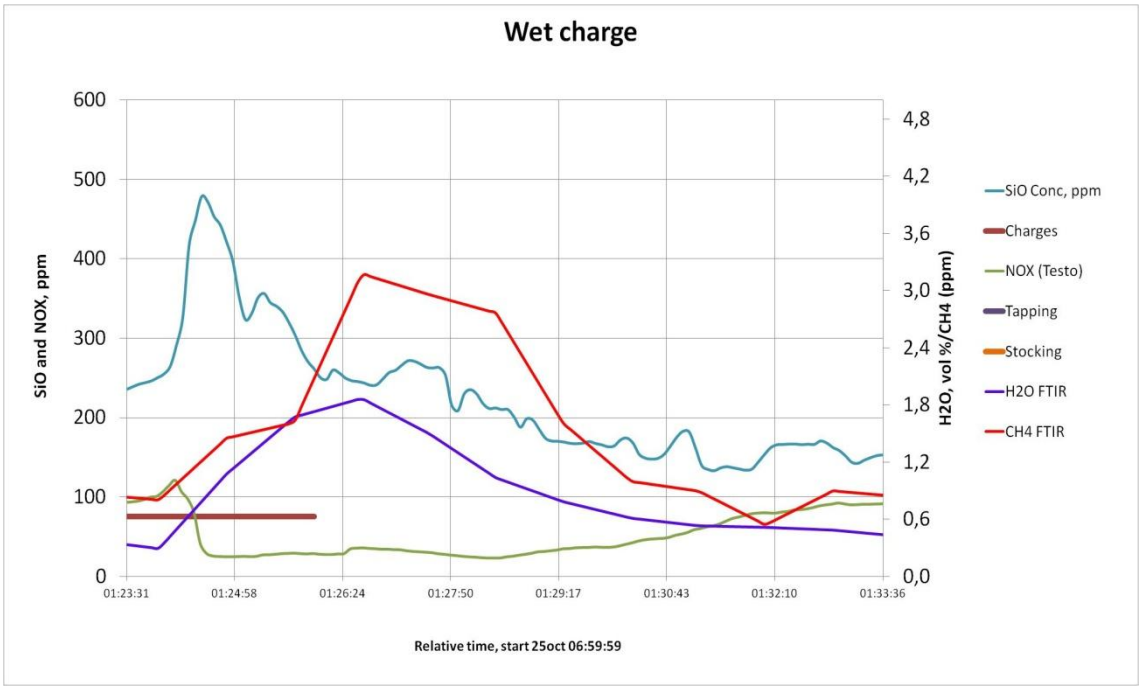

Fig. A.7.12: "Wet Charge + Lower Openings", the effect of charging.

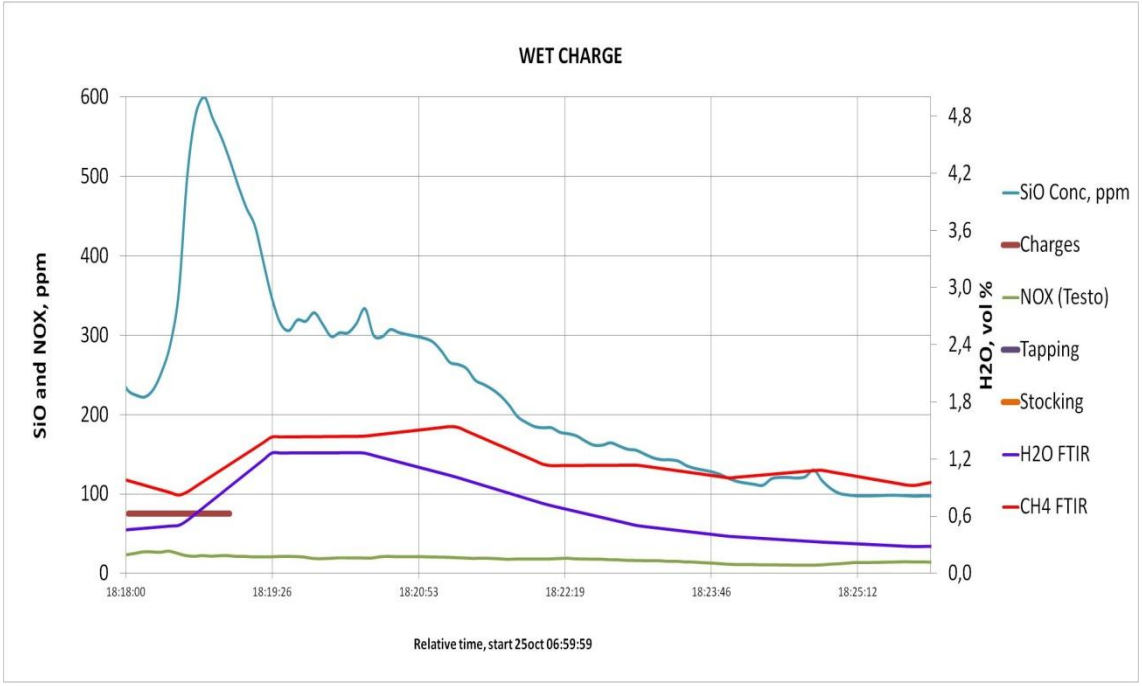

Fig. A.7.13: "Wet Charge + Upper Openings", the effect of charging.

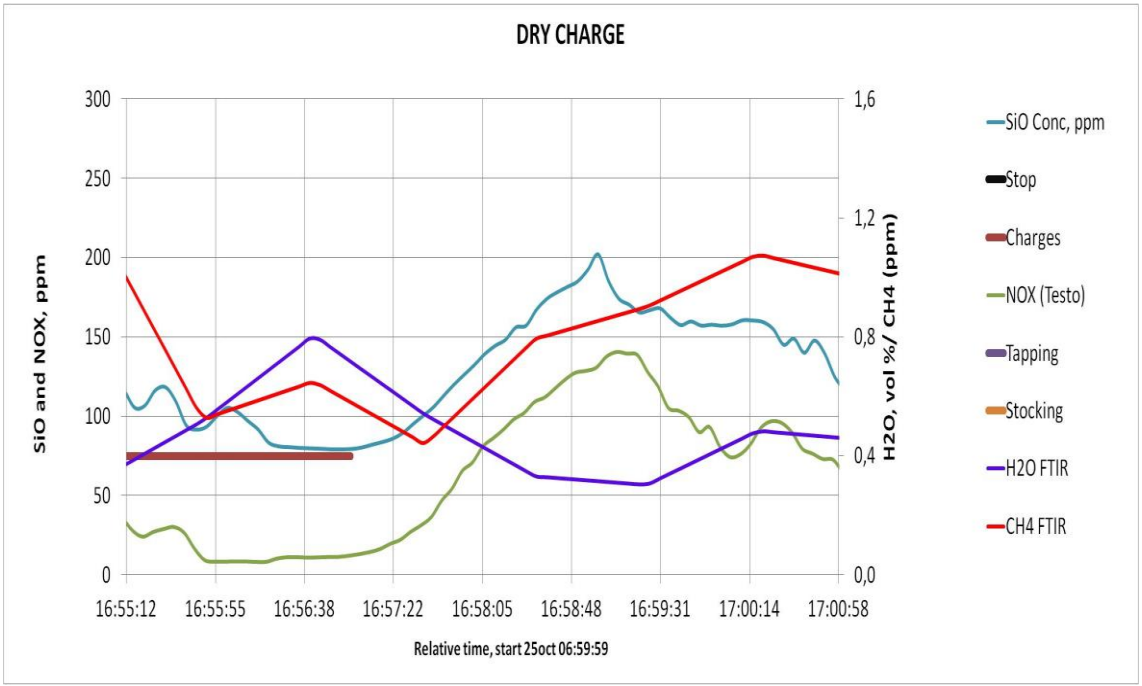

Fig. A.7.14: "Dry Charge + Lower Openings", the effect of charging.

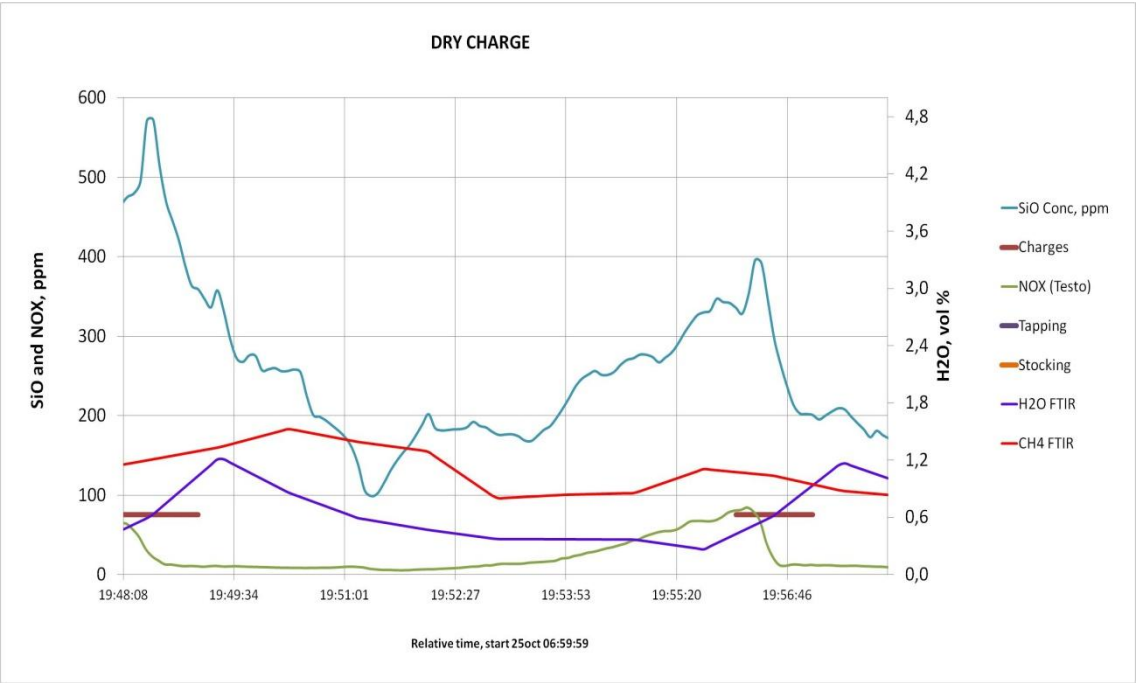

Fig. A.7.15: "Dry Charge + Upper Openings", the effect of charging.

A.8 Industrial charge experiment

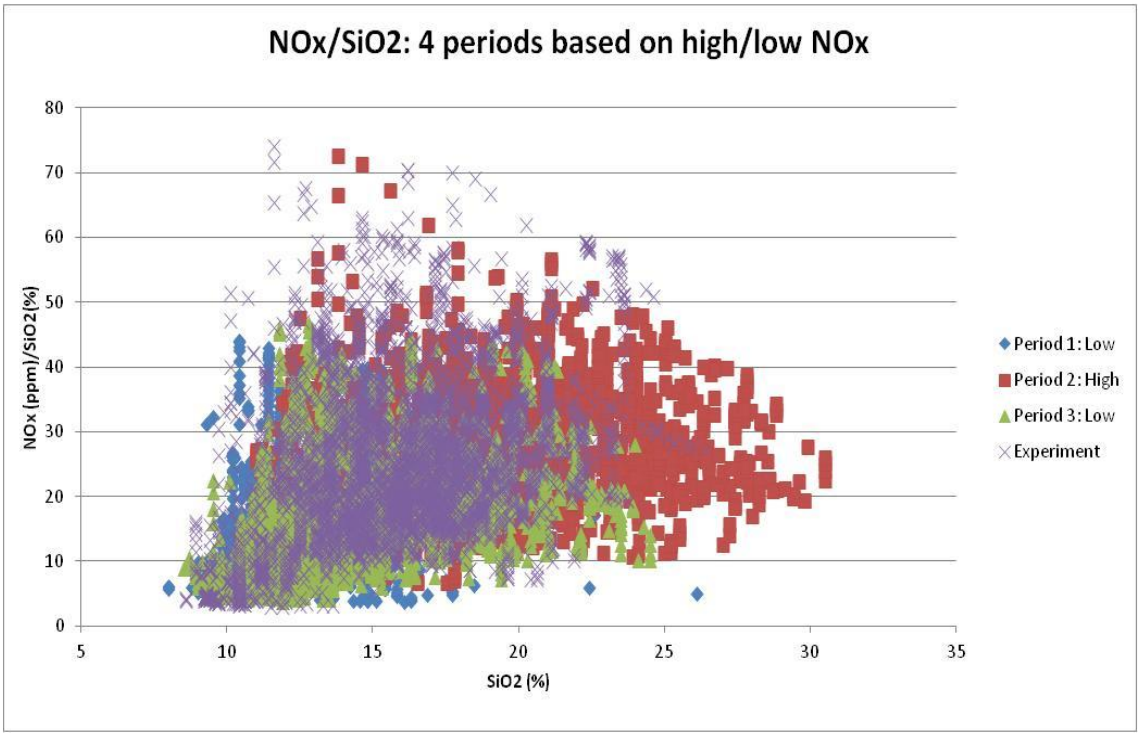

Fig. A.8.1: This is the plot used to find the slopes of the four periods in the results.

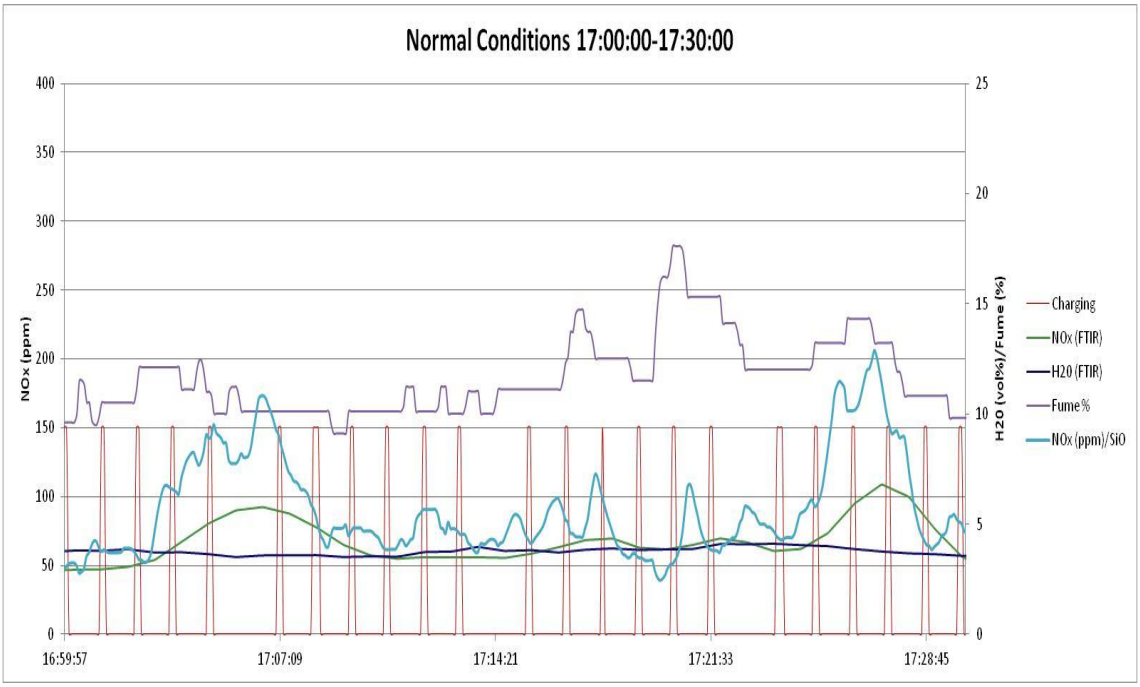

Fig. A.8.2: The dynamics for the normal conditions showing that the water content is stabile and the variations in emissions are low.

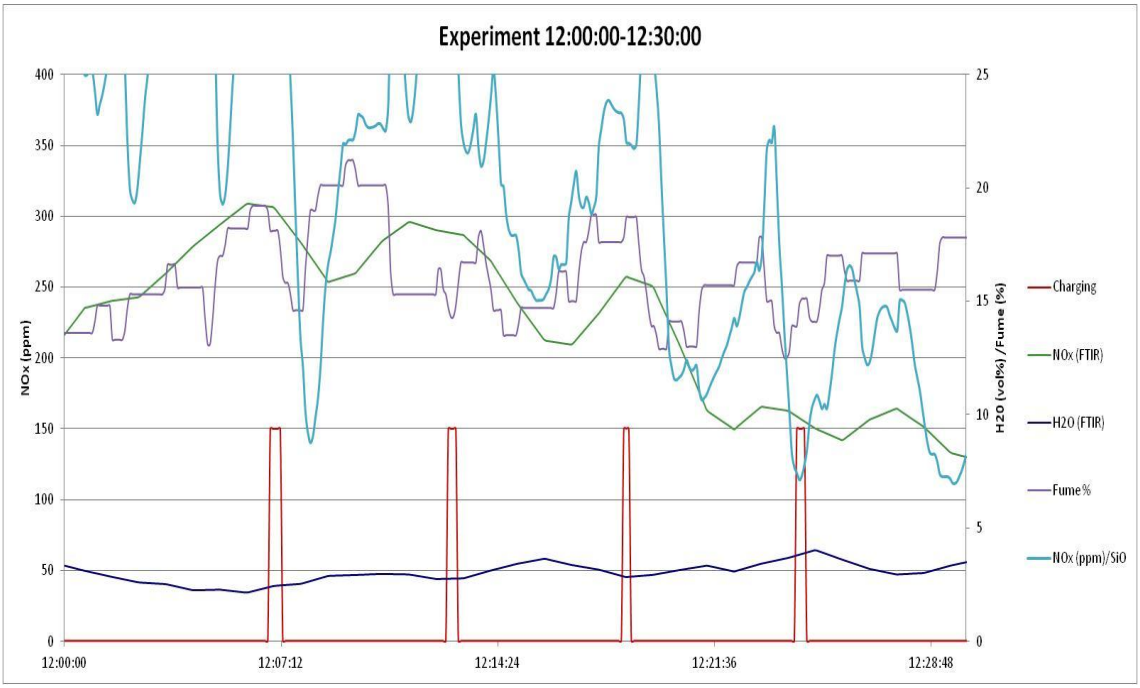

Fig. A.8.3: This figure illustrates the dynamics during the experiment.

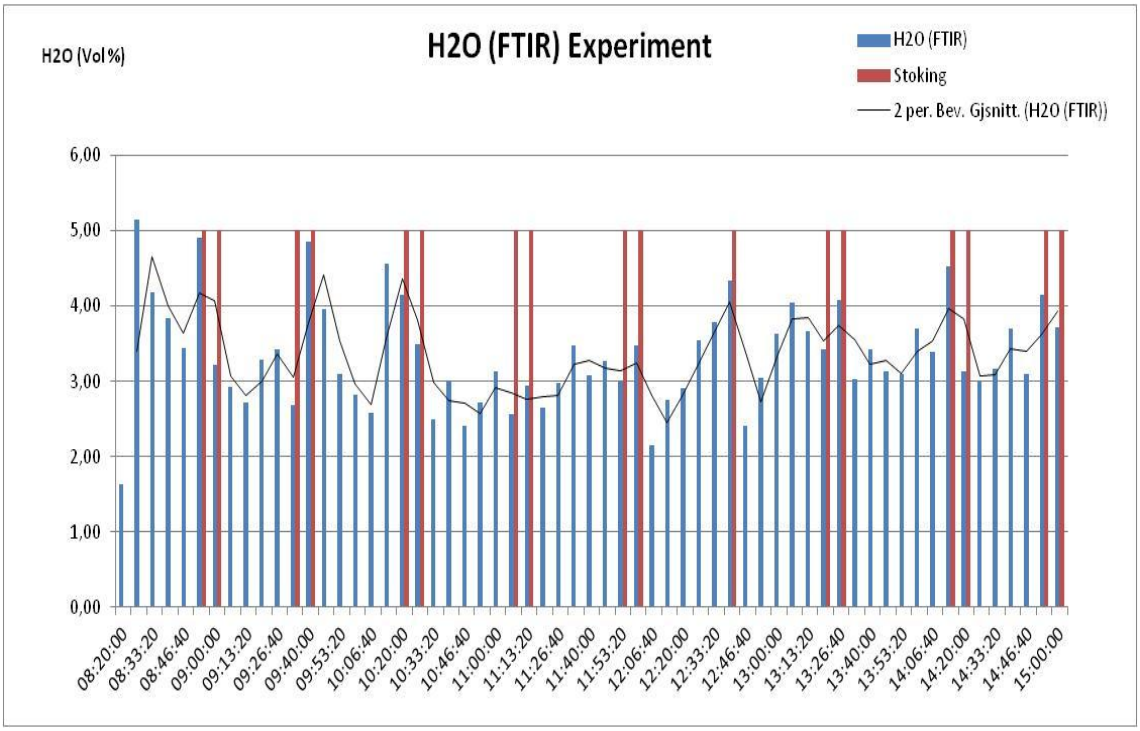

Fig. A.8.4: The effect of stoking on the water content during the experiment.